



**UNIWERSYTET  
MIKOŁAJA KOPERNIKA  
W TORUNIU**

Collegium Medicum  
im. Ludwika Rydygiera w Bydgoszczy

**Bydgoszcz 2021 r.**



**UNIwersytet  
MIKOŁAJA KOPERNIKA  
W TORUNIU**  
Wydział Lekarski  
Collegium Medicum w Bydgoszczy

**Lek. Sara Kierońska-Siwak**

**Ocena przydatności i wykorzystania traktografii w oparciu o tensor dyfuzji jako narzędzia obrazowania w postępowaniu neurochirurgicznym.**

**Rozprawa na stopień doktora nauk medycznych**

**Promotor:  
dr hab. n. med. Paweł Sokal, prof. UMK**

**Bydgoszcz 2021 r.**

## Spis treści

1. Nota informacyjna i wykaz publikacji stanowiący rozprawę doktorską .....	4
2. Wykaz skrótów .....	6
3. Wstęp .....	8
3.1. Artykuł „ <i>The usefulness and limitations of diffusion tensor imaging – a review study.</i> ” .....	10
4. Cel pracy doktorskiej.....	19
5. Cykl publikacji .....	20
5.1. Omówienie pracy „ <i>Tractography-Based Analysis of Morphological and Anatomical Characteristics of the Uncinate Fasciculus in Human Brains</i> ” .....	20
5.2. Artykuł „ <i>Tractography-Based Analysis of Morphological and Anatomical Characteristics of the Uncinate Fasciculus in Human Brains</i> ” .....	21
5.3. Omówienie pracy „ <i>Tractography Alterations in the Arcuate and Uncinate Fasciculi in Post-Stroke Aphasia</i> ” .....	36
5.4. Artykuł „ <i>Tractography Alterations in the Arcuate and Uncinate Fasciculi in Post-Stroke Aphasia</i> ” .....	37
5.5. Omówienie pracy „ <i>Tractography-guided surgery of brain tumours: what is the best method to outline the corticospinal tract?</i> ” .....	49
5.6. Artykuł „ <i>Tractography-guided surgery of brain tumours: what is the best method to outline the corticospinal tract?</i> ” .....	50
5.7. Omówienie pracy „ <i>Reliability of diffusion tensor tractography of facial nerve in cerebello-pontine angle tumours</i> ” .....	57
5.8. Artykuł „ <i>Reliability of diffusion tensor tractography of facial nerve in cerebello-pontine angle tumours</i> ” .....	58
6. Podsumowanie .....	68
7. Wnioski.....	69
8. Piśmiennictwo.....	70

## **1. Nota informacyjna i wykaz publikacji stanowiący rozprawę doktorską**

Zgodnie z warunkami ubiegania się o stopień naukowy doktora nauk medycznych, które zostały wyszczególnione w uchwale 115/2020 RDNM z dnia 24.06.2020 r w sprawie zasad postępowania o nadanie stopnia doktora w dyscyplinie nauki medyczne niniejsza rozprawa doktorska "Ocena przydatności i wykorzystania traktografii w oparciu o tensor dyfuzji jako narzędzia obrazowania w postępowaniu neurochirurgicznym" ma formę spójnego tematycznie zbioru pięciu artykułów opublikowanych w czasopismach naukowych wymienionych w części A listy czasopism publikowanych Ministerstwa Nauki i Szkolnictwa Wyższego.

Doktorant jest pierwszym autorem w czterech publikacjach (w jednej z nich jest równorzędnym pierwszym autorem). Jedna praca jest pracą przeglądową stanowiącą rozwinięcie wstępu do pracy. Pozostałe cztery prace są pracami oryginalnymi. Łączna wartość współczynnika Impact Factor dla cyklu wynosi **8,64**, a łączna wartość punktów ministerialnych według wykazu czasopism punktowanych Ministerstwa Nauki i Szkolnictwa Wyższego wynosi **280**.

Lista prac:

- 1) **Sara Kierońska**, Paweł Słoniewski; The usefulness and limitations of diffusion tensor imaging – a review study. European Journal of Translational and clinical medicine 2019;2 (2):43-51, liczba punktów MniSW: 20
- 2) **Sara Kierońska**, Paweł Sokal, Marta Dura, Magdalena Jabłońska, Marcin Rudaś, Renata Jabłońska; Tractography-Based Analysis of Morphological and Anatomical Characteristics of the Uncinate Fasciculus in Human Brains. Brain Sciences 2020 Oct 6;10(10):709. doi: 10.3390/brainsci10100709, współczynnik impact factor 3,34, liczba punktów MNiSW 100.

3) **Sara Kierońska**, Milena Świtońska, Grzegorz Meder, Magdalena Piotrowska, Paweł Sokal; Tractography Alterations in the Arcuate and Uncinate Fasciculi in Post-Stroke Aphasia. Brain Sciences . 2021 Jan 5;11(1):53. doi: 10.3390/brainsci11010053; współczynnik impact factor 3,34, liczba punktów MNiSW 100.

4) T. Szmuda , **S. Kierońska\*** , S. Ali, P. Słoniewski , M. Pacholski, J. Dzierżanowski , A. Sabisz, E. Szurowska; Tractography-guided surgery of brain tumours: what is the best method to outline the corticospinal tract?Folia MorphologicaVol 80, No 1 (2021);współczynnik impact factor 0,941;liczba punktów MNiSW 20. \* równorzędny pierwszy autor

5) Tomasz Szmuda, Paweł Słoniewski, Shan Ali, Pedro M. Gonçalves Pereira, Mateusz Pacholski, Fanar Timemy, Agnieszka Sabisz, Edyta Szurowska,**Sara Kierońska**; Reliability of diffusion tensor tractography of facial nerve in cerebello-pontine angle tumours. Polish Journal of Neurology and Neurosurgery 2020, Volume 54, no. 1, pages: 73–82, DOI: 10.5603/PJNNS.a2020.0001; współczynnik impact factor 1,025, liczba punktów MNiSW 40.

## **2. Wykaz skrótów**

**ADC** (apparent diffusion coefficient) – rzeczywisty współczynnik dyfuzji

**AF** (arcuate fasciculus)- pęczek łukowaty

**CP**(cerebral peduncle)- konar mózgu

**CM** (contrast medium) – środek kontrastowy

**CST** (corticospinal tract)-droga korowo-rdzeniowa

**DEC** (directionally encoded colour)- kolor kodowany kierunkowo

**DWI** (diffusion weighted imaging) – obrazowanie zależne od dyfuzji

**DTI** (diffusion tensor imaging) – obrazowanie tensora dyfuzji

**DTI-FN** (diffusion tensor imaging-facial nerve)- traktografia nerwu twarzowego

**DTT** (diffusion tensor tractography) – traktografia tensora dyfuzji

**FA** (fractional anisotropy) – parametr frakcjonowanej anizotropii

**FL** (frontal lobe)-płat czołowy

**FOV** (field of view) – pole widzenia

**FN**(facial nerve)- nerw twarzowy

**GFI** (gyrus frontalis inferior)- zakręt czołowy dolny

**GFS** (gyrus frontalis superior)-zakręt czołowy górny

**MD** (mean diffusivity)- średnia dyfuzyjność

**MR** (magnetic resonance) – rezonans magnetyczny

**MRI** (magnetic resonance imaging) – obrazowanie metodą rezonansu magnetycznego

**POCG** (postcentral gyrus)- zakręt zaśrodkowy

**PLIC** (posterior limb of internal capsule)- odnoga tylna torebki wewnętrznej

**ROI** (region of interest) – obszar zainteresowania

**SMA** (supplementary motor area)-pole ruchowe dodatkowe

**SD** (standard deviation) – odchylenie standardowe

**STIR** (short tau inversion recovery) – sekwencja zależna od czasu inwersji T1 (tau) dla tkanki

**T** – Tesla, jednostka indukcji magnetycznej

**T1 zależny** – obraz zależny od czasu relaksacji T1

**T2 zależny** – obraz zależny od czasu relaksacji T2

**TE** (echo time) – czas echa

**tDCS** (transcranial direct current stimulation)-przezczaszkowa stymulacja mózgu

**TI** (inversion time) – czas inwersji

**TK** – tomografia komputerowa

**TR** (repetition time) – czas repetycji

**UF** (uncinate fasciculus)- pęczek haczykowaty

**WHO** (World Health Organization) – Światowa Organizacja Zdrowia

### 3.Wstęp

Traktografia z wykorzystaniem tensora dyfuzji (DTI) jest nieinwazyjną techniką rezonansu magnetycznego uznawaną za metodę obrazowania przestrzennego. Tensor dyfuzji opiera się na pomiarze ruchów Browna cząsteczek wody. Jest to operacja matematyczna, stanowiąca opis wartości dyfuzji w trzech płaszczyznach [17,18].

W istocie białej cząsteczki wody mają tendencję do swobodnego dyfundowania wzdłuż aksonów. Taka kierunkowa zależność dyfuzyjności nazywana jest anizotropią. Ten kierunek maksymalnej dyfuzyjności wzdłuż włókien istoty białej rzutowany jest na ostateczny obraz radiologiczny. Powstałe obrazy można zapisywać w różnorodnych formatach i przekazywać bezpośrednio do sal operacyjnych lub wykorzystać dla celów naukowych. Najbardziej istotnym klinicznie aspektem jest prezentacja graficzna DTI jako sekwencja kolorów (DEC) [4]. DEC jest uwarunkowane kierunkiem wektora dyfuzji. W traktografii powszechnie stosuje się termin anizotropii, której wielkość bada się za pomocą frakcjonowanej anizotropii (FA). Dzięki temu możliwe jest stworzenie kolorowych map FA. Obrazy parametryczne FA kodowane kolorem ukazują zarówno kierunek maksymalnej składowej tensora dyfuzji przedstawiane jako określony kolor: czerwony (pravo–lewo), zielony (przód–tył), niebieski (góradół) oraz wielkość FA, od której zależna jest intensywność danego koloru [19-21]. Według wbudowanych, automatycznych, anatomicznych atlasów aplikacje pozwalają na precyzyjne określenie struktury neuronowe i niektóre z głównych ścieżek światłowodowych. Struktury te są nazywane regionami zainteresowania (ROI). Ustawiając jeden lub więcej ROI, aplikacja automatycznie oblicza i rysuje włókna istoty białej [5,6].

Neurochirurgia i operacje resekcji guzów mózgu na przestrzeni ostatnich lat poczyniły ogromne postępy. W chirurgii guzów mózgu dla neurochirurga priorytetem jest doszczętność resekcji bez dokonania deficytów neurologicznych, dlatego nauka dąży do wprowadzania nowoczesnych technik neuroobrazowania, które ułatwią zachowanie struktur elokwentnych [5].



Wiedza o przebiegu i anatomii poszczególnych włókien nerwowych pozwala na precyzyjne i dokładne zaplanowanie zabiegu operacyjnego oraz w znaczący sposób zwiększa bezpieczeństwo interwencji neurochirurgicznej[1-3].

Dla rozwinięcia wstępu do rozprawy doktorskiej poniżej przedstawiono opublikowany artykuł poglądowy “The usefulness and limitations of diffusion tensor imaging – a review study.”

# The usefulness and limitations of diffusion tensor imaging – a review study

Sara Kierońska<sup>1,2</sup> , Paweł Słoniewski<sup>2</sup> 

<sup>1</sup>Jan Biziel University Hospital Collegium Medicum Nicolaus Copernicus University,  
Department of Neurosurgery and Neurology, Bydgoszcz, Poland

<sup>2</sup>Department of Neurosurgery, Medical University of Gdańsk, Poland

## Abstract

Diffusion tensor tractography (DTI) has been used for planning of a brain pathology surgeries. Knowledge about the distances between neural tracts and brain tumours is believed to increase the patient safety and implies the extent of resection. The aim of the study was to demonstrate the contemporary possibilities and the clinical usefulness of DTI. Following the explanation of the technical basics of DTI, we presented the drawbacks and limitations of this visualisation technique. The most commonly outlined tracts are corticospinal tract (CST), arcuate fasciculus (AF) and frontal aslant tract (FAT). Tumour located in frontal, parietal or temporal lobe can affect the course of the CST. There are two basic possibilities to visualise CST: deterministic and probabilistic. The usefulness of DTI seems limited in imaging the neoplasms of either frontal or temporal region causing aphasia, which infiltrate the AF or the FAT. This limitation is probably related to divergent and patient-specific location of functional speech areas. Acquisition disturbances, ill-defined mathematical algorithms, surgery-related brain shift and defining wrong non-functional brain area are the sources of DTI inaccuracy, which is limiting its clinical application.

**Keywords:** Diffusion Tensor Imaging · tractography · corticospinal tract · arcuate fasciculus · frontal aslant tract

## Citation

Kierońska S, Słoniewski P. The usefulness and limitations of diffusion tensor imaging – a review study.  
Eur J Transl Clin Med. 2019;2(2):43-51.  
DOI: 10.31373/ejtcmm/112437

## Introduction

Tractography is a non-invasive method of visualizing the white matter of central nervous system (CNS) structures in vivo. It is possible to determine the direction and continuity of neural fibres in either

CNS or peripheral nervous system by using diffusion tensor imaging (DTI), a specific sequence of magnetic resonance (MR) [1]. Tractography allows reconstructing the neural fibres in colourful projections that run simultaneously through particular anatomical regions of the brain. Important neural pathways are tracked

### Corresponding author:

Sara Kierońska, Jan Biziel University Hospital Collegium Medicum Nicolaus Copernicus University, Department of Neurosurgery and Neurology, Bydgoszcz, Poland  
e-mail: sara.kieronska@gmail.com

No external funds.

Available online: [www.ejtcmm.gumed.edu.pl](http://www.ejtcmm.gumed.edu.pl)

Copyright © Medical University of Gdańsk

This is Open Access article distributed under the terms of the Creative Commons Attribution-ShareAlike 4.0 International.



by utilising the connection map and their course correlates with some pathological changes in the CNS [2-3]. That information is essential in neurosurgeon's pre-operative planning, as it leads to an improvement in setting boundaries for tumour resection and decrease of post-surgery neurological deficits.

Tractography utilises the data provided by the MR tensor, which returns information about size and the direction of the diffusion. The sketch of the white matter pathways through the selected anatomical points is based on the principles of voxel continuity [4]. There are several analytical methods used in the assessment of anatomical differences between specific groups of patients. Nevertheless, the most commonly used is the voxel-based analysis. It is easily adjustable to the needs of the neurosurgeon and makes it possible to assess the degree of tissue diffusion simultaneously throughout the encephalon, which points out the possible locations of tumour infiltrations. Another widely used method is an analysis of the region of interest (ROI) which enables the precise assessment of the degree of diffusion in hypothetically determined locations [5-6].

Studies conducted on neurosurgical patients revealed that total or subtotal brain tumor resection leads to improved survival. The specific success rate is directly connected with a lower risk of tumour relapse [7-8]. From the patient's perspective, it is crucial to maintain quality of life, motor function and speech after undergoing surgery [9]. The vast majority of available literature refers to the preclinical technical aspects of DTI and rarely describes its practical application. Currently, only several of these practical possibilities that DTI gives are utilised in modern neurosurgery. These need to be summarised in a comprehensive review, which is not only directed at neurosurgeons but also radiologists and neurologists. In this study, we reviewed not only the usefulness but also the potential limitations of DTI in brain tumour surgery.

## Tractography

Tractography is a method of spatial imaging of computational radiological data. It allows various neural fibres to be tracked, which is a result of different diffusion of a single voxel. Many professional applications, both

paid and freeware, are used for tracking, fusing of the sequences and comparative analyses. These are widely available and have great flexibility in the data processing. Images can be saved in a variety of formats, printed and transferred to operating rooms or used for research purposes. The most clinically valid and nonetheless spectacular graphic presentation of DTI is a directionally encoded colour (DEC) sequence. DEC is conditioned by the direction of the diffusion vector of white matter. According to built-in, automatic, anatomical atlases, applications allow precise determination of neural structures and some of the main fibre pathways. These structures are named regions of interest (ROIs). By setting one or more ROI, the application automatically calculates and draws white matter fibres. To note, visualising an individual neural pathway is also possible. The software also allows sketching the location of the tumour concerning the previously designated path.

At our department, we performed DTI for all patients with suspected tumour infiltration, according to internal DTI protocol, resulting in a total of 60 diffusion sampling directions acquired. Parameters of those MRI examinations were as follows:

- b-value: 1000 s/mm<sup>2</sup>,
- in-plane resolution: 1.95313 mm,
- thickness: 2 mm,
- angular threshold: 90°.

The obtained pattern of neural tracts, as well as the outlined tumour, can be imported into the neuronavigation system, which seems to be the leading, practical advantage of all DTI methods.

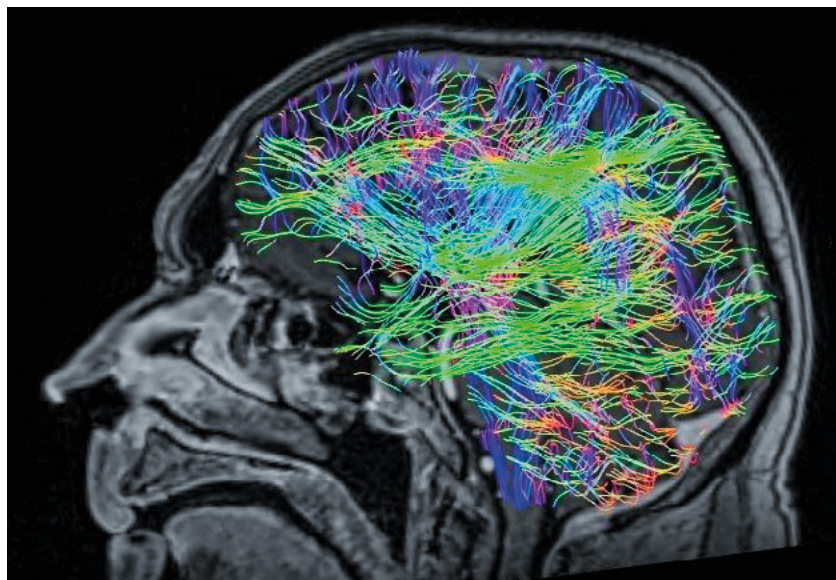


**Figure 1.** Directionally encoded colour (DEC) sequence of the diffusion tensor tractography depicts the course of white matter fibres. In standard markings, the red colour means left-right, green front-back and blue top-to-bottom directions of white matter fibres

There are two basic techniques for creating models of neural pathways: probabilistic and deterministic. The deterministic approach implies drawing the fibres in the system by marking one starting point and another ROI. Utilising this technique, the defined neural bundle assumes only one direction assigned to

the single voxel. Therefore, the main limitation of this approach is the high anatomical variability of neural pathways and the fact that some of the fibres intersect each other [10]. Table 1 presents selected articles comparing both methods.

**Table 1. Comparison of methods of tractography: the probabilistic and deterministic. The practical application of each technique was extracted from the studies**

Author	Title	Year	Tract	Probabilistic vs. Deterministic	Clinical impact
Zolal A et al. [1]	Comparison of probabilistic and deterministic fibre tracking of cranial nerves	2017	Cranial nerves: II, III,V, VII,VIII	Probabilistic	Probabilistic tracking is more effective than the previously described deterministic
Schlaier JR et al. [2]	Probabilistic vs. deterministic fibre tracking and the influence of different seed regions to delineate cerebellar-thalamic fibers in deep brain stimulation	2017	Dentate-rubro thalamic tract	Probabilistic	Probabilistic fibre tracking was more sensitive and provides more accurate tracking solutions for dentate-rubro-thalamic tract
Jenabi M et al. [3]	Identification of the Corticobulbar Tracts of the Tongue and Face Using Deterministic and Probabilistic DTI Fibre Tracking in Patients with Brain Tumor	2015	Corticobulbar tract	Probabilistic	Probabilistic tractography successfully reconstructs the face- and tongue-associated corticobulbar tracts from the lateral primary motor cortex to the pons in both hemispheres
Jenabi M et al. [4]	Probabilistic fibre tracking of the language and motor white matter pathways of the supplementary motor area (SMA) in patients with brain tumors	2014	Broca's area to SMA	Probabilistic	The identification of unique areas of white matter according to the probabilistic method allows the location of the tract connecting Broca's area to SMA
Li Z et al. [5]	Diffusion tensor tractography of the arcuate fasciculus in patients with brain tumors: Comparison between deterministic and probabilistic models	2013	Arcuate fasciculus	Probabilistic	Probabilistic tractography reconstructs the arcuate fasciculus more completely and performs better through areas of tumor and/or edema

Burkett DJ et al. [6]	Deterministic Tractography of the Descending Tract of the Spinal Trigeminal Nerve Using Diffusion Tensor Imaging	2017	descending tract of the trigeminal nerve	Deterministic	The identification of unique areas of white matter according to the probabilistic method allows the location of the tract connecting Broca's area to SMA
Anthofer JM et al. [7]	DTI-based deterministic fibre tracking of the medial forebrain bundle	2015	medial forebrain bundle	Deterministic	Deterministic tractography with different ROIs provides variable delineations of the course of the medial forebrain bundle

Most authors use a probabilistic method for ascertaining a specific tract. The obtained images of DTI are easy to interpret for most of them [17-18]. The advantage of probabilistic tractography is an obtained sketch of neural tracts that presents any structural changes of white matter adjacent to pathological changes [18]. On the other hand, the deterministic method, is mostly used for the analysis of the course of fibres that have their ending in the voxels with the lowest FA value [10]. For the clinical purpose, the deterministic model is chosen less frequently, although it has some clinical advantages. In our experience, the deterministic approach results in better visualisation of the corticospinal tract (CST) adhering to tumours of the medial frontal lobe.

There are over 50 patients who had deterministic tracking of the CST before undergoing surgery at the Neurosurgery Department of the Medical University of Gdańsk (Poland). Those surgeries confirmed the position of CST with the clinical findings. Other studies confirm our observations [19].

### Clinical application of tractography

The precise visualisation of the neural pathways and their topographic relation to the tumour increases the safety of the surgery, even though DTI fibres are not the same as the actual neural pathways [19-20]. Optimal preoperative planning allows the operating team to minimise the potential damage of vital white matter during the surgery [21-22]. The images created during the preoperative planning can be superimposed in realtime onto the view shown in the operative

microscope. This way the neurosurgeon can remove the tumour relying solely on the preoperative planning in what is known as 'image-guided surgery' [23].

### Corticospinal tract

The CST is the main neuronal route responsible for motor functions of the face, limbs and trunk. CST is composed of descending fibres starting in the pre-centre bend (4th Brodmann area) which transmits neural impulses through the pyramid up to the spinal cord [24]. Infiltration or destruction of CST caused by a brain tumour, ischemic stroke or subarachnoid haemorrhage affects the density of the fibres. Sterr et al demonstrated that the degree of the damage to the pyramidal pathway is closely related to subsequent motor deficits in patients after ischemic stroke [25]. The anatomy of the CST and its topography in relation to the tumour is essential when those two are close to each other [26]. Based on tractographic parameters, we can estimate the degree of CST injury and predict the postoperative neurological outcome [26]. The CST is the neural bundle most commonly tracked by neurosurgeons, including at our centre [27]. Various ROIs can be used to track CST, resulting in high variability rate. Weiss et al showed that an ROI set at the anterior inferior pontine region yielded better tracking results compared to the ROI set at the internal capsule [28-30]. Furthermore, CST was reconstructed from neural bundles passing through by cerebral peduncle, posterior limb of internal capsule and corona radiata in a patient after stroke [31]. This study confirmed the significance of a hind limb of the internal capsule as an ROI for CST

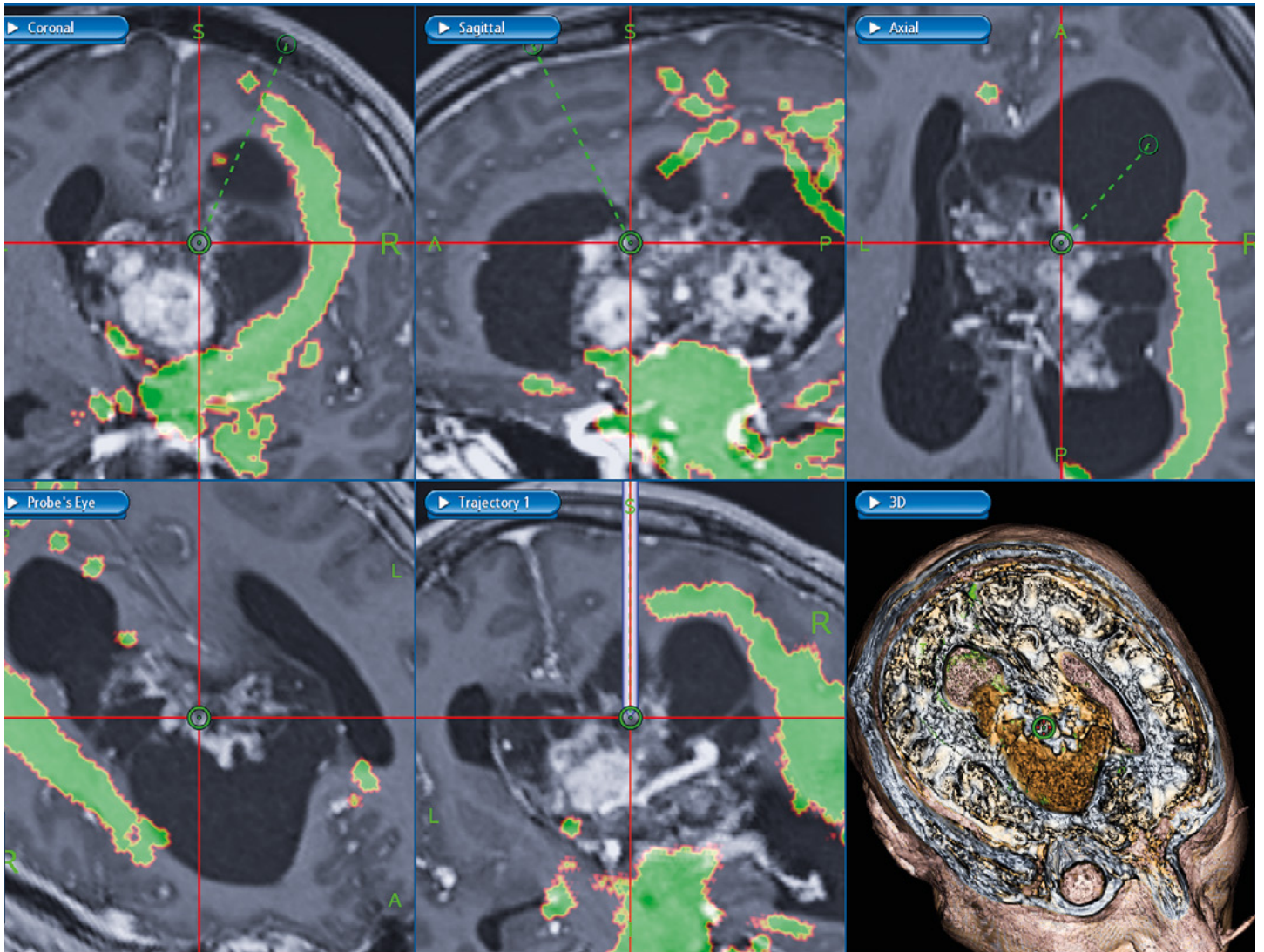


Figure 2. Planning of the surgical approach with the visualisation of the corticospinal tract of a patient with ventricular neurocytoma

tractography. Based on the above suggestions, our department has commenced the DTI analysis comparing the differences between CSTs with various

ROIs. In our experience, we defined two main types of the anatomical ROIs (the cerebral peduncle and posterior limb of the internal capsule) and four additional

endpoints: precentral gyrus, post-central gyrus, supplementary motor area and frontal lobe.

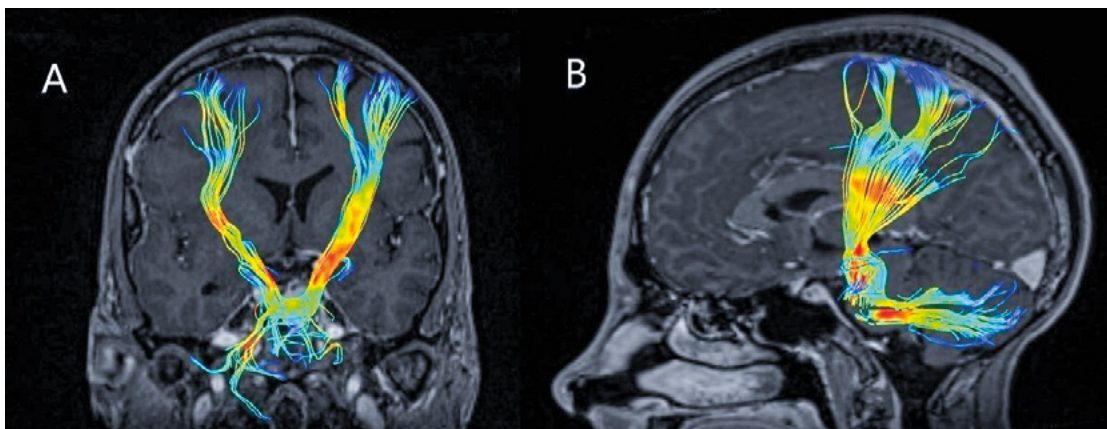


Figure 3. Corticospinal tract on preoperative tractography on coronal (A) and sagittal (B) planes

## Arcuate Fasciculus (AF)

AF is the white matter pathway connecting the Broca speech centre (located in the frontal lobe) with the Wernicke speech centre (temporal lobe). CNS lesions infiltrating AF affect speech because the communication between the Broca and Wernicke areas becomes severed. The patient usually presents with so-called conduction aphasia [32-33]. DTI-based visualisation of AF is an widely accepted management for tumours of eloquent areas. The synchronisation of the tractography with the navigation system determines the precise location of the AF. Therefore, DTI sets boundaries for resection of a tumour located near AF and helps to prevent iatrogenic injury of the speech centre [34]. However, AF alone tractography could not always prevent postoperative aphasia. Cortical mapping, together with neurophysiological monitoring, could be applied for some more demanding tumours, although some surgeons prefer awake craniotomy [35]. Awake craniotomy also improves patient safety in terms of preserving speech functions [36]. The different location of both Broca and Wernicke area among individuals preclude the correct prediction of functionally active AF in DTI, what seems to be the main drawback of DTI tracking of AF, also confirmed by our experience.

Nevertheless, functional MRI also can unambiguously estimate the exact location of speech areas. Researchers should put more effort into studying DTI in terms of speech preservation as awake craniotomy resection is still more reliable in this case [37].

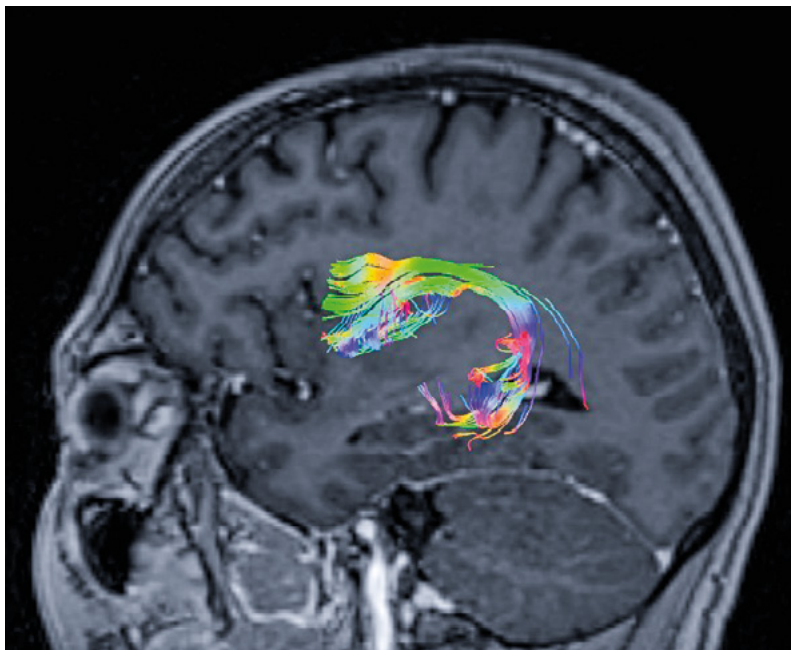


Figure 4. Arcuate Fasciculus connecting Broca's and Wernicke's areas

## Frontal aslant tract

The frontal aslant tract (FAT), first described in DTI by Catani et al, contains neural fibres connecting the lower frontal bend (pars triangularis and pars opercularis of the operculum) with the supplementary motor area (SMA) and pre-SMA [38]. Tumors infiltrating SMA or pre-SMA may impede some motor functions, learning and aphasia. In a majority of patients, the FAT projected to the opercularis part of inferior frontal gyrus (IFG) and a greater number of fibres terminated at the triangularis part of IFG in left-handed patients [39]. The course of FAT through the inferior frontal lobe and the Broca's area suggests its significant role in the proper functioning of speech. Patients with progressive aphasia with a significant change within the FAT show particularly large changes in the correlation with AF [38-40]. In studies of the surgical treatment of patients with brain tumours, FAT lesions are associated with transient speech disorders and the occurrence of mutism and motor aphasia [34, 41]. The accurate prediction of the FAT location is possible thanks to the neuromonitoring techniques and direct stimulation of the cerebral cortex. In one study, the intraoperative stimulation of the left hemisphere FAT during craniotomy caused transient speech disorder of the stuttering type [34, 42].

In clinical practice, FAT could be determined to be a means of DTI in patients for whom an awake craniotomy is planned [43]. Baker et al. suggested that FAT and "crossed FAT" are of great importance for tumours infiltrating SMA and pre-SMA [37, 44].

## Limitations and future of tractograph

DTI is an imaging method used as a radiological tool for years. However, only the recent development of visualisation of neural tracts, tractography, makes it possible to use on personal computers. Frequent use of tractography leads to the constant improvement of reconstruction methods and these directly influenced the precision of treatment in the clinical setting. The correlation of DTI with a patient's neurological condition is sufficient for an adequate therapeutic process

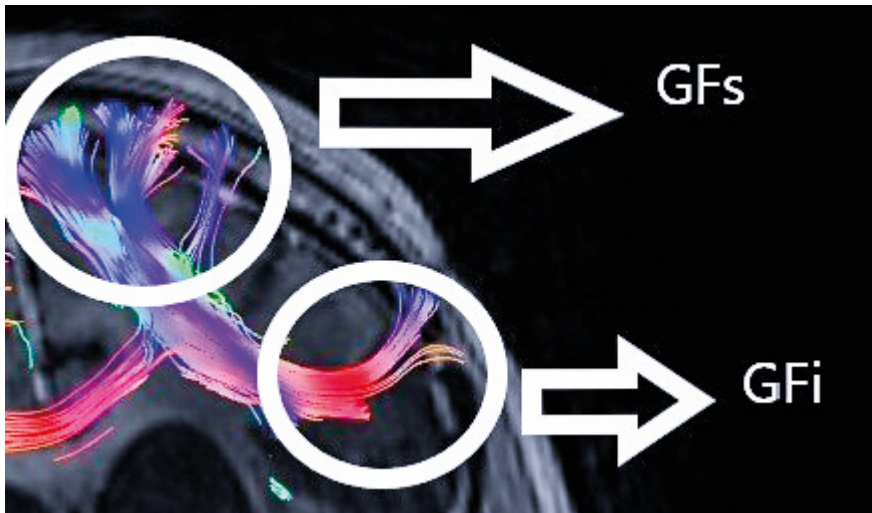


**Figure 5.** Frontal aslant tract based on two regions of interest—gyrus frontalis superior (GFs) and gyrus frontalis inferior (GFi). Abbreviations: GFs –gyrus frontalis superior, GFi – gyrus frontalis inferior

[45-47]. However, tractography is not considered as a standard approach due to its limitations, variability of obtained data and lack of standardisation of image acquisition parameters.

As mentioned earlier, tractography is a method of spatial imaging of computational radiological data and because of that use of DTI in surgical planning remains virtual. For patients with malignant tumours or significant brain edema, the identification of neural pathways is inaccurate [47]. Furthermore, in the case of sizable cerebrospinal fluid flow, there is a risk of motion artefacts occurring during the DTI acquisition. This functional limitation substantially affects the precision of tractography. For these reasons, DTI techniques should be regarded as complementary in surgical planning or as an educational tool [48].

On the other hand, DTI is still dynamically evolving. Thanks to its widespread use by neurosurgeons, we need continuous research to discover new clinical uses and possibilities of DTI. The main contemporary issue is to find the functional significance of each visualised neural tract. On the contrary, even if a particular

amount of fibres is damaged during the surgery, it does not necessarily lead to noticeable neurological deficits [21]. It seems that the future of neural tract tracking lies in the development of a universal mathematical model for precise delineation of anatomic-functional structures [23].

Tractography, as a method of imaging, has been used for several years. We've been using it at our department since 2010. In most cases, acquisition parameters are the same but

ways of determining the nerve path of our patients are based on the experience of the researcher currently responsible for the patient. Nevertheless, conclusions of all the researchers are in line with each other. Also other review articles coincide with our observations about the utility and reliability of the tractography as a standard diagnostic procedure. Furthermore, our results are in line with the experiences published by other teams about the necessity of using the tractography as an essential tool in treatment in patients with a brain tumour.

## Conclusions

DTI is a clinically significant tool in the daily neurosurgical practice. In the current review, we provide examples where tractography is a valuable imaging adjunct. Owing to the limitations of DTI, combining tractography with intraoperative monitoring would allow more accurate preoperative planning and then increase the safety of the surgery. Further standardisation of DTI protocols is needed.

## References

1. Basser PJ, Pajevic S, Pierpaoli C, Duda J, Aldroubi A. In vivo fiber tractography using DT-MRI data. *Magn Reson Med* [Internet]. 2000;44(4):625–32. Available from: <http://www.ncbi.nlm.nih.gov/pubmed/11025519>
2. Catani M. Occipito-temporal connections in the human brain. *Brain* [Internet]. 2003 Sep 1;126(9):2093–107. Available from: <https://academic.oup.com/brain/article-lookup/doi/10.1093/brain/awg203>
3. Gierek T, Paluch J, Pencak P, Kaźmierczak B, Klimczak-Gołab L. [Magnetic resonance tractography in neuroradiological diagnostic aspects]. *Otolaryngol Pol = Polish Otolaryngol* [Internet]. 2009;63(5):403–6. Available from: <http://linkinghub.elsevier.com/retrieve/pii/S0030665709701519>



4. Radek M, Wiśniewski K, Grochal M, Jastrzębski K, Gębski P, Snopkowska-Wiaderna D, et al. Traktografia rdzenia jako metoda diagnostyczna w trudnych przypadkach guzów śródrdzeniowych. *Neurol Neurochir Pol* [Internet]. 2013;47(1):74–9. Available from: <https://linkinghub.elsevier.com/retrieve/pii/S0028384314602747>
5. Gawłowska-Sawosz M, Pawełczyk A, Gębski P, Pawełczyk T, Strzelecki D, Rabe-Jabłońska J. Evaluation of white matter structure changes, as assessed in tractography, and cognitive dysfunctions in patients with early onset schizophrenia and their first-degree relatives. *Psychiatr Pol* [Internet]. 2017;51(4):735–50. Available from: <http://psychiatriapolska.pl/735750>
6. Shizukuishi T, Abe O, Aoki S. Diffusion tensor imaging analysis for psychiatric disorders. *Magn Reson Med Sci* [Internet]. 2013;12(3):153–9. Available from: <http://www.ncbi.nlm.nih.gov/pubmed/23857149>
7. Smith JS, Chang EF, Lamborn KR, Chang SM, Prados MD, Cha S, et al. Role of Extent of Resection in the Long-Term Outcome of Low-Grade Hemispheric Gliomas. *J Clin Oncol* [Internet]. 2008 Mar 10;26(8):1338–45. Available from: <http://ascopubs.org/doi/10.1200/JCO.2007.13.9337>
8. Dubey A, Kataria R, Sinha V. Role of diffusion tensor imaging in brain tumor surgery. *Asian J Neurosurg* [Internet]. 2018;13(2):302. Available from: <http://www.asianjns.org/text.asp?2018/13/2/302/228537>
9. Ulmer JL, Salvan C V, Mueller WM, Krouwer HG, Stroe GO, Aralasmak A, et al. The role of diffusion tensor imaging in establishing the proximity of tumor borders to functional brain systems: Implications for preoperative risk assessments and postoperative outcomes. *Technol Cancer Res Treat* [Internet]. 2004;3(6):567–76. Available from: <https://journals.sagepub.com/doi/abs/10.1177/153303460400300606>
10. Klein J, Grötsch A, Betz D, Barbieri S, Friman O, Stieltjes B, et al. Qualitative and quantitative analysis of probabilistic and deterministic fiber tracking. In: Dawant BM, Haynor DR, editors. *Medical Imaging 2010: Image Processing* [Internet]. 2010. p. 76232A. Available from: <http://proceedings.spiedigitallibrary.org/proceeding.aspx?doi=10.1117/12.843472>
11. Zolal A, Sobottka SB, Podlesek D, Linn J, Rieger B, Juratli TA, et al. Comparison of probabilistic and deterministic fiber tracking of cranial nerves. *J Neurosurg* [Internet]. 2017;127(3):613–21. Available from: <https://thejns.org/view/journals/j-neurosurg/127/3/article-p613.xml>
12. Schlaier JR, Beer AL, Faltermeier R, Fellner C, Steib K, Lange M, et al. Probabilistic vs. deterministic fiber tracking and the influence of different seed regions to delineate cerebellar-thalamic fibers in deep brain stimulation. Roesper J, editor. *Eur J Neurosci* [Internet]. 2017;45(12):1623–33. Available from: <https://doi.org/10.1111/ejn.13575>
13. Jenabi M, Peck KK, Young RJ, Brennan N, Holodny AI. Identification of the Corticobulbar Tracts of the Tongue and Face Using Deterministic and Probabilistic DTI Fiber Tracking in Patients with Brain Tumor. *Am J Neuroradiol* [Internet]. 2015;36(11):2036–41. Available from: <http://www.ajnr.org/lookup/doi/10.3174/ajnr.A4430>
14. Jenabi M, Peck KK, Young RJ, Brennan N, Holodny AI. Probabilistic fiber tracking of the language and motor white matter pathways of the supplementary motor area (SMA) in patients with brain tumors. *J Neuroradiol* [Internet]. 2014 Dec 1 [cited 2019 Sep 30];41(5):342–9. Available from: <https://www.sciencedirect.com/science/article/pii/S0150986113001302>
15. Li Z, Peck KK, Brennan NP, Jenabi M, Hsu M, Zhang Z, et al. Diffusion tensor tractography of the arcuate fasciculus in patients with brain tumors: Comparison between deterministic and probabilistic models. *J Biomed Sci Eng* [Internet]. 2013;6(2):192–200. Available from: <https://www.ncbi.nlm.nih.gov/pubmed/25328583>
16. Burkett DJ, Garst JR, Hill JP, Kam A, Anderson DE. Deterministic Tractography of the Descending Tract of the Spinal Trigeminal Nerve Using Diffusion Tensor Imaging. *J Neuroimaging* [Internet]. 2017 Sep;27(5):539–44. Available from: <http://doi.wiley.com/10.1111/jon.12425>
17. Anthofer JM, Steib K, Fellner C, Lange M, Brawanski A, Schlaier J. DTI-based deterministic fibre tracking of the medial forebrain bundle. *Acta Neurochir (Wien)* [Internet]. 2015 Mar 15;157(3):469–77. Available from: <http://link.springer.com/10.1007/s00701-014-2335-y>
18. Jbabdi S, Johansen-Berg H. Tractography: Where Do We Go from Here? *Brain Connect* [Internet]. 2011 Sep;1(3):169–83. Available from: <http://www.liebertpub.com/doi/10.1089/brain.2011.0033>
19. Schonberg T, Pianka P, Hendler T, Pasternak O, Assaf Y. Characterization of displaced white matter by brain tumors using combined DTI and fMRI. *Neuroimage* [Internet]. 2006 May;30(4):1100–11. Available from: <https://linkinghub.elsevier.com/retrieve/pii/S1053811905024626>
20. Witwer BP, Moftakhar R, Hasan KM, Deshmukh P, Haughton V, Field A, et al. Diffusion-tensor imaging of white matter tracts in patients with cerebral neoplasm. *J Neurosurg* [Internet]. 2002;97(3):568–75. Available from: <https://thejns.org/view/journals/j-neurosurg/97/3/article-p568.xml>
21. Provenzale JM, Mukundan S, Barboriak DP. Diffusion-weighted and Perfusion MR Imaging for Brain Tumor Characterization and Assessment of Treatment Response. *Radiology* [Internet]. 2006;239(3):632–49. Available from: <http://pubs.rsna.org/doi/10.1148/radiol.2393042031>
22. Al-Okaili RN, Krejza J, Wang S, Woo JH, Melhem ER. Advanced MR Imaging Techniques in the Diagnosis of Intraaxial Brain Tumors in Adults. *RadioGraphics* [Internet]. 2006 Oct;26(suppl\_1):S173–89. Available from: <http://pubs.rsna.org/doi/10.1148/rg.26si065513>
23. Krakowiak M, Stoniewski P, Dzierżanowski J, Szmuda T. Future of the nerve fibres imaging: tractography application and development directions. *Folia Morphol (Warsz)* [Internet]. 2015 Sep 2;74(3):290–4. Available from: [https://journals.via-medica.pl/fovia\\_morphologica/article/view/38825](https://journals.via-medica.pl/fovia_morphologica/article/view/38825)
24. Tracey D. Ascending and Descending Pathways in the Spinal Cord. In: *The Rat Nervous System* [Internet]. Elsevier; 2004. p. 149–64. Available from: <https://linkinghub.elsevier.com/retrieve/pii/B9780125476386500080>
25. Sterr A, Shan Shen, Szameitat AJ, Herron KA. The Role of Corticospinal Tract Damage in Chronic Motor Recovery and Neurorehabilitation: A Pilot Study. *Neurorehabil Neural Repair* [Internet]. 2010 Jun;24(5):413–9. Available from: <http://journals.sagepub.com/doi/10.1177/1545968309348310>
26. Seo JP, Jang SH. Different Characteristics of the Corticospinal Tract According to the Cerebral Origin: DTI Study. *Am J Neuroradiol* [Internet]. 2013 Jul;34(7):1359–63. Available from: <http://www.ajnr.org/lookup/doi/10.3174/ajnr.A3389>

27. Min Z, Niu C, Zhang Q, Zhang M, Qian Y. Optimal Factors of Diffusion Tensor Imaging Predicting Corticospinal Tract Injury in Patients with Brain Tumors. *Korean J Radiol* [Internet]. 2017;18(5):844. Available from: <https://synapse.koreamed.org/DOIx.php?id=10.3348/kjr.2017.18.5.844>
28. Morita N, Wang S, Kadakia P, Chawla S, Poptani H, Melhem ER. Diffusion Tensor Imaging of the Corticospinal Tract in Patients with Brain Neoplasms. *Magn Reson Med Sci* [Internet]. 2011;10(4):239–43. Available from: <http://joi.jlc.jst.go.jp/JST.JSTAGE/mrms/10.239?from=CrossRef>
29. Gao B, Shen X, Shiroishi MS, Pang M, Li Z, Yu B, et al. A pilot study of pre-operative motor dysfunction from gliomas in the region of corticospinal tract: Evaluation with diffusion tensor imaging. Fung SH, editor. *PLoS One* [Internet]. 2017 Aug 22;12(8):e0182795. Available from: <https://dx.plos.org/10.1371/journal.pone.0182795>
30. Weiss C, Tursunova I, Neuschmelting V, Lockau H, Nettekoven C, Oros-Peusquens A-M, et al. Improved nTMS- and DTI-derived CST tractography through anatomical ROI seeding on anterior pontine level compared to internal capsule. *NeuroImage Clin* [Internet]. 2015;7:424–37. Available from: <https://linkinghub.elsevier.com/retrieve/pii/S2213158215000078>
31. Maraka S, Jiang Q, Jafari-Khouzani K, Li L, Malik S, Hamidian H, et al. Degree of corticospinal tract damage correlates with motor function after stroke. *Ann Clin Transl Neurol* [Internet]. 2014;1(11):891–9. Available from: <http://doi.wiley.com/10.1002/acn3.132>
32. Geranmayeh F, Brownsett SLE, Wise RJS. Task-induced brain activity in aphasic stroke patients: what is driving recovery? *Brain* [Internet]. 2014 Oct;137(10):2632–48. Available from: <https://academic.oup.com/brain/article-lookup/doi/10.1093/brain/awu163>
33. Fridriksson J, Guo D, Fillmore P, Holland A, Rorden C. Damage to the anterior arcuate fasciculus predicts non-fluent speech production in aphasia. *Brain* [Internet]. 2013 Nov;136(11):3451–60. Available from: <https://academic.oup.com/brain/article-lookup/doi/10.1093/brain/awt267>
34. Fujii M, Maesawa S, Motomura K, Futamura M, Hayashi Y, Koba I, et al. Intraoperative subcortical mapping of a language-associated deep frontal tract connecting the superior frontal gyrus to Broca's area in the dominant hemisphere of patients with glioma. *J Neurosurg* [Internet]. 2015 Jun;122(6):1390–6. Available from: <https://thejns.org/view/journals/j-neurosurg/122/6/article-p1390.xml>
35. De Witte E, Mariën P. The neurolinguistic approach to awake surgery reviewed. *Clin Neurol Neurosurg* [Internet]. 2013;115(2):127–45. Available from: <https://linkinghub.elsevier.com/retrieve/pii/S0303846712004933>
36. Sitnikov AR, Grigoryan YA, Mishnyakova LP. Awake craniotomy without sedation in treatment of patients with lesional epilepsy. *Surg Neurol Int* [Internet]. 2018;9:177. Available from: <http://www.ncbi.nlm.nih.gov/pubmed/30221022>
37. Chernoff BL, Teghipco A, Garcea FE, Sims MH, Paul DA, Tivarus ME, et al. A Role for the Frontal Aslant Tract in Speech Planning: A Neurosurgical Case Study. *J Cogn Neurosci* [Internet]. 2018 May;30(5):752–69. Available from: [https://www.mitpressjournals.org/doi/abs/10.1162/jocn\\_a\\_01244](https://www.mitpressjournals.org/doi/abs/10.1162/jocn_a_01244)
38. Catani M, Dell'Acqua F, Vergani F, Malik F, Hodge H, Roy P, et al. Short frontal lobe connections of the human brain. *Cortex* [Internet]. 2012 Feb;48(2):273–91. Available from: <https://linkinghub.elsevier.com/retrieve/pii/S0010945211003170>
39. Szmuda T, Rogowska M, Słoniewski P, Abuhaimed A, Szmuda M, Springer J, et al. Frontal aslant tract projections to the inferior frontal gyrus. *Folia Morphol (Warsz)* [Internet]. 2017 Dec 1;76(4):574–81. Available from: [https://journals.via-medica.pl/fovia\\_morphologica/article/view/50306](https://journals.via-medica.pl/fovia_morphologica/article/view/50306)
40. Mandelli ML, Caverzasi E, Binney RJ, Henry ML, Lobach I, Block N, et al. Frontal White Matter Tracts Sustaining Speech Production in Primary Progressive Aphasia. *J Neurosci* [Internet]. 2014 Jul 16;34(29):9754–67. Available from: <http://www.jneurosci.org/cgi/doi/10.1523/JNEUROSCI.3464-13.2014>
41. Sierpowska J, Gabarrós A, Fernandez-Coello A, Camins À, Castañer S, Juncadella M, et al. Morphological derivation overflow as a result of disruption of the left frontal aslant white matter tract. *Brain Lang* [Internet]. 2015 Mar;142:54–64. Available from: <https://linkinghub.elsevier.com/retrieve/pii/S0093934X15000061>
42. Kemerdere R, de Champfleury NM, Deverdun J, Cochereau J, Moritz-Gasser S, Herbet G, et al. Role of the left frontal aslant tract in stuttering: a brain stimulation and tractographic study. *J Neurol* [Internet]. 2016 Jan 11;263(1):157–67. Available from: <http://link.springer.com/10.1007/s00415-015-7949-3>
43. Andrea GD, Trillo G, Picotti V, Raco A. Trends in Reconstructive Neurosurgery [Internet]. Visocchi M, Mehdorn HM, Katayama Y, von Wild KRH, editors. Cham: Springer International Publishing; 2017. 241–250 p. (Acta Neurochirurgica Supplement; vol. 124). Available from: <http://link.springer.com/10.1007/978-3-319-39546-3>
44. Varriano F, Pascual-Diaz S, Prats-Galino A. When the FAT goes wide: Right extended Frontal Aslant Tract volume predicts performance on working memory tasks in healthy humans. He H, editor. *PLoS One* [Internet]. 2018 Aug 1;13(8):e0200786. Available from: <https://dx.plos.org/10.1371/journal.pone.0200786>
45. Essayed WI, Zhang F, Unadkat P, Cosgrove GR, Golby AJ, O'Donnell LJ. White matter tractography for neurosurgical planning: A topography-based review of the current state of the art. *NeuroImage Clin* [Internet]. 2017;15(January):659–72. Available from: <https://linkinghub.elsevier.com/retrieve/pii/S2213158217301444>
46. Abdullah KG, Lubelski D, Nucifora PGP, Brem S. Use of diffusion tensor imaging in glioma resection. *Neurosurg Focus* [Internet]. 2013 Apr;34(4):E1. Available from: <https://thejns.org/view/journals/neurosurg-focus/34/4/article-pE1.xml>
47. Castellano A, Bello L, Michelozzi C, Gallucci M, Fava E, Iadanza A, et al. Role of diffusion tensor magnetic resonance tractography in predicting the extent of resection in glioma surgery. *Neuro Oncol* [Internet]. 2012 Feb 1;14(2):192–202. Available from: <https://academic.oup.com/neuro-oncology/article-lookup/doi/10.1093/neuonc/nor188>
48. Zhukov VY, Goryaynov SA, Ogurtsova AA, Ageev IS, Protskiy S V, Pronin IN, et al. [Diffusion tensor imaging tractography and intraoperative neurophysiological monitoring in surgery of intracranial tumors located near the pyramidal tract]. *Zh Vopr Neurokhir Im N N Burdenko* [Internet]. 2016;80(1):5–18. Available from: [https://www.researchgate.net/profile/Ivan\\_Ageev/publication/301315444\\_Diffusion\\_tensor\\_imaging\\_tractography\\_and\\_intraoperative\\_neurophysiological\\_monitoring\\_in\\_surgery\\_of\\_intracranial\\_tumors\\_located\\_near\\_the\\_pyramidal\\_tract/links/5873d42008ae8fce4924cc91.pdf](https://www.researchgate.net/profile/Ivan_Ageev/publication/301315444_Diffusion_tensor_imaging_tractography_and_intraoperative_neurophysiological_monitoring_in_surgery_of_intracranial_tumors_located_near_the_pyramidal_tract/links/5873d42008ae8fce4924cc91.pdf)

#### **4. Cel pracy doktorskiej**

Wyniki dotychczasowych prac naukowych uwzględniają traktografię jako jedną z metodą stosowaną w neurochirurgii dla wizualizacji dróg nerwowych istoty białej. Traktografia zajmuje szczególnie miejsce w neuroonkologii, ze szczególnym uwzględnieniem chirurgii glejaków, jako zmian charakteryzujących się w resekcji wysoką problematycznością. Neuroobrazowanie z wykorzystaniem traktografii umożliwia ocenę: położenia oraz przebiegu włókien istoty białej względem guza oraz ich wzajemnej korelacji, uszkodzeń włókien w obrębie istoty białej, a także zmian zaistniałych w tkankach w bezpośrednim sąsiedztwie guza tj.: naciek nowotworowy czy obrzęk.

Biorąc pod uwagę powyższe przesłanki cele pracy obejmowały:

1. Określenie znaczenia traktografii oraz przedstawienia sposobów wyznaczania istotnych dróg nerwowych w oparciu o tensor dyfuzji.
2. Ocenę przydatności traktografii jako narzędzia neuroobrazowania w praktyce neurochirurgicznej podczas planowania zabiegów neuroonkologicznych.
3. Ocenę zmian w anatomii dróg nerwowych i nerwu twarzowego związanych z naciekiem nowotworowym i niedokrwieniem mózgu.

## 5. Cykl publikacji

### 5.1 Omówienie pracy “Artykuł “Tractography-Based Analysis of Morphological and Anatomical Characteristics of the Uncinate Fasciculus in Human Brains”

Artykuł “Tractography-Based Analysis of Morphological and Anatomical Characteristics of the Uncinate Fasciculus in Human Brains” opublikowany w czasopiśmie Brain Sciences prezentuje anatomiczne aspekty pęczka haczykowatego u pacjentów u których wykluczono patologię wewnątrzczaszkową. Materiał obejmuje analizę 34 pacjentów u których wykonano badanie rezonansu magnetycznego z uwzględnieniem DTI.

W artykule analizie poddana została objętość drogi, ilość włókien oraz kształt pęczka haczykowatego w zależności od płci oraz półkuli mózgu. Całkowita liczba włókien UF była istotnie wyższa w prawej półkuli w porównaniu z lewą (prawa  $M \pm SD = 52 \pm 24$ ; lewa:  $39 \pm 25$ ,  $p < 0,05$ ). Kolejnym kluczowym aspektem tej publikacji było wyróżnienie różnorodnych kształtów pęczka haczykowatego: kształt haka, kształt U, kształt Y. Dotychczas w publikacjach naukowych pęczek haczykowaty nie został sklasyfikowany pod względem kształtów. W zaprezentowanej grupie badanych dominował kształt haka. U części badanych badany pęczek układał się w sposób nietypowy tworząc kształt litery “U” lub “Y” co może stanowić punkt dla kolejnych badań anatomicznych.

Istotnym aspektem była również analiza objętości UF, która była istotnie większa u mężczyzn ( $1410 \pm 150,7 \text{ mm}^3$ ) w porównaniu z kobietami ( $1325 \pm 133,2 \text{ mm}^3$ ) ( $p < 0,05$ ). Natomiast średnie wartości anizotropii frakcyjnej (FA) UF były istotnie większe po lewej stronie 0,597, podczas gdy po prawej UF średnio 0,346 ( $p < 0,05$ ).

Communication

# Tractography-Based Analysis of Morphological and Anatomical Characteristics of the Uncinate Fasciculus in Human Brains

Sara Kierońska <sup>1</sup>, Paweł Sokal <sup>1,2,\*</sup>, Marta Dura <sup>3</sup>, Magdalena Jabłońska <sup>4</sup>, Marcin Rudaś <sup>1</sup> and Renata Jabłońska <sup>1,5</sup>

<sup>1</sup> Department of Neurosurgery and Neurology, Jan Biziel University Hospital No 2, Collegium Medicum, Nicolaus Copernicus University, 85-168 Bydgoszcz, Poland; sara.kieronska@bizeil.pl (S.K.); marcin.rudas@bizeil.pl (M.R.); renata.jablonska@cm.umk.pl (R.J.)

<sup>2</sup> Faculty of Health Science, The Ludwik Rydygier Collegium Medicum, Nicolaus Copernicus University, 85-067 Bydgoszcz, Poland

<sup>3</sup> Department of Radiology, Jan Biziel University Hospital No. 2, Collegium Medicum Nicolaus Copernicus University, 85-168 Bydgoszcz, Poland; marta.dura@cm.umk.pl

<sup>4</sup> Students' Scientific Circle, Department of Neurosurgery and Neurology, Jan Biziel University Hospital No 2, Collegium Medicum, Nicolaus Copernicus University, 85-168 Bydgoszcz, Poland; magdalena.jablonska14@gmail.com

<sup>5</sup> Department of Neurological and Neurosurgical Nursing, Faculty of Health Science, The Ludwik Rydygier Collegium Medicum, Nicolaus Copernicus University, 85-067 Bydgoszcz, Poland

\* Correspondence: pawel.sokal@cm.umk.pl; Tel.: +48-600-954-415

Received: 29 August 2020; Accepted: 30 September 2020; Published: 6 October 2020



**Abstract:** (1) Background: The uncinat fasciculus (UF) is a white matter bundle connecting the prefrontal cortex and temporal lobe. The functional role of the uncinat fasciculus is still uncertain. The role of the UF is attributed to the emotional empathy network. The present study aimed to more accurately describe anatomical variability of the UF by focusing on the volume of fibers and testing for correlations with sex and age. (2) Material and Methods: Magnetic resonance imaging of adult patients with diffusion tensor imaging (DTI) was performed on 34 patients. The total number of fibers, volume of UF, and number of tracts were processed using DSI studio software. The DSI studio allows for mapping of different nerve pathways and visualizing of the obtained results using spatial graphics. (3) Results: The total number of UF tracts was significantly higher in the right hemisphere compared to the left hemisphere (right  $M \pm SD = 52 \pm 24$ ; left:  $39 \pm 25$ ,  $p < 0.05$ ). A hook-shaped UF was the most common variant (91.7%). The UF volumes were larger in men ( $1410 \pm 150.7 \text{ mm}^3$ ) as compared to women ( $1325 \pm 133.2 \text{ mm}^3$ ) ( $p < 0.05$ ). The mean fractional anisotropy (FA) values of the UF were significantly larger on the left side 0.597, while the right UF had an average of 0.346 ( $p < 0.05$ ). Patients older than 50 years old had a significantly higher value of mean diffusivity (MD) ( $p = 0.034$ ). In 73.5% of patients, a greater number of fibers terminated in the inferior part of the inferior frontal gyrus. (4) Conclusions: The morphological characteristics of the UF, unlike the shape, are associated with sex and are characterized by hemispheric dominance. These findings confirm the results of the previous studies. Future research should examine the potential correlation among the UF volume, number of fibers, and total brain volume in both sexes and patient psychological state.

**Keywords:** uncinat fasciculus; tractography; fractional anisotropy; diffusion tensor imaging

## 1. Introduction

The uncinat fasciculus (UF) was first described by Reil in 1809. It is a white matter tract in the human brain that connects limbic regions in the temporal lobe to the frontal lobe [1,2].

Although the functional role of the uncinate fasciculus is still unknown, the UF is recognized as the major fiber tract connecting the anterior part of the temporal lobe with the orbitofrontal cortex and the frontopolar cortex [3–5]. It is attributed to the emotional empathy network and in addition, these nerve fibers are sent to components of the limbic system, including terminating projections to the hippocampus and amygdala [6,7]. The UF as well as the superior longitudinal fasciculus (SLF) and inferior fronto-occipital fasciculus (IFOF) are the main long association fibers in the brain [1,8].

The UF is also known as a ‘hook-shaped’ fascicle connecting the prefrontal cortex and the anteromedial temporal lobe. The traditional anatomical description outlines a temporal stem that hooks around the posterior insula, a subinsular body, and two prefrontal stems that extend to the lateral orbital gyri and the frontopolar cortex [9]. The UF interconnects regions that support acoustic memory, visual information, and emotional responses [10].

UF abnormalities are associated with impaired socio-emotional processing and symptom severity in patients with autism spectrum disorder [11].

Tractography is a valuable tool in imaging the central nervous system. Diffusion tensor imaging (DTI) studies have shown that UF is divided into different parts: frontal, insular, and temporal pole [12]. The UF corresponds to the uncus (i.e., Brodmann areas 28, 34, and 36) and the temporal lobe (Brodmann areas 20 and 38) [3,13].

The present study aimed to more accurately describe the anatomical variability of the UF by focusing on the shape of the tract, considering the volume of fibers (with the number of fibers as a side parameter) and testing for correlations with sex and age. We further aimed to present the relationship between the UF in each hemisphere, sex, and age in illustrated and tractography series.

Numerous software packages available allow for an even more robust use of this technique. One example is the DSI studio (<http://dsi-studio.labsolver.org>) developed by Fang-Cheng. The DSI studio allows for mapping of different nerve pathways and visualizing of the obtained results using spatial graphics.

## 2. Materials and Methods

Patients treated at an academic Neurosurgery Department from 2019 to 2020 were prospectively enrolled into this project.

Participants in this study were 34 adult patients (14 males and 20 females) with an average age of 53.5 years (range: 25–82 years; standard deviation [SD] = 14.69). Handedness was determined by a questionnaire completed by patients (right/left = 29/5). Patients with lesions interfering with the regions of interest (ROIs) or the UF were excluded. Informed consent was obtained from all participants and the study protocol was approved by the local Ethics Committee. The study was conducted in accordance with the Declaration of Helsinki, and the protocol was approved by the Ethics Committee of NKBBN/65/2019.

### 2.1. MRI and DTI Acquisition

Human brains were scanned by MRI (T1, T2-weighted, and DTI with echo planar imaging) using a 20-channel head/neck coil on a single 3.0 T Siemens Magnetom Aera scanner (Erlangen, Germany).

We used the following DTI acquisition parameters: slice thickness 5.0 mm; matrix—128 × 128; field of view—240 × 240 mm; repetition time—3500 ms; echo time—83.0 ms. Outcome measures of interest included fractional anisotropy (FA), mean diffusivity (MD), and apparent diffusion coefficient (ADC). DTI is most commonly performed using a single-shot, spin-echo, echo planar image acquisition at b-values similar to those used for conventional DWI (typically  $b = 1000 \text{ s/mm}^2$ ). ROIs were defined automatically based on an anatomical atlas loaded into the DSI studio program (Figure 1).

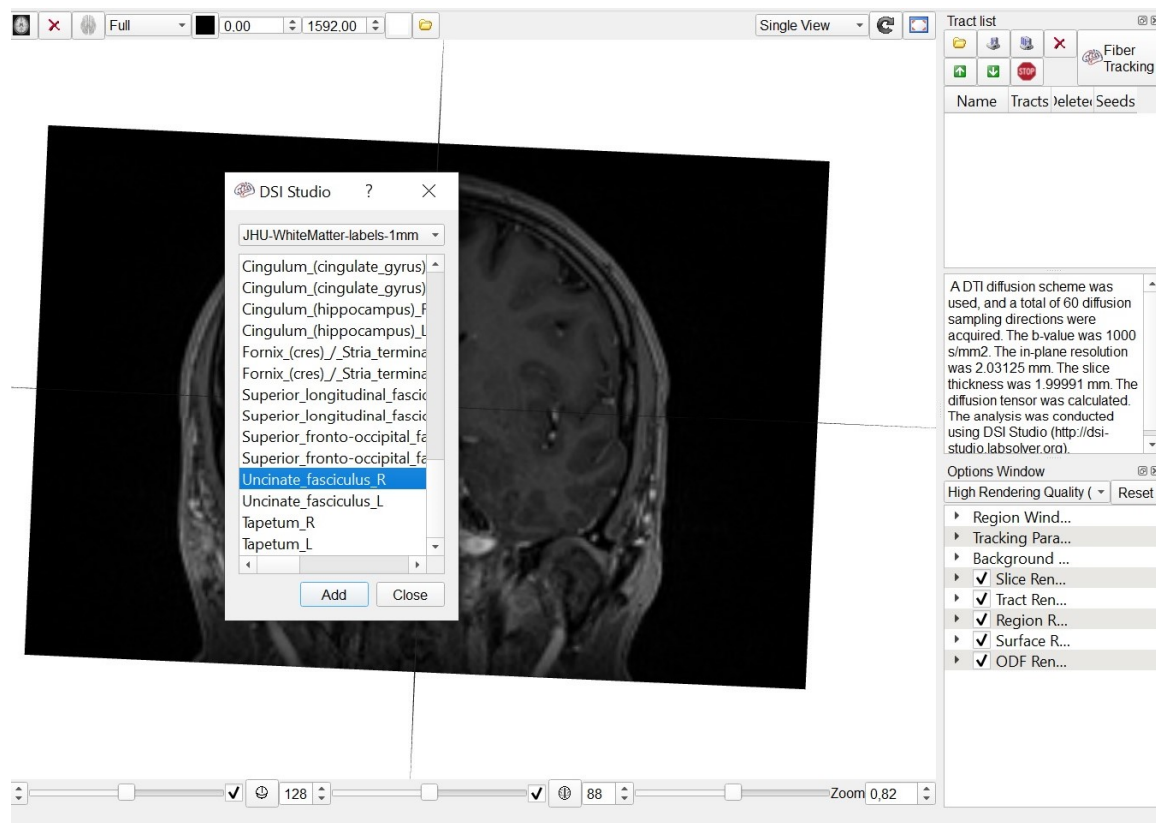


**Figure 1.** Anatomical atlas loaded in to the DSI studio software.

## 2.2. Fiber Tracking

Diffusion tensor images were processed using DSI studio software, BSD License. A DTI diffusion scheme was used and a total of 60 diffusion sampling directions were acquired. The number of directions was based on the experience of previous researchers [14–16]. Lebel et al. in their manuscript pointed out that in their study, 30- and 60-direction protocols resulted in either more or longer tracts [16]. The b-value was 1000 s/mm<sup>2</sup>. The in-plane resolution was 1.95 mm. The slice thickness was 2 mm. A deterministic fiber tracking algorithm was used and all of the fiber tracts were determined using the Runge–Kutta algorithm, which was the default for all of the visualizations [17]. The angular threshold was 90 degrees. The step size was 0.98 mm and a total of 200,000 seeds were placed. Fiber trajectories were smoothed by averaging the propagation direction with 30% of the previous directions. Tracts with a length less than 25 mm were discarded. A total of 15,000 tracts were calculated.

## 2.3. Statistical Analyses

Statistica 13 software (Tibco Software Inc., Palo Alto, CA, USA) was used for statistical analysis. The normality of the data distribution was tested qualitatively using the Shapiro–Wilk test. In the event of normal distribution, parametric tests were applied (i.e., Student’s *t*-test for non-dependent and dependent variables and Pearson’s rank correlation test). In the event of non-normal distribution, the data were analyzed using non-parametric tests (i.e., between-group comparisons using the Mann–Whitney test and for dependent variables, the Wilcoxon test; Spearman’s rank correlation test for correlation analysis). All analyses were considered significant at a  $p < 0.05$  threshold.

### 3. Results

The UF was identified in both hemispheres in all patients.

A significantly greater number of UF tracts were observed in the right as compared to the left hemisphere (right:  $M \pm SD = 52 \pm 24$ ; left:  $39 \pm 25$ ,  $p < 0.05$ ). The shapes of the UF in three different patients are presented in Figures 2–4. The blue color represents terminating fibers, whereas the green color represents fibers forming the central part of the tract. The colors are selected automatically by the DSI studio program. The hook-shaped (91.7%;  $n = 31$ , Figure 2), U-shaped (5.8%;  $n = 2$ , Figure 3), and Y-shaped (2.9%;  $n = 1$ , Figure 4) were the most common anatomical variants of the UF.

The volume of the UF ranged from 1270 to  $1440 \pm 170 \text{ mm}^3$ . The volume of the UF was larger in men ( $1410 \pm 150.7 \text{ mm}^3$ ) as compared to women ( $1325 \pm 133.2 \text{ mm}^3$ ) ( $p < 0.05$ ).

We compared the FA and MD values of the UF in terms of hemisphere, sex, and patient's age. Mean values of FA (MV of FA) were significantly larger on the left side ( $M = 0.596$ ) as compared to the right side ( $M = 0.344$ ) ( $p < 0.05$ ). The charts of distributions of FA in the left hemisphere are presented in Figure 5, whereas for the right hemisphere in Figure 6. MD values (distribution presented in the Figures 7 and 8) were significantly higher among patients older than 50 years of age on the left side ( $p = 0.034$ ). In addition, Figure 9 shows a correlation between MV of FA and age for both men and women.

As expected, the analysis of the UF revealed that fibers ended in the frontal and temporal lobes. In 73.5% of patients ( $n = 25$  patients), a greater number of fibers terminated in the inferior part of the inferior frontal gyrus (IFG); in 14.7% of patients ( $n = 5$ ), fibers terminated in the gyrus rectus (GyR); and in 11.7% ( $n = 4$  patients), fibers terminated in the middle temporal gyrus (MTG).

Factors influencing the variety of UF fibers distribution were analyzed. The total number of UF fibers was not correlated with the ending points of the bundle.

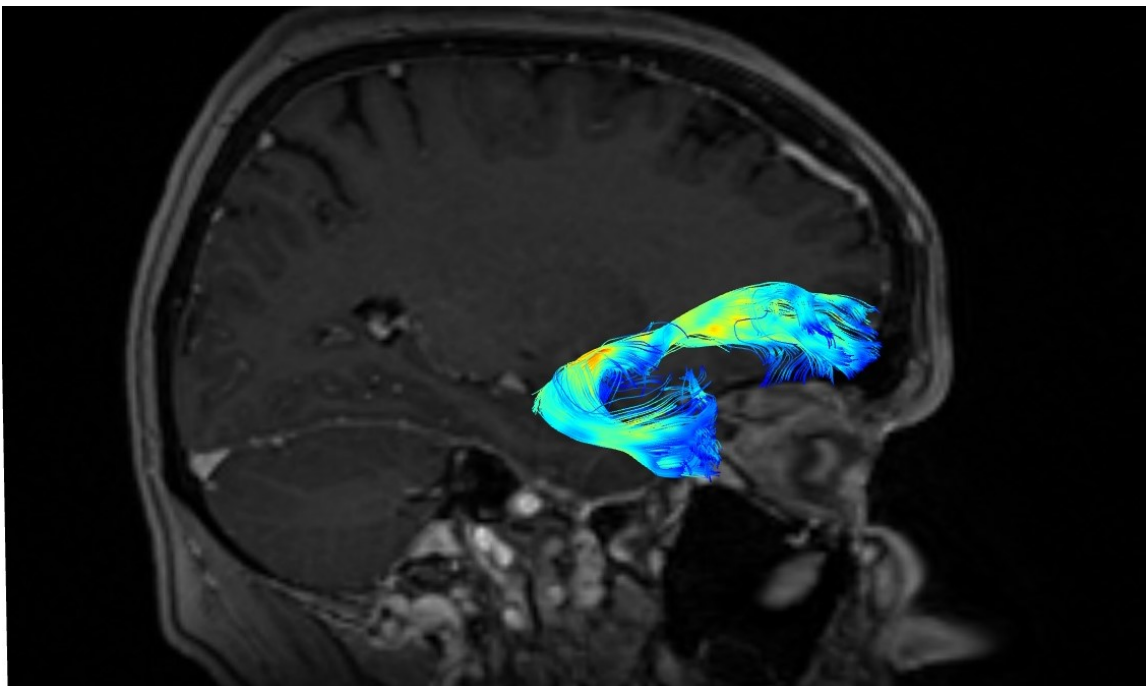


**Figure 2.** Hook-shape of the uncinate fasciculus (UF).



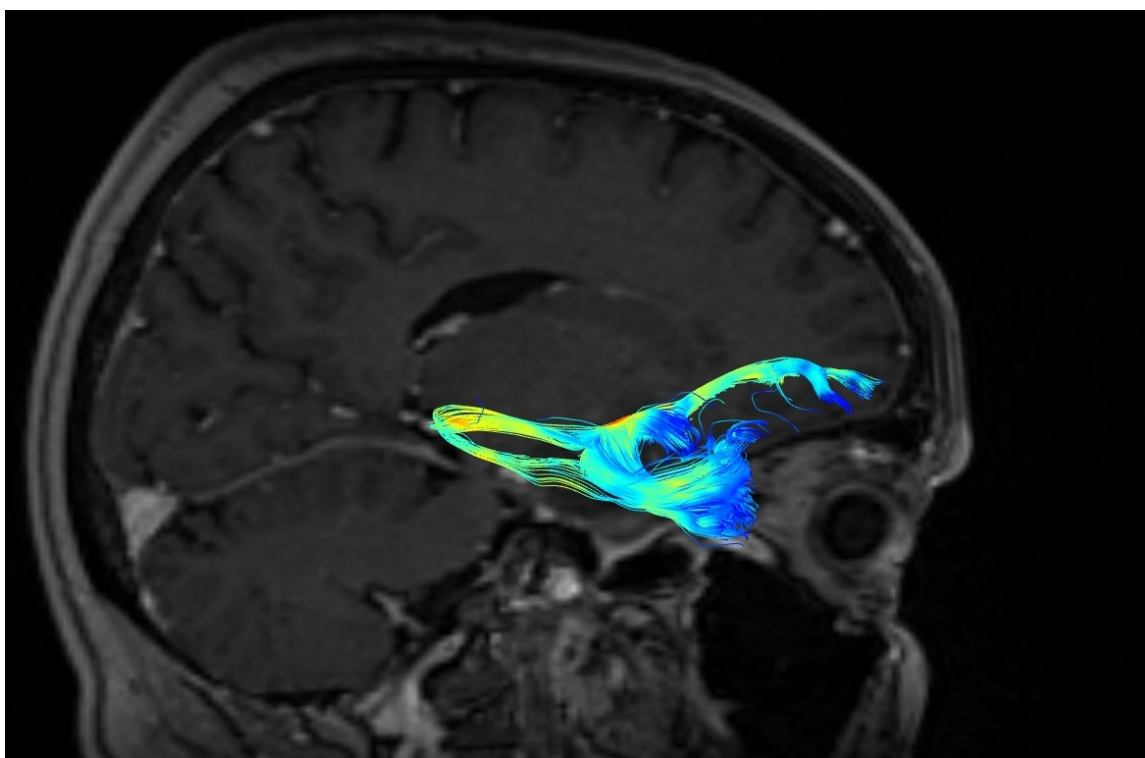


**Figure 3.** U-shape of the uncinate fasciculus (UF).

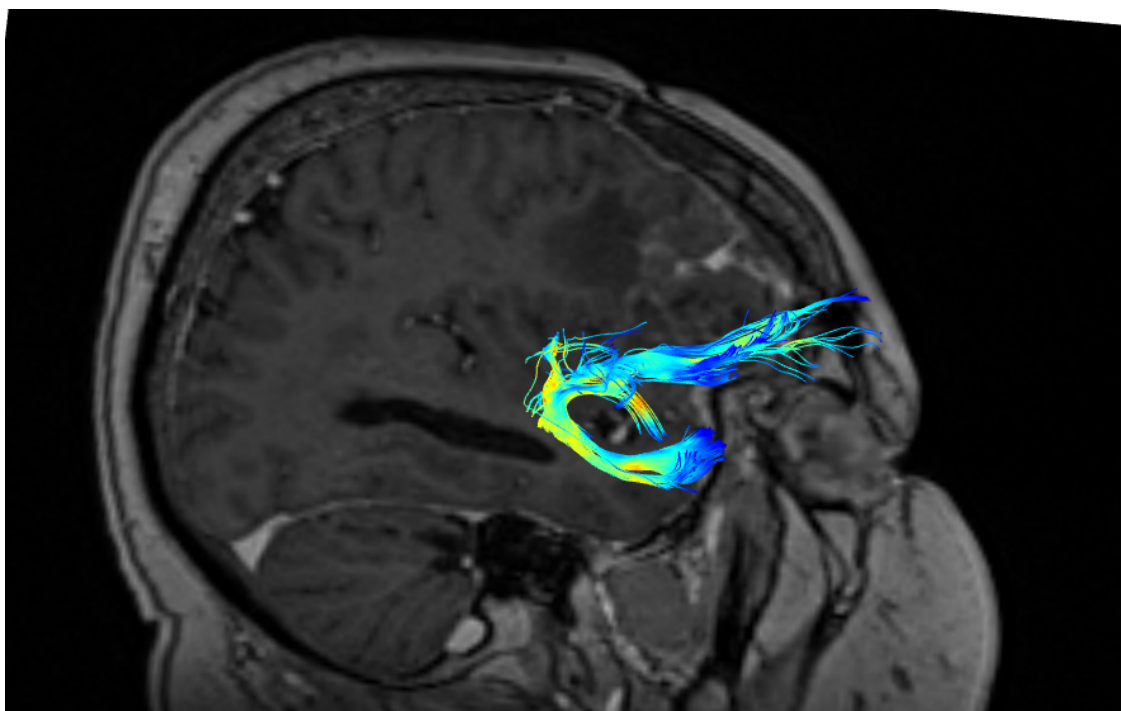


**Figure 4.** Y-shape of the uncinate fasciculus (UF).

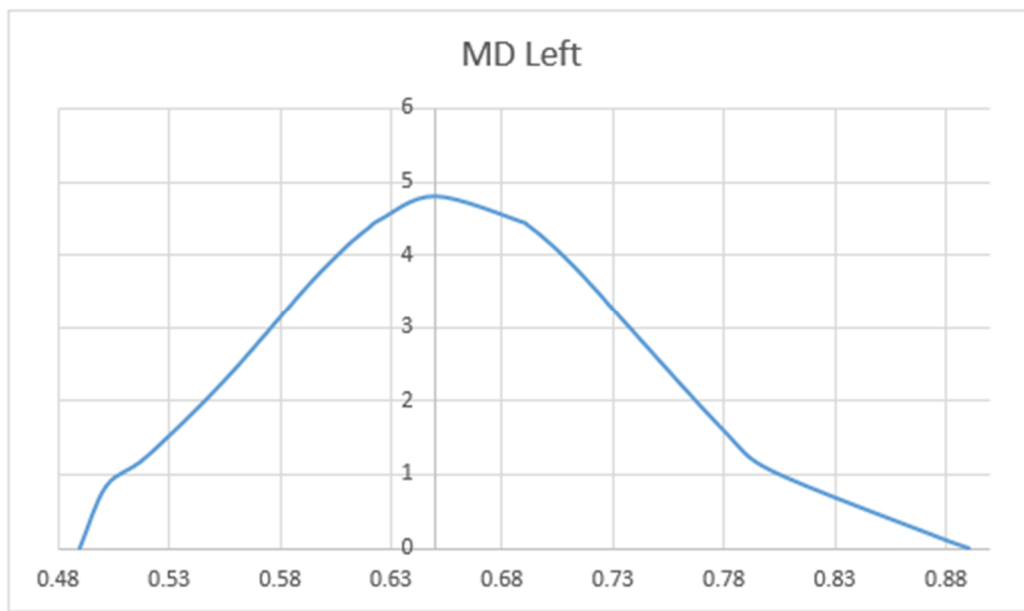


**Figure 5.** Distribution charts of mean diffusivity (MD) in the left hemisphere of the group of 34 patients aged 25–82.

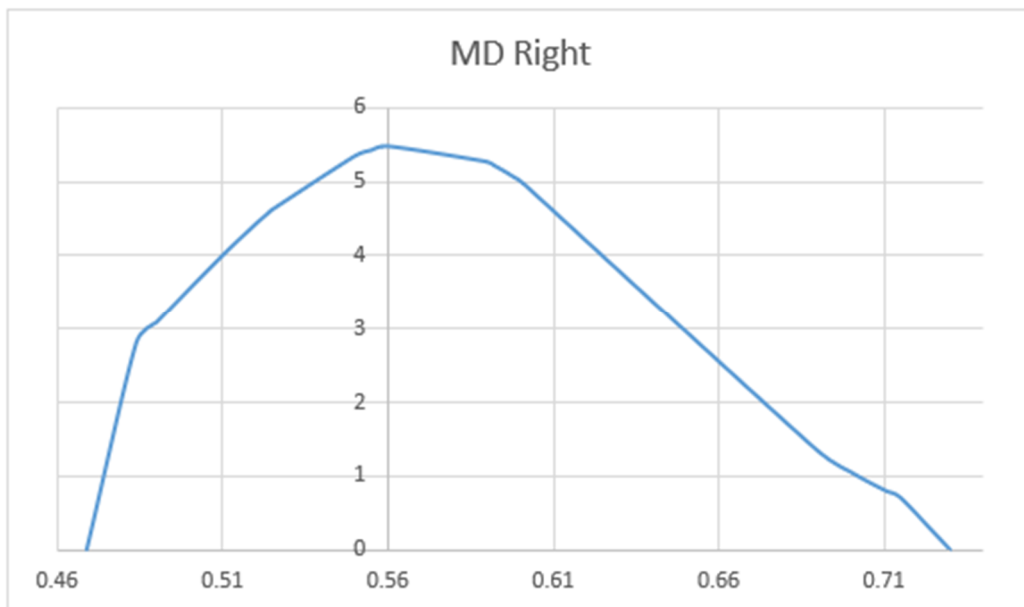


**Figure 6.** Distribution charts of MD in the right hemisphere of the group of 34 patients aged 25–82.

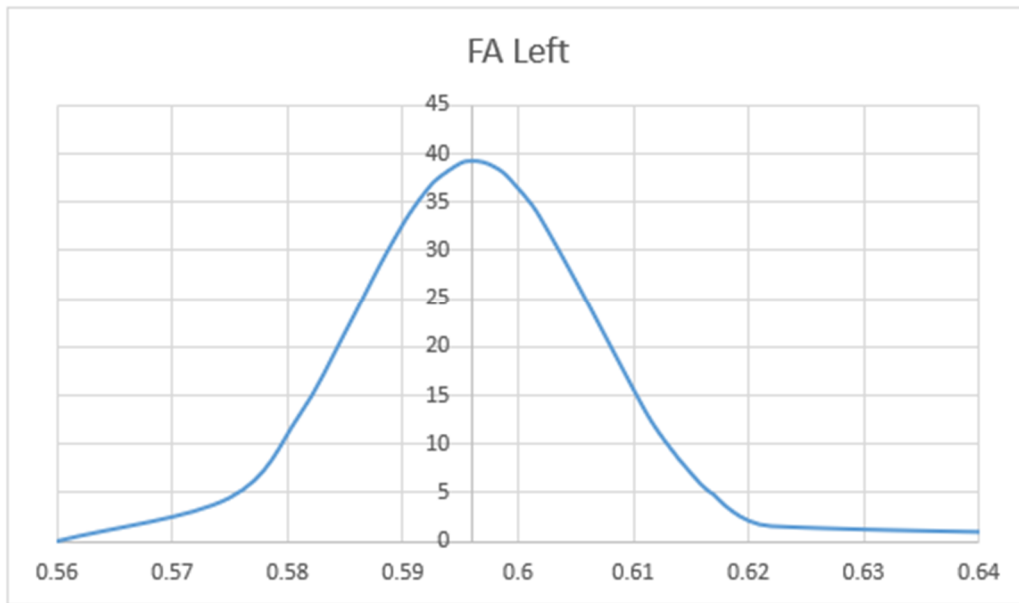


**Figure 7.** Distribution charts of fractional anisotropy (FA) in the left hemisphere of the group of 34 patients aged 25–82.

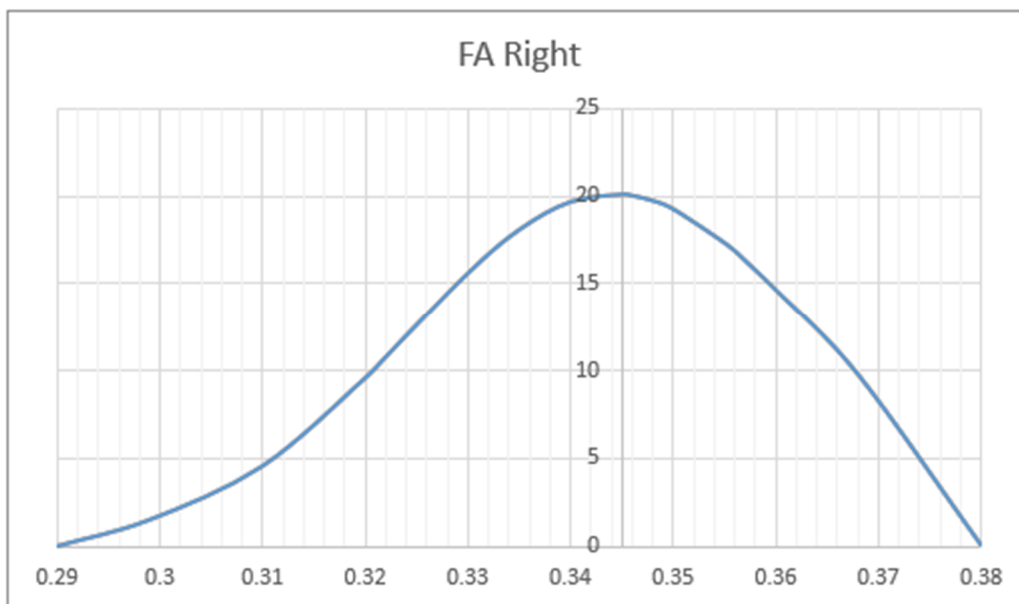


**Figure 8.** Distribution charts of FA in the right hemisphere of the group of 34 patients aged 25–82.

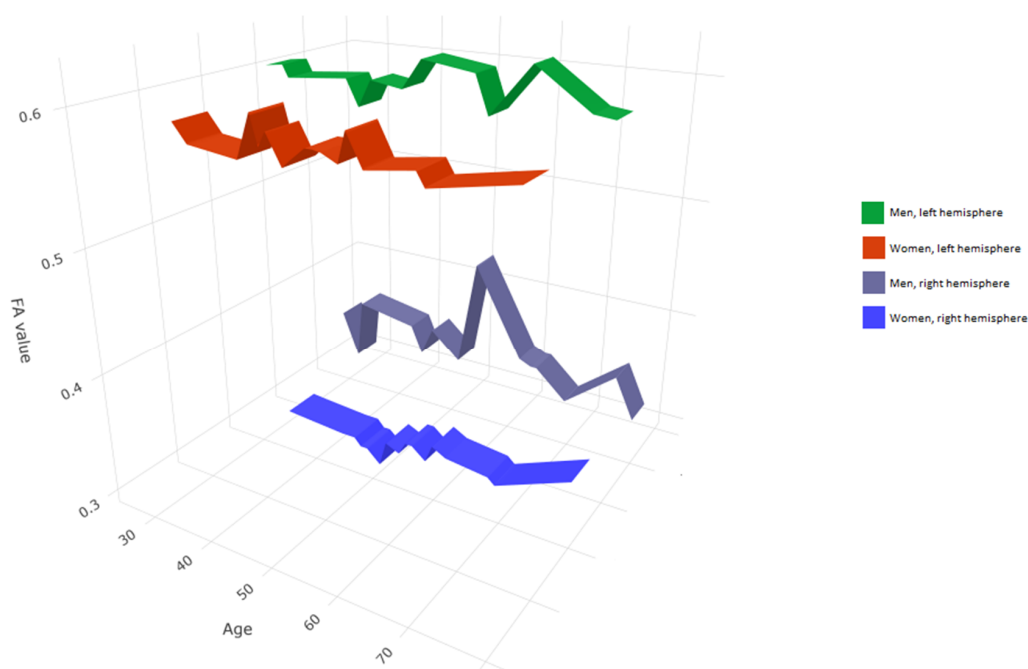


**Figure 9.** Correlation between FA value, sex, and age in the right and left hemisphere for the group of 34 patients aged 25–82.

#### 4. Discussion

DTI is a modern MRI method that allows for the identification of white matter microstructures [18–20]. DTI allows for in vivo spatial visualization of the projection of nerve fibers, and also allows for the determination of the number, lateralization, and direction of the course of the fibers. Several previous reports have demonstrated the multicomponent structure of the UF [4,21,22]. The advent of tractography allowed for one to accurately trace UF fibers. Yagmurlu et al. in their study found that three-dimensional (3D) anatomic organization of the brain tracts is also important in understanding the correct anatomy of the UF, including planning of neurosurgical operations [23].

The role of the UF is still a matter of discussion. Gaffan and Wilson showed that the UF is directly related to the limbic system, which plays an important role in emotion and memory [24].

In light of the current knowledge, the UF is involved in the creation of associative and episodic memory, and also participates in the implementation of socio-emotional and linguistic memory [25]. Changes within the UF are implicated in several mental diseases and disorders, including schizophrenia, anxiety disorders, and Alzheimer’s disease. The results of the DTI analysis may also be used in psychiatry. The use of DTI allows for the visualization of changes in the micro- and macro-structure of white matter in individuals with diagnosed mental disorders [1,3,26,27]. Changes in white matter are reflected in white matter biomarkers such as FA and MD. Several studies have linked lower FA values in the left UF with negative symptoms in schizophrenia, and this pattern was not seen in patients with non-deficit schizophrenia [25,26]. Bahatia et al. demonstrated a reduction in white matter integrity of the UF, which may translate to risk of mental disorders such as first-onset and chronic depression [9]. However, these studies are not equivocal because some researchers have reported an increase or no change in the FA values and indicate a small share of the bundle in the pathogenesis of schizophrenia [28,29]. On the other hand, research involving people with psychopathic personalities consistently demonstrates reduced FA values and significantly increased MD values in the right UF as compared to control subjects [30,31]. In addition, it has been shown that the orbital frontal cortex and temporal pole connection have a smaller volume and are thinner [1,3]. Changes in the UF have also been implicated in the pathogenesis of anxiety disorders. Interestingly, lesions in the UF may result in the occurrence of temporal lobe epilepsy. In addition, the UF is likely associated with behavioral

disorders. Indeed, prior studies link anatomical changes in the UF with antisocial behavior and the pathogenesis of Asperger's syndrome [32,33]. Similar studies of the UF have been conducted in a group of patients with autism spectrum disorder (ASD) [34]. That study demonstrated higher FA values in the left hemisphere in the ASD group as compared to the control group, which may suggest compensatory overgrowth in the ASD [34]. The same study also reported higher FA values in child patients as compared to adult patients [34].

One of the limitations of the study is that the morphology and anatomy of the UF was not correlated with psychological status or personality disorders among patients. Further research should include psychological tests and assessment of the infiltration of the UF by pathological lesions. As in other clinical trials, we showed UF volume asymmetry. Malykhin et al. reported that 71% of patients showed at least 10% asymmetry between the right and left UF, and the average difference between hemispheres was over 40% [35]. Similar conclusions were reached in a post mortem study by Higley et al. [29]. The results of the present study are consistent with these prior studies. The observed hemispheric asymmetry in UF volumes may result from a more consistent or less curly arrangement of the UF fibers in the left hemisphere as compared to the right hemisphere. The value of FA is influenced by many factors, most notably the structural integrity of the fibers, their packing density, degree of myelination, and fiber diameter [25,36,37]. The results of the present study demonstrate that long tracts have significantly higher FA values than anterior tracts. In a post mortem study of normal subjects and patients with schizophrenia, Higley et al. found that the UF is asymmetric in both sexes, such that the UF was 27% larger in the right hemisphere and contained 33% more fibers than in the left hemisphere [29].

Sex differences in the brain are commonly reported. Sexual dimorphism is also reported in studies that use DTI and show differences in the size of the parameters (i.e., volume, FA, and MD), which are most likely caused by differences in the microstructure of white matter between men and women [1,38]. It has been suggested that white matter differences result from different rates of pubertal development, during which there is also dramatic development of white matter in the brain. At the same time, it should be noted that the relative volume of the brain increases faster in boys than girls [39]. It is also worth noting the influence of other, obvious, gender-specific features [38]. For example, men may have a proportionally larger skull and thus, a larger proportion of white matter in the brain as compared to women. On the other hand, the percentage of gray matter in the brain has shown to be higher among women than men [40,41].

During adolescence, FA values and white matter volume gradually increase, which is likely due, in part, to the degree of myelination of nerve fibers [38]. At the same time, after reaching a peak between 28 and 35 years of age, the values of these parameters become inversely proportional to age and therefore, are systematically reduced. This is an expression of brain aging manifested as a loss of myelinated fibers and myelin itself [1,38,39].

Based on the analysis of the collected data, we showed a significant difference in FA values for the left side compared to the right side of the UF (0.596 vs. 0.344). Due to the fact that the group of patients differed both in age and gender, the question arises as to the reason for the difference in FA. It was assumed that a higher FA value reflects a more directed movement of water molecules in nerve fibers, as well as greater coherence of themselves [42]. The asymmetry in the distribution of FA values reflects the difference in the structure and functioning of the UF in both hemispheres of the brain, as well as their different development [42]. The higher value of FA on the left side, compared to the right side, may indicate that it is composed of a greater number of fibers included in the bundle or that their greater density or the arrangement of the fibers is less winding [36,43]. The FA parameter depends on the microstructural properties of nerve fibers; it may indirectly reflect the speed of conduction, thus differences in the values of this parameter may indicate different functioning of the cerebral hemispheres. The obtained results, taking into account the different age and sex structure of the participants, may indicate the lateralization of brain functions [43].

It should be noted that the available literature data are inconsistent with regard to the asymmetric distribution of FA values for the UF. The likely reasons for the discrepancies between the research results are the differences in their methodology, as well as the heterogeneity of the population. Part of the research work showed higher FA values for the UF on the left side [42–46]. However, there are also data in the literature showing rightward FA asymmetry [47] or no asymmetry in FA values at all [48,49]. A 2011 study by Kitamura et al. showed that the FA value for the right (but not left) UF is significantly higher in men as compared to women. This result suggests the presence of sexual dimorphism in the frontotemporal area [41]. A 2015 study by Alm et al. demonstrated higher MD values in both the right and left UF in women as compared to men [50].

In addition, it is important to note that FA and MD values are influenced by the mutual relationship of age and sex, and future data should be collected based on the correlation of these variables. Given the known influence of age and sex, data should be collected on the same MRI scanner and analyzed using a similar tracking algorithm.

Another limitation of the present study was that the UF was measured in patients following a traumatic brain injury (TBI). We found that FA values were higher in the left hemisphere in men as compared to women, and there were no sex differences in MD. Kurki also pointed out that the fibers located in the central part of the UF are characterized by high FA values, which decrease towards the peripherally located fibers [51].

The value of FA is conditioned by many factors. The anatomical aspects of the brain have a significant influence on the parameters of FA tractography. In the work of Hsu et al. the relationship between age, gender, brain anatomy and FA values for 145 adults was analyzed. The results of this analysis proved that the MV of FA is inversely correlated with age. However, the anatomical points where FA was examined were a very important parameter. Hsu et al. while analyzing the anterior part of the corpus callosum, internal capsule and posterior paraventricular region, shown that these anatomical points correlate most with the age-related FA decrease. However, FA values in the temporal and occipital lobes were not correlated with age at all. In the same study, differences between the anatomy of the brain and the gender of patients undergoing FA were also found. Men had higher FA values than women, especially in the right deep temporal regions [52].

In our study, we did not analyze individual anatomical regions in the course of the UF, but subsequent analyses should be carried out based on the exact anatomy of the bundle, taking into account the age and sex of the patients. It should be noted that the accuracy of imaging using DTI depends on the homogeneity of the magnetic field gradients, which translate into the value of the b-matrix. System errors, including equipment-dependent restrictions and scanner or gradient coils, are associated with the spatial heterogeneity of diffusion gradients. [53,54]. The spatial heterogeneity of diffusion gradients, in turn, causes vector distortion and ultimately, falsification of the resulting image. Thus, it became necessary to develop a model that would eliminate the problem as much as possible. The first experimental mathematical scheme to retrospectively correct the effects of spatial gradient field distortions on diffusion-dependent imaging was developed by Bammer et al. [54]. However, to optimally eliminate and correct measurements of the diffusion tensor caused by heterogeneity in the magnetic field gradients, the calibration technique BSD-DTI (b-matrix spatial Distribution DTI technique) was developed and introduced, which significantly improved the fiber tracking procedure. The technique was first introduced in the literature in 2015 by Krzyżak et al. [55]. A year later, Kłodowski et al. conducted a clinical verification that demonstrated the correctness and clinical usefulness of BSD-DTI [56]. Thanks to the introduction of BSD-DTI, it is possible to eliminate conversion errors and account for the spatial distribution of the b-matrix [55,57].

BSD-DTI increases the representativeness and replicability of the obtained results, which allows for comparisons between the obtained images. The BSD-DTI technique allows the correction of not only the magnitude, but also the direction of the diffusion gradient, which is crucial for accurate fiber tracking [53,55].

Fiber tracking has become a valuable method of qualitatively describing many nerve pathways in the brain of a living organism that remain inaccessible to conventional imaging. However, the quantitative assessment of visualized connections has a high risk of false-positive results. Due to the complexity of nerve fibers in the human brain, fiber tracking is undoubtedly subject to a high risk of errors that can arise from the spatial arrangement of the fibers. Crossing, branching, or narrowing of fibers are examples of configurations that can result in identical voxel signals. This is due to the diversity of the spatial arrangement of the white matter fibers, including, for e.g., their intersection. This diversity in fiber arrangement can lead to false lengths of reconstructed fiber tracts [58]. To optimize imaging fidelity, higher-order computational models aimed at precisely eliminating false positive nerve pathways should be used. Despite the introduction of software that creates more and more accurate neuro-anatomical models, in the case of practical use of fiber tracking, the limitations of the method should still be considered [59,60].

In tractography, determining the number of fibers is still a big challenge. Metrics “number of fibers” and “spatial extent of pathways” in direct viewing suggests that the result obtained determines the actual number of white matter fibers identified by axon projections.

These terms are more commonly used in the literature; however, these parameters are not a real numerical representation of the number of fibers and the obtained measurements are associated with a high risk of obtaining a result with an error.

According to data from Jones et al., the reconstruction is influenced by variables such as fiber length, as well as their branching, curvature, and the degree of myelination. Their influence may cause the reconstructed number of fibers to differ from the actual state. Therefore, it should be added that in order to maximize the reliability of quantitative assessments, one should strive to develop procedures correcting the influence of variables on the identification and reconstruction of the actual number of nerve fibers. The authors suggest that when interpreting the obtained results, the term “improvement counter” should be used [58,61]. Tractography has proven to be a useful tool for identifying cortical connections. At the same time, on the basis of measurements obtained by means of probabilistic tractography, it became possible to develop maps of cortical tract length (CTL). This will allow the assessment of which fibers are involved in the projection of distant or local connections. Analysis by Bajada et al. from 2018 provided information on the variability of the distribution of projections of different lengths in the cerebral cortex, as well as the correlation between fiber length and structural features (myelination, cortex thickness) and the relationship between the degree of network complexity at rest and the fiber length profile [62].

## 5. Conclusions

This study presents the anatomy and morphology of the UF. The patient group selected in the study and the criteria used for the research suggest that, under such parameters, the most common UF shape is a hook-shape. Under these same assumptions, the MV of FA was shown to be higher in the left hemisphere as compared to the right hemisphere. The present study demonstrated that morphological characteristics of the UF are associated with sex and are characterized by hemispheric dominance. These findings confirm the results of previous studies. The shape of the UF was not correlated with sex differences nor laterality of the brain hemisphere. Future research should examine the potential correlation between UF anatomy and patient’s psychological state. Future research should also test for correlations among UF volume and total brain volume in both sexes.

**Author Contributions:** Conceptualization, S.K. and P.S.; Data curation, S.K., P.S. and M.J.; Formal analysis, S.K. and M.J.; Investigation, S.K., P.S., M.R., R.J. and M.J.; Methodology, S.K., P.S., M.D. and M.J.; Project administration, S.K. and P.S.; Resources, S.K., P.S. and M.D.; Software, S.K., M.D. and M.J.; Supervision, S.K. and P.S.; Validation, S.K., P.S., M.R. and R.J.; Visualization, S.K. and M.D.; Writing—Original draft, S.K. and P.S.; Writing—Review & editing, S.K. and P.S. All authors have read and agreed to the published version of the manuscript.

**Funding:** This research received no external funding.

**Conflicts of Interest:** The authors declare no conflict of interest.

## References

- Olson, I.R.; Von Der Heide, R.J.; Alm, K.H.; Vyas, G. Development of the uncinate fasciculus: Implications for theory and developmental disorders. *Dev. Cogn. Neurosci.* **2015**, *14*, 50–61. [[CrossRef](#)] [[PubMed](#)]
- Donner, F. Untersuchungen über den Bau des grossen Gehirn im Menschen. *DMW Dtsch. Med. Wochenschr.* **1878**, *4*, 471–473.
- Von Der Heide, R.J.; Skipper, L.M.; Klobusicky, E.; Olson, I.R. Dissecting the uncinate fasciculus: Disorders, controversies and a hypothesis. *Brain* **2013**, *136*, 1692–1707. [[CrossRef](#)] [[PubMed](#)]
- Hau, J.; Sarubbo, S.; Houde, J.C.; Corsini, F.; Girard, G.; Deledalle, C.; Crivello, F.; Zago, L.; Mellet, E.; Jobard, G.; et al. Revisiting the human uncinate fasciculus, its subcomponents and asymmetries with stem-based tractography and microdissection validation. *Brain Struct. Funct.* **2017**, *222*, 1645–1662. [[CrossRef](#)] [[PubMed](#)]
- Wycoco, V.; Shroff, M.; Sudhakar, S.; Lee, W. White Matter Anatomy. What the Radiologist Needs to Know. *Neuroimaging Clin. N. Am.* **2013**, *23*, 197–216. [[CrossRef](#)]
- Fujiwara, S.; Sasaki, M.; Kanbara, Y.; Inoue, T.; Hirooka, R.; Ogawa, A. Feasibility of 1.6-mm isotropic voxel diffusion tensor tractography in depicting limbic fibers. *Neuroradiology* **2008**, *50*, 131–136. [[CrossRef](#)]
- Heimer, L.; Van Hoesen, G.; Trimble, M. *The Anatomy of Neuropsychiatry: The New Anatomy of the Basal Forebrain and and Its Implication for the Neuropsychiatric Illness*, 1st ed.; Academic Press: Cambridge, MA, USA, 2008; ISBN 9780123742391.
- Krestel, H.; Annoni, J.M.; Jagella, C. White matter in aphasia: A historical review of the Dejerines' studies. *Brain Lang.* **2013**, *127*, 526–532. [[CrossRef](#)]
- Bhatia, K.; Henderson, L.; Yim, M.; Hsu, E.; Dhaliwal, R. Diffusion Tensor Imaging Investigation of Uncinate Fasciculus Anatomy in Healthy Controls: Description of a Subgenual Stem. *Neuropsychobiology* **2018**, *75*, 132–140. [[CrossRef](#)]
- Seitz, J.; Zuo, J.X.; Lyall, A.E.; Makris, N.; Kikinis, Z.; Bouix, S.; Pasternak, O.; Fredman, E.; Duskin, J.; Goldstein, J.M.; et al. Tractography analysis of 5 white matter bundles and their clinical and cognitive correlates in early-course schizophrenia. *Schizophr. Bull.* **2016**, *42*, 762–771. [[CrossRef](#)]
- Li, Z.; Peck, K.K.; Brennan, N.P.; Jenabi, M.; Hsu, M.; Zhang, Z.; Holodny, A.I.; Young, R.J. Diffusion tensor tractography of the arcuate fasciculus in patients with brain tumors: Comparison between deterministic and probabilistic models. *J. Biomed. Sci. Eng.* **2013**, *6*, 192–200. [[CrossRef](#)]
- Ebeling, U.; Cramon, D.V. Topography of the uncinate fascicle and adjacent temporal fiber tracts. *Acta Neurochir.* **1992**, *115*, 143–148. [[CrossRef](#)] [[PubMed](#)]
- Yağmurlu, K.; Oguz, K.K.; Shaffrey, M.E.; Mut, M. Orbitofrontal extensions of the insular glioma based on subdivision of the uncinate fasciculus. *J. Clin. Neurosci.* **2020**, *78*, 376–386. [[CrossRef](#)] [[PubMed](#)]
- Ni, H.; Kavcic, V.; Zhu, T.; Ekholm, S.; Zhong, J. Effects of number of diffusion gradient directions on derived diffusion tensor imaging indices in human brain. *Am. J. Neuroradiol.* **2006**, *27*, 1776–1781. [[PubMed](#)]
- Jones, D.K. The Effect of Gradient Sampling Schemes on Measures Derived from Diffusion Tensor MRI: A Monte Carlo Study. *Magn. Reson. Med.* **2004**, *51*, 807–815. [[CrossRef](#)] [[PubMed](#)]
- Lebel, C.; Benner, T.; Beaulieu, C. Six is enough? Comparison of diffusion parameters measured using six or more diffusion-encoding gradient directions with deterministic tractography. *Magn. Reson. Med.* **2012**, *68*, 474–483. [[CrossRef](#)] [[PubMed](#)]
- Yoldemir, B.; Acar, B.; Firat, Z.; Kiliçkesmez, Ö. SMT: A reliability based interactive DTI tractography algorithm. *IEEE Trans. Med. Imaging* **2012**, *31*, 1929–1940. [[CrossRef](#)]
- Larroza, A.; Moratal, D.; D'ocón Alcañiz, V.; Arana, E. Tractography of the uncinate fasciculus and the posterior cingulate fasciculus in patients with mild cognitive impairment and Alzheimer disease. *Neurologia (Engl. Ed.)* **2014**, *29*, 11–20. [[CrossRef](#)]
- Sato, T.; Maruyama, N.; Hoshida, T.; Minato, K. Correlation between uncinate fasciculus and memory tasks in healthy individual using diffusion tensor tractography. In Proceedings of the 2012 Annual International Conference of the IEEE Engineering in Medicine and Biology Society, San Diego, CA, USA, 28 August–1 September 2012; pp. 424–427. [[CrossRef](#)]
- Witwer, B.P.; Moftakhar, R.; Hasan, K.M.; Deshmukh, P.; Haughton, V.; Field, A.; Arfanakis, K.; Noyes, J.; Moritz, C.H.; Meyerand, M.E.; et al. Diffusion-tensor imaging of white matter tracts in patients with cerebral neoplasm. *J. Neurosurg.* **2002**, *97*, 568–575. [[CrossRef](#)]



21. Oishi, K.; Faria, A.V.; Hsu, J.; Tippett, D.; Mori, S.; Hillis, A.E. Critical Role of the Right Uncinate Fasciculus in Emotional Empathy. *Ann. Neurol.* **2008**, *23*, 1–7. [[CrossRef](#)]
22. Steffens, D.C.; Taylor, W.D.; Denny, K.L.; Bergman, S.R.; Wang, L. Structural integrity of the uncinate fasciculus and resting state functional connectivity of the ventral prefrontal cortex in late life depression. *PLoS ONE* **2011**, *6*, e22697. [[CrossRef](#)]
23. Yagmurlu, K.; Vlasak, A.L.; Rhoton, A.L., Jr. Three-dimensional topographic fiber tract anatomy of the cerebrum. *Oper. Neurosurg.* **2015**, *11*, 274–305. [[CrossRef](#)] [[PubMed](#)]
24. Gaffan, D.; Wilson, C.R.E. Medial temporal and prefrontal function: Recent behavioural disconnection studies in the macaque monkey. *Cortex* **2008**, *44*, 928–935. [[CrossRef](#)] [[PubMed](#)]
25. Kitis, O.; Ozalay, O.; Zengin, E.B.; Haznedaroglu, D.; Eker, M.C.; Yalvac, D.; Oguz, K.; Coburn, K.; Gonul, A.S. Reduced left uncinate fasciculus fractional anisotropy in deficit schizophrenia but not in non-deficit schizophrenia. *Psychiatry Clin. Neurosci.* **2012**, *66*, 34–43. [[CrossRef](#)] [[PubMed](#)]
26. Baker, C.M.; Burks, J.D.; Briggs, R.G.; Smitherman, A.D.; Glenn, C.A.; Conner, A.K.; Wu, D.H.; Sughrue, M.E. The crossed frontal aslant tract: A possible pathway involved in the recovery of supplementary motor area syndrome. *Brain Behav.* **2018**, *8*, e00926. [[CrossRef](#)]
27. Mahon, K.; Burdick, K.E.; Szeszko, P.R. A role for white matter abnormalities in the pathophysiology of bipolar disorder. *Neurosci. Biobehav. Rev.* **2010**, *34*, 533–554. [[CrossRef](#)]
28. Dalamagkas, K.; Tsintou, M.; Rathi, Y.; O'Donnell, L.J.; Pasternak, O.; Gong, X.; Zhu, A.; Savadjiev, P.; Papadimitriou, G.M.; Kubicki, M.; et al. Individual variations of the human corticospinal tract and its hand-related motor fibers using diffusion MRI tractography. *Brain Imaging Behav.* **2019**, 1–40. [[CrossRef](#)]
29. Highley, J.R. Asymmetry of the Uncinate Fasciculus: A Post-mortem Study of Normal Subjects and Patients with Schizophrenia. *Cereb. Cortex* **2002**, *12*, 1218–1224. [[CrossRef](#)]
30. Motzkin, J.C.; Newman, J.P.; Kiehl, K.A.; Koenigs, M. Reduced prefrontal connectivity in psychopathy. *J. Neurosci.* **2011**, *31*, 17348–17357. [[CrossRef](#)]
31. Sundram, F.; Deeley, Q.; Sarkar, S.; Daly, E.; Latham, R.; Craig, M.; Raczek, M.; Fahy, T.; Picchioni, M.; Barker, G.J.; et al. White matter microstructural abnormalities in the frontal lobe of adults with antisocial personality disorder. *Cortex* **2012**, *48*, 216–229. [[CrossRef](#)]
32. Catani, M.; Dell'Acqua, F.; Bizzi, A.; Forkel, S.J.; Williams, S.C.; Simmons, A.; Murphy, D.G.; de Schotten, M.T. Beyond cortical localization in clinico-anatomical correlation. *Cortex* **2012**, *48*, 1262–1287. [[CrossRef](#)]
33. Pugliese, L.; Catani, M.; Ameis, S.; Dell'Acqua, F.; de Schotten, M.T.; Murphy, C.; Robertson, D.; Deeley, Q.; Daly, E.; Murphy, D.G.M. The anatomy of extended limbic pathways in Asperger syndrome: A preliminary diffusion tensor imaging tractography study. *Neuroimage* **2009**, *47*, 427–434. [[CrossRef](#)] [[PubMed](#)]
34. Li, Y.; Zhou, Z.; Chang, C.; Qian, L.; Li, C.; Xiao, T.; Xiao, X.; Chu, K.; Fang, H.; Ke, X. Anomalies in uncinate fasciculus development and social defects in preschoolers with autism spectrum disorder. *BMC Psychiatry* **2019**, *19*, 399. [[CrossRef](#)]
35. Malykhin, N.; Concha, L.; Seres, P.; Beaulieu, C.; Coupland, N.J. Diffusion tensor imaging tractography and reliability analysis for limbic and paralimbic white matter tracts. *Psychiatry Res. Neuroimaging* **2008**, *164*, 132–142. [[CrossRef](#)] [[PubMed](#)]
36. Beaulieu, C. The basis of anisotropic water diffusion in the nervous system—A technical review. *NMR Biomed.* **2002**, *15*, 435–455. [[CrossRef](#)] [[PubMed](#)]
37. Park, C.H.; Kou, N.; Boudrias, M.H.; Playford, E.D.; Ward, N.S. Assessing a standardised approach to measuring corticospinal integrity after stroke with DTI. *NeuroImage Clin.* **2013**, *2*, 521–533. [[CrossRef](#)] [[PubMed](#)]
38. Fjell, A.M.; Westlye, L.T.; Greve, D.N.; Fischl, B.; Benner, T.; Van Der Kouwe, A.J.W.; Salat, D.; Bjørnerud, A.; Due-Tønnessen, P.; Walhovd, K.B. The relationship between diffusion tensor imaging and volumetry as measures of white matter properties. *Neuroimage* **2008**, *42*, 1654–1668. [[CrossRef](#)] [[PubMed](#)]
39. Simmonds, D.J.; Hallquist, M.N.; Asato, M.; Luna, B. Developmental stages and sex differences of white matter and behavioral development through adolescence: A longitudinal diffusion tensor imaging (DTI) study. *Neuroimage* **2014**, *92*, 356–368. [[CrossRef](#)]
40. Ingallhalikar, M.; Smith, A.; Parker, D.; Satterthwaite, T.D.; Elliott, M.A.; Ruparel, K.; Hakonarson, H.; Gur, R.E.; Gur, R.C.; Verma, R. Sex differences in the structural connectome of the human brain. *Proc. Natl. Acad. Sci. USA* **2014**, *111*, 823–828. [[CrossRef](#)]

41. Kitamura, S.; Morikawa, M.; Kiuchi, K.; Taoka, T.; Fukusumi, M.; Kichikawa, K.; Kishimoto, T. Asymmetry, sex differences and age-related changes in the white matter in the healthy elderly: A tract-based study. *BMC Res. Notes* **2011**, *4*, 378. [[CrossRef](#)]
42. Kubicki, M.; Westin, C.; Maier, S.E.; Frumin, M.; Nestor, P.G.; Ph, D.; Salisbury, D.F.; Ph, D.; Kikinis, R.; Jolesz, F.A.; et al. Uncinate Fasciculus Findings in Schizophrenia: A Magnetic Resonance Diffusion Tensor Imaging Study. *Am. J. Psychiatry* **2002**, *5*, 813–820. [[CrossRef](#)]
43. Hasan, K.M.; Iftikhar, A.; Kamali, A.; Kramer, L.A.; Ashtari, M.; Cirino, P.T.; Papanicolaou, A.C.; Fletcher, J.M.; Ewing-cobbs, L. Development and aging of the healthy human brain uncinate fasciculus across the lifespan using diffusion tensor tractography. *Brain Res.* **2009**, *1276*, 67–76. [[CrossRef](#)] [[PubMed](#)]
44. Rocca, M.A.; Valsasina, P.; Ceccarelli, A.; Absinta, M.; Ghezzi, A.; Riccitelli, G.; Pagani, E.; Falini, A.; Comi, G.; Scotti, G.; et al. Structural and functional MRI correlates of stroop control in benign MS. *Hum. Brain Mapp.* **2009**, *30*, 276–290. [[CrossRef](#)] [[PubMed](#)]
45. Danielian, L.E.; Iwata, N.K.; Thomasson, D.M.; Floeter, M.K. Reliability of Fiber Tracking Measurements in Diffusion Tensor Imaging for Longitudinal Study. *NIH Public Access* **2011**, *49*, 1572–1580. [[CrossRef](#)] [[PubMed](#)]
46. Eluvathingal, T.J.; Hasan, K.M.; Kramer, L.; Fletcher, J.M.; Ewing-Cobbs, L. Quantitative diffusion tensor tractography of association and projection fibers in normally developing children and adolescents. *Cereb. Cortex* **2007**, *17*, 2760–2768. [[CrossRef](#)]
47. Rodrigo, S.; Oppenheim, C.; Chassoux, F.; Golestani, N. Uncinate fasciculus fiber tracking in mesial temporal lobe epilepsy. Initial findings. *Eur. Radiol.* **2007**, *17*, 1663–1668. [[CrossRef](#)]
48. Park, H.J.; Westin, C.F.; Kubicki, M.; Maier, S.E.; Niznikiewicz, M.; Baer, A.; Frumin, M.; Kikinis, R.; Jolesz, F.A.; McCarley, R.W.; et al. White matter hemisphere asymmetries in healthy subjects and in schizophrenia: A diffusion tensor MRI study. *Neuroimage* **2004**, *23*, 213–223. [[CrossRef](#)]
49. Yasmin, H.; Aoki, S.; Abe, O. Tract-specific analysis of white matter pathways in healthy subjects: A pilot study using diffusion tensor MRI. *Neuroradiology* **2009**, 831–840. [[CrossRef](#)]
50. Alm, K.H.; Rolheiser, T.; Mohamed, F.B.; Olson, I.R. Fronto-temporal white matter connectivity predicts reversal learning errors. *Front. Hum. Neurosci.* **2015**, *9*, 343. [[CrossRef](#)]
51. Kurki, T.J.I.; Laalo, J.P.; Oksaranta, O.M. Diffusion tensor tractography of the uncinate fasciculus: Pitfalls in quantitative analysis due to traumatic volume changes. *J. Magn. Reson. Imaging* **2013**, *38*, 46–53. [[CrossRef](#)]
52. Hsu, J.; Leemans, A.; Bai, C.; Lee, C.; Tsai, Y.; Chiu, H.; Chen, W. Gender differences and age-related white matter changes of the human brain: A diffusion tensor imaging study. *Neuroimage* **2008**, *39*, 566–577. [[CrossRef](#)]
53. Borkowski, K.; Krzyżak, A.T. Analysis and correction of errors in DTI-based tractography due to diffusion gradient inhomogeneity. *J. Magn. Reson.* **2018**, *296*, 5–11. [[CrossRef](#)] [[PubMed](#)]
54. Bammer, R.; Markl, M.; Barnett, A.; Acar, B.; Alley, M.T.; Pelc, N.J.; Glover, G.H.; Moseley, M.E. Analysis and generalized correction of the effect of spatial gradient field distortions in diffusion-weighted imaging. *Magn. Reson. Med.* **2003**, *50*, 560–569. [[CrossRef](#)] [[PubMed](#)]
55. Krzyżak, A.T.; Olejniczak, Z. Improving the accuracy of PGSE DTI experiments using the spatial distribution of b matrix. *Magn. Reson. Imaging* **2015**, *33*, 286–295. [[CrossRef](#)] [[PubMed](#)]
56. Kłodowski, K.; Krzyżak, A.T. Innovative anisotropic phantoms for calibration of diffusion tensor imaging sequences. *Magn. Reson. Imaging* **2016**, *34*, 404–409. [[CrossRef](#)] [[PubMed](#)]
57. Borkowski, K.; Krzyżak, A.T. Assessment of the systematic errors caused by diffusion gradient inhomogeneity in DTI-computer simulations. *NMR Biomed.* **2019**, *32*, 1–12. [[CrossRef](#)] [[PubMed](#)]
58. Jones, D.K.; Knösche, T.R.; Turner, R. White matter integrity, fiber count, and other fallacies: The do's and don'ts of diffusion MRI. *Neuroimage* **2013**, *73*, 239–254. [[CrossRef](#)]
59. Jeurissen, B.; Descoteaux, M.; Mori, S.; Leemans, A. Diffusion MRI fiber tractography of the brain. *NMR Biomed.* **2019**, *32*, 1–22. [[CrossRef](#)]
60. Maier-Hein, K.H.; Neher, P.F.; Houde, J.C.; Côté, M.A.; Garyfallidis, E.; Zhong, J.; Chamberland, M.; Yeh, F.C.; Lin, Y.C.; Ji, Q.; et al. The challenge of mapping the human connectome based on diffusion tractography. *Nat. Commun.* **2017**, *8*, 1349. [[CrossRef](#)]

61. Jones, D.K. Challenges and limitations of quantifying brain connectivity in vivo with diffusion MRI. *Imaging Med.* **2010**, *2*, 341–355. [[CrossRef](#)]
62. Bajada, C.J.; Schreiber, J.; Caspers, S. Fiber length profiling: A novel approach to structural brain organization. *Neuroimage* **2019**, *186*, 164–173. [[CrossRef](#)]



© 2020 by the authors. Licensee MDPI, Basel, Switzerland. This article is an open access article distributed under the terms and conditions of the Creative Commons Attribution (CC BY) license (<http://creativecommons.org/licenses/by/4.0/>).

### **5.3 Omówienie pracy “Tractography Alterations in the Arcuate and Uncinate Fasciculi in Post-Stroke Aphasia”**

W publikacji “Tractography Alterations in the Arcuate and Uncinate Fasciculi in Post-Stroke Aphasia” opublikowanej w Brain Sciences przedstawiono zmiany w zakresie pęczka haczykowatego i łukowatego u pacjenta po przebytych udarze niedokrwiennym z afazją mieszaną.

Celem pracy było zaprezentowanie różnic w anatomii wybranych dróg nerwowych u pacjenta przy przyjęciu do szpitala oraz w 3 miesiącu po udarze niedokrwiennym mózgu.

W opublikowanym artykule przedstawiono przypadek 41-letniego pacjenta przyjętego do Kliniki Neurochirurgii i Neurologii z powodu narastających zaburzeń o typie afazji mieszanej. U chorego wykonano badanie TK głowy oraz MR głowy z opcją DTI uwidaczniające ognisko niedokrwienne w obrębie lewego płąta skroniowego. U chorego zastosowano trombektomię mechaniczną, terapię przezskórną stymulację magnetyczną (tDCS) oraz wczesną rehabilitację ruchową i logopedyczną.

Na podstawie badania MR głowy z DTI przy przyjęciu oraz po 3 miesiącach po udarze niedokrwiennym wykreślono pęczek haczykowaty i łukowaty obustronnie w oparciu o program DST studio wykorzystując algorytm deterministyczny.

Po 3 miesiącach stwierdzono zwiększenie wartości frakcjonowanej anizotropii w zakresie obu badanych dróg nerwowych po stronie lewej. Ponadto uzyskano zwiększenie objętości obu wykreślanych dróg nerwowych oraz ilość włókien nerwowych tworzących pęczek haczykowaty i łukowaty. Klinicznie stan chorego uległ znaczącej poprawie. Cechy afazji uległy regresji w stopniu znacznym, chory powrócił do aktywności zawodowej.

W artykule przedstawiono traktografię jako metodę monitorowania stanu klinicznego pacjenta oraz postępy w rehabilitacji mowy co może mieć związek ze zmianą integralności istoty białej.

Case Report

# Tractography Alterations in the Arcuate and Uncinate Fasciculi in Post-Stroke Aphasia

Sara Kierońska <sup>1</sup>, Milena Świtońska <sup>1,2</sup>, Grzegorz Meder <sup>3</sup>, Magdalena Piotrowska <sup>1</sup> and Paweł Sokal <sup>1,2,\*</sup>

- <sup>1</sup> Department of Neurosurgery and Neurology, Jan Biziel University Hospital No. 2, Collegium Medicum, Nicolaus Copernicus University, 85-168 Bydgoszcz, Poland; sara.kieronska@bizeil.pl (S.K.); m.switonska@cm.umk.pl (M.Ś.); piotrowska.magdalena@wp.pl (M.P.)
- <sup>2</sup> Faculty of Health Science, Ludwik Rydygier Collegium Medicum, Nicolaus Copernicus University, 85-067 Bydgoszcz, Poland
- <sup>3</sup> Department of Interventional Radiology, Jan Biziel University Hospital No. 2, 85-168 Bydgoszcz, Poland; grzegorz.meder@gmail.com
- \* Correspondence: pawel.sokal@cm.umk.pl; Tel.: +48-600954415

**Abstract:** Fiber tractography based on diffuse tensor imaging (DTI) can reveal three-dimensional white matter connectivity of the human brain. Tractography is a non-invasive method of visualizing cerebral white matter structures in vivo, including neural pathways surrounding the ischemic area. DTI may be useful for elucidating alterations in brain connectivity resulting from neuroplasticity after stroke. We present a case of a male patient who developed significant mixed aphasia following ischemic stroke. The patient had been treated by mechanical thrombectomy followed by an early rehabilitation, in conjunction with transcranial direct current stimulation (tDCS). DTI was used to examine the arcuate fasciculus and uncinate fasciculus upon admission and again at three months post-stroke. Results showed an improvement in the patient's symptoms of aphasia, which was associated with changes in the volume and numbers of tracts in the uncinate fasciculus and the arcuate fasciculus.

**Keywords:** diffusion-tensor imaging; diffusion-tensor tractography; stroke; arcuate fasciculus; thrombectomy



**Citation:** Kierońska, S.; Świtońska, M.; Meder, G.; Piotrowska, M.; Sokal, P. Tractography Alterations in the Arcuate and Uncinate Fasciculi in Post-Stroke Aphasia. *Brain Sci.* **2021**, *11*, 53. <https://doi.org/10.3390/brainsci11010053>

Received: 22 November 2020

Accepted: 2 January 2021

Published: 5 January 2021

**Publisher's Note:** MDPI stays neutral with regard to jurisdictional claims in published maps and institutional affiliations.



**Copyright:** © 2021 by the authors. Licensee MDPI, Basel, Switzerland. This article is an open access article distributed under the terms and conditions of the Creative Commons Attribution (CC BY) license (<https://creativecommons.org/licenses/by/4.0/>).

## 1. Introduction

Stroke is the second leading cause of death and one of the most common causes of disability in adults worldwide [1]. Recent studies have shown that 26% of stroke survivors have disabilities related to activities of daily living (ADL). Fifty percent of people who have suffered a stroke have reduced mobility due to hemiparesis [2]. Aphasia is one of the most devastating cognitive impairments following stroke, affecting 21–38% of acute stroke patients [3]. Aphasia following stroke can affect communication and quality of life. About one third of patients report persistent aphasia at least three months following a stroke [4]. Functional recovery most likely involves both spontaneous and learning-dependent processes [5].

Conventional computed tomography (CT) and magnetic resonance imaging (MRI) techniques play an important role in the acute diagnosis and medical management of stroke patients. Lesion characteristics are undoubtedly associated with functional impairments at the time of scanning, and likely predict long-term clinical outcomes [6]. More recent neuroimaging techniques, such as diffusion tensor imaging (DTI) and tractography, can be used to aid in the differentiation between those who recover vs. don't recover. These techniques can also identify patients who will respond vs. not respond to different therapeutic approaches (e.g., rehabilitation) [7].

Magnetic resonance tractography is a valuable neuroimaging type of DTI that allows for the in vivo visualization of white matter pathways. This technique leverages the phenomenon of anisotropic diffusion of water to visualize the axons of nerve cells. In this

technique, the diffusion of water protons is determined by coefficients that characterize the direction of diffusion change. The highly organized structure of the axon and natural barriers (e.g., cell membranes, myelin sheaths) determine the anisotropic direction of diffusion [7,8]. DTI parameters, including fractionated anisotropy (FA) and mean diffusivity (MD) parameters, allow for the more precise differentiation of grey and white matter and to track the course of nerve pathways. Given that the values of FA and MD parameters are closely related to the microstructure of neurons, this allows for the quantitative and qualitative assessment of changes occurring in the brain in the course of natural and pathological processes [8]. Importantly, the parameters obtained on the basis of DTI imaging can serve as a kind of marker, helpful in assessing the advancement of a stroke, predicting response to therapies or their long-term results [9,10]. Due to the fact that motor deficits are a particularly common consequence of stroke, the area of interest in research on the use of DTI as a biomarker was in the cortical-spinal system (CST) [9]. It has been shown that there is a significant correlation between the parameters obtained thanks to the DTI technique and the results of physical fitness obtained subsequently. This dependence concerned the FA parameter, which reflects the regenerative abilities of CST, turns out to be particularly useful, making it a potential marker of motor outcomes recovery [10,11]. However, it should be remembered that, in order to unequivocally determine the usefulness, further multi-center studies are necessary, allowing for the standardization of the obtained data [9].

Moreover, important fiber tract, especially in the aspect of post-stroke aphasia is arcuate fasciculus which is the white matter pathway connecting the Broca speech center (located in the frontal lobe) with the Wernicke speech center (temporal lobe). The AF is a bundle of associative fibers that connect Wernicke's area, which is responsible for sensory aspects of speech, with Broca's area, which is responsible for motor aspects of speech. This fiber bundle is largely responsible for central speech control by coordinating information between the motor and sensory speech areas [12]. The uncinata fasciculus as a hook fascicle connecting the prefrontal cortex and temporal lobe. The UF mainly interconnects regions that support empathy and emotional responses.

Transcranial stimulation with direct current (tDCS) is a non-invasive method of neurorehabilitation based on neuromodulation. The technique consists of placing electrodes on the head soaked in a physiological saline solution and in contact with a direct current source with an intensity in the range of 1–2 mA. Although the exact mechanism of operation of this technique is still unclear, it is postulated that the current flowing through the cerebral cortex modulates cortical excitation by changing the potential of the cell membrane of neurons and the activity of neuronal receptors [13,14]. The type of modulation depends on the polarity of the electrode located above the area to be treated. The use of anodic stimulation is associated with the intensification of cortical excitation and spontaneous cortical activity, while the use of a cathode has the opposite effect [13–15]. The available literature data indicate that tDCS contributes to the improvement of language and behavioral functions in patients with post-stroke aphasia [14–16]. It has been suggested that tDCS, when used in the treatment of aphasia, in combination with commonly used neurologopedic rehabilitation techniques is a potentially beneficial therapeutic tool [16].

The aim of the case report is present tractography as a method to assess neural functional rehabilitation after stroke. Moreover, in this study, we explored how neuroimaging, and specifically diffusion tensor tractography, might add to predictive models of stroke functional recovery. To address this, we reviewed key findings in the literature and present data from a relatively rare case wherein DTI findings were important for understanding deficits over time.

## 2. Case

### 2.1. Case History

This case study reports on a 41-year old, right-handed man with no past medical history. The patient was admitted to the Stroke Intervention Treatment Unit in the Department of Neurosurgery and Neurology in University Hospital No. 2 in Bydgoszcz due to

difficulty speaking and inability to understand words for five hours. Total sensory and partial motor aphasia was diagnosed, which gave us the diagnosis of mixed aphasia. The patient's consciousness was clear without evident abnormalities in muscle tone, reflex, or gait. The patient gave informed consent form on the usage of personal data.

## 2.2. Results of Tests

The patient's vital signs were as follows: temperature: 37 °C orally, BP: 170/90 mmHg, heart rate: 86 beats/min, respiratory rate: 16 breaths/min. The clinical neurological deficits of the patient were assessed using the National Institutes of Health Stroke Scale (NIHSS) and were rated 6 points- Responsiveness 0 point (responsive), Questions 2 points (patient didn't correctly answer either question), Commands 2 points (patient didn't correctly perform tasks), Horizontal Eye Movement 0 point (normal), Visual field test 0 point (no vision loss), facial palsy 0 point (normal), Motor arm 0 point (no arm drift), Motor leg 0 point (no motor drift), Limb ataxia 0 point (normal), sensory 0 point (no sensor loss), and Speech 2 points (Severe aphasia)

Brain CT scan performed 30 min after admission to the hospital didn't reveal any abnormalities. However, CT scan performed after 24 h after admission to the hospital showed moderate ischemic infarction in the left temporal lobe (Figure 1). Additionally, 48 h after admission to the hospital, MRI examination was performed (Figure 2). Three months after ischemic stroke, MRI was performed according to the same protocol as baseline (Figure 3.)



**Figure 1.** CT scan of the brain after 24 h after admission to the hospital shows an ischemic stroke (30 × 25 × 60 mm) in the left temporal lobe.

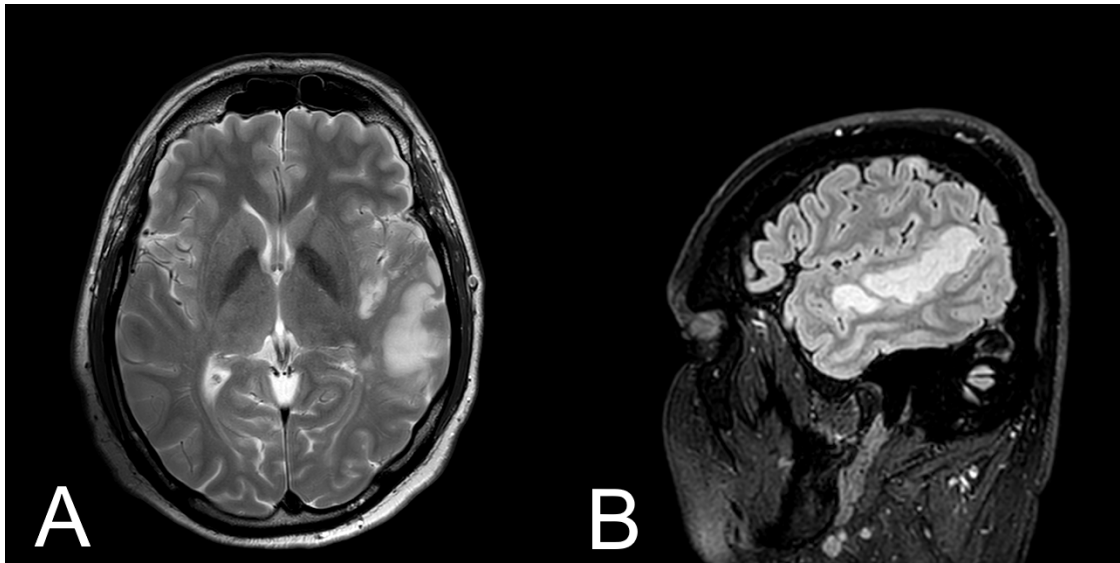


**Figure 2.** Initial conventional magnetic resonance imaging (MRI) of the patient. (A) T2-weighted image with axial plane (T2WI) showed moderate ischemic lesion in the left temporal lobe; (B) FLAIR image with sagittal plane showed ischemic lesion with oedema of the left temporal lobe.

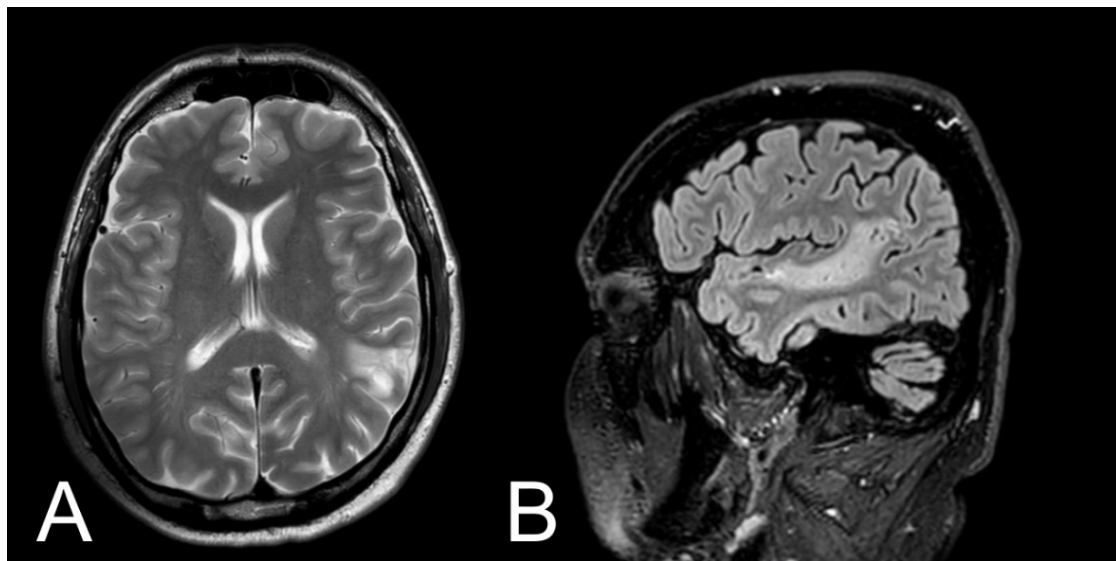


**Figure 3.** Magnetic resonance imaging (MRI) of the patient after 3 months. (A) T2-weighted image with axial plane (T2WI) showed decrease ischemic lesion in the left temporal lobe; (B) FLAIR image with sagittal plane showed decrease ischemic lesion without oedema of left temporal lobe.

### 2.3. Treatment

The patient underwent mechanical thrombectomy within six hours after symptom onset. The patient did not qualify for intravenous thrombolysis due to exceeding the time criterion (i.e., 4.5 h from the onset of stroke symptoms). During digital subtraction angiography (DSA), an occlusion of the inferior trunk of the left middle cerebral artery (MCA) was found. Using a small stent retriever (Catch mini 3 × 15 mm, Balt), mechanical thrombectomy (MT) was performed and a thrombus from the affected branch of the MCA was removed. A control run revealed a short, narrowed segment in the treated MCA branch, which quickly started to thrombose again. Two more passes with the device were performed and yielded the same result, which raised the suspicion of branch dissection.



Implantation of the stent into the affected branch was deliberated, but, finally, further attempts to recanalize were terminated. As a result, a slight reperfusion—TICI 1—was obtained.

#### 2.4. Outcome after Treatment

The patient was assessed 24 h following admission to the hospital by a speech therapist, using the Frenchay Aphasia Screening Test (FAST Test) and the Boston Naming Test (BNT Test, elaborate by Pachalska and MacQueen) [17,18]. The FAST Test measures Comprehension, Expression, Reading and Writing, whereas the Boston Naming Test measures naming skills. The patient obtained the following results: FAST 0/30 points, BNT 2/60 points. The patient displayed symptoms of mixed, primarily sensory aphasia and showed significantly impaired understanding of speech, including simple and complex commands. The patient also had profound difficulties in naming the items in the illustrations in the course of the Boston Naming Test (BNT), i.e., he could correctly name only two out of 60 items. The patient was diagnosed with alexia and agraphia.

#### 2.5. MRI Protocol

Human brains were scanned by MRI (T1, T2-weighted, and DTI with echo planar imaging) using a 20-channel head/neck coil on a single 3.0 T Siemens Magnetom Aera scanner (Erlangen, Germany). We used the following DTI acquisition parameters: slice thickness 5.0 mm; matrix— $128 \times 128$ ; field of view— $240 \times 240$  mm; repetition time—3500 ms; echo time—83.0 ms. Outcome measures of interest included fractional anisotropy (FA), mean diffusivity (MD) and apparent diffusion coefficient (ADC) DTI is most commonly performed using a single-shot, spin-echo, echo planar image acquisition at b-values similar to those used for conventional DWI (typically  $b = 1000$  s/mm<sup>2</sup>). The scanners of MRI and the fiber tracking protocols at baseline and after three months were the same [19,20].

#### 2.6. Fiber Tracking Protocol

Diffusion tensor images were processed using DSI studio software, BSD License. A DTI diffusion scheme was used and a total of 60 diffusion sampling directions were acquired. longer tracts [16]. The b-value was 1000 s/mm<sup>2</sup>. The in-plane resolution was 1.95 mm. The slice thickness was 2 mm. A deterministic fiber tracking was used. A total of 15,000 tracts were calculated. ROIs were defined automatically based on an anatomical atlas loaded into the DSI studio program.

By determining arcuate fasciculus, the first Region of Interest (ROI) was drawn in the coronal section under the central sulcus, and a second ROI had been drawn in the axial view at the temporo-parietal junction. Moreover, for uncinat fasciculus, the first ROI was plotted such that it covered the entire temporal lobe; the second ROI covered the projections over the frontal lobe.

#### 2.7. tDCS Protocol

The patient received scheduled, conventional rehabilitation (exercises with a physio-therapist in the rehabilitation room) and received transcranial direct current stimulation (tDCS, Sooma Helsinki, Finland) as a rehabilitation tool during the first 10 days following stroke. TDCS was administered for 30 min daily with 2 mA amplitude. According to protocol which was used in Sebastian's et al. article, anodal tDCS was applied to the left hemisphere language areas to increase cortical excitability (increasing the threshold of activation), and cathodal tDCS was applied to the right hemisphere homotopic areas to inhibit over activation in contralesional right homologues of language areas [21].

#### 2.8. Outcome at Discharge

On the tenth day of hospitalization, the patient underwent a follow-up neurological evaluation. The patient obtained the following results: FAST 20/30 points, BNT 45/60 points. A reduction in aphasic disorders and an improvement in verbal and

logical contact with the patient were observed. The patient understood and followed simple and complex commands. Improvements in updating the names of items were observed (perseveration, verbal paraphrases, amnesty gaps). The patient was helped by the hint of the first syllable. The patient correctly recreated the automated word sequences (counting, names of days of the week, months). He was repeating simple sounds and single words correctly. Difficulties with longer words with a complicated grammatical structure and sentences (phonetic paraphrases) were still difficult to repeat. Improvement in reading function was observed in the patient. The patient was correctly recognizing names of individual letters, reading individual words and sentences (paralexia persisted). The patient was properly oriented auto- and allopsychically. The patient was advised to continue further speech therapy after discharge from the hospital ward provided by trained and qualified speech and language therapists, including tasks devoted to naming, comprehension, and increasing verbal output.

The patient received ongoing treatment of ASA 75 mg, enoxaparine 40 mg, and cerebrolysin 30 mg daily starting from the second day of hospitalization. The patient was discharged from the hospital 14 days following stroke and received ASA 150 mg, Atorvastatin 40 mg, Citicoline 1000 mg daily for the next 20 days.

### 2.9. Outcome at Follow Up

Three months after the stroke, the patient underwent a follow-up neurologopedic evaluation. The speech therapy examination upon admission and after three months was performed by the same speech therapist. The patient obtained the following results: FAST 29/30 points, BNT 60/60 points. The assessment showed full independence of the patient, and he was able to perform all social functions, but with slight aphasic disorders. These assessments indicated that the patient would soon be able to start gainful employment, which was important for him to return to pre-stroke functioning and regain lost social roles. Three months after the stroke, the patient was allowed to return to work as a sales representative.

### 3. Analysis

Based on MRI with DTI, the arcuate fasciculus (AF) and uncinate fasciculus (UF) were delineated upon admission (AF Figure 4, UF Figure 5) and three months following the ischemic stroke (AF Figure 6, UF Figure 7). Analyses computed the number of fibers, tract length, and volume.

Differences in the parameters of the nerve tracts upon admission and three months after hospitalization for the UF and AF are presented in Tables 1 and 2, respectively.

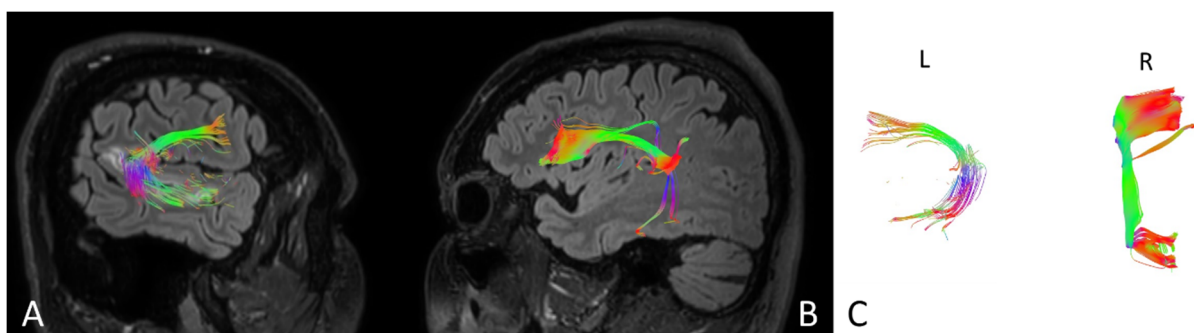


**Figure 4.** Anatomy of the arcuate fasciculus (AF) upon the patient's admission to the hospital. (A) right hemisphere, (B) left hemisphere, (C) comparison of left and right axial plane of AF.

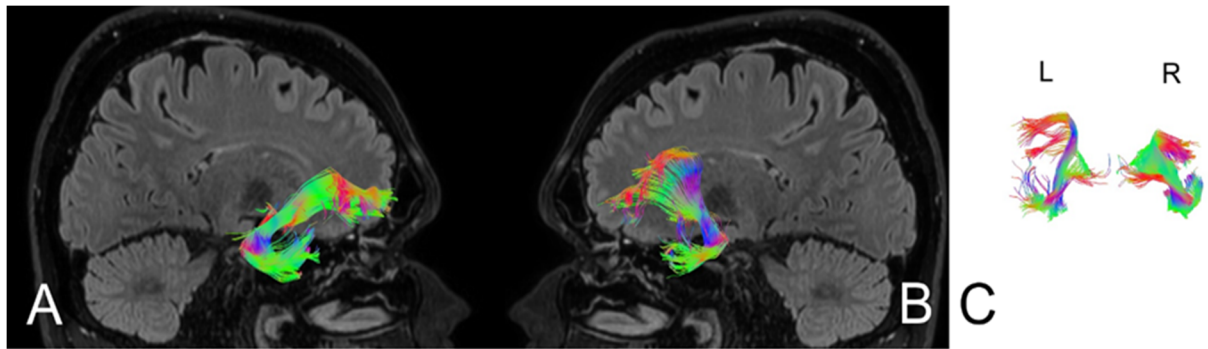


**Figure 5.** Anatomy of the uncinus fasciculus (UF) upon the patient’s admission to the hospital. (A) right hemisphere, (B) left hemisphere, (C) comparison of left and right axial plane of UF.

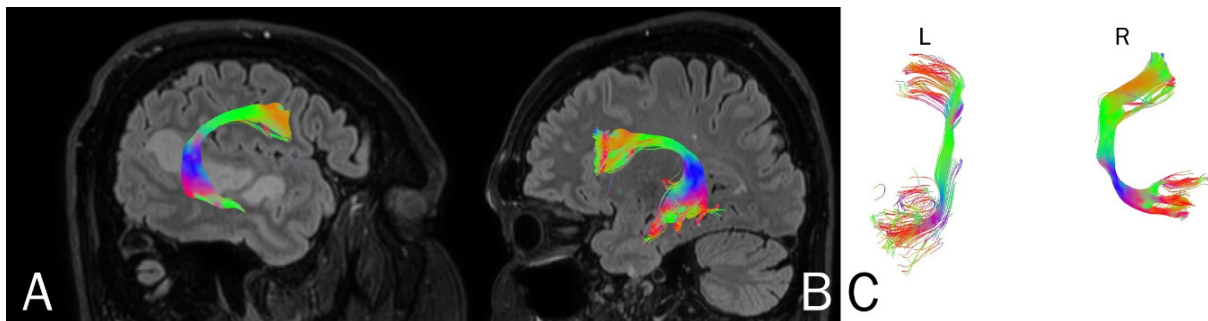


**Figure 6.** Anatomy of the patient’s arcuate fasciculus (AF) at 3 months following stroke. (A) right hemisphere, (B) left hemisphere, (C) comparison of left and right axial plane of the AF.

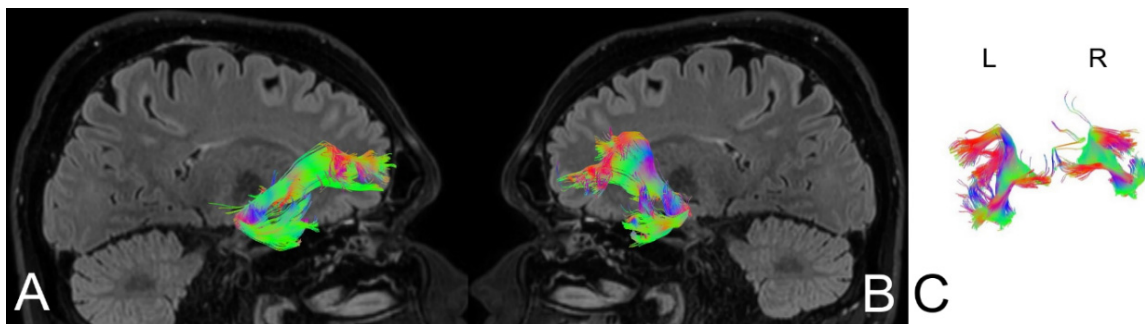


**Figure 7.** Anatomy of the patient’s uncinus fasciculus (UF) at 3 months following stroke. (A) right hemisphere, (B) left hemisphere, (C) comparison of left and right axial plane of the UF.

**Table 1.** The patient’s morphological data of the uncinus fasciculus (UF) upon admission and three months following stroke.

Parameters	Admission		3 Month Follow-Up	
	Left side	Right side	Left side	Right side
Number of fibers	148	183	155	152
Volume of tract [mm <sup>2</sup> ]	13305	16440	14400	16338
Length of tract [mm]	88.5	98.3	87.5	97.1
FA	0.675	0.895	0.705	0.880

**Table 2.** The patient's morphological data of the arcuate fasciculus (AF) upon admission and three months following stroke.

Parameters	Admission		3 Month Follow-Up	
	Left side	Right side	Left side	Right side
Number of fibres	160	205	185	208
Volume of tract [mm <sup>2</sup> ]	1125	18440	1280	18559
Length of tract [mm]	75.5	88.0	86.4	89.0
FA	0.715	0.885	0.785	0.880

#### 4. Discussion

To the best of our knowledge, this is the first case report on the use of tractography to monitor processes related to neural functional restoration in a patient after thrombectomy. However, the use of the DTI technique to assess the functional recovery of selected areas of the cerebral cortex has been in the past. An example of this is the case by Seghier et al. from 2005 concerning the restoration of visual ability in a patient after a perinatal stroke. The authors of this study also pointed to the usefulness of information obtained thanks to the DTI technique in planning rehabilitation and in predicting the return of functions lost due to brain damage [22,23]. In the present study, we found substantial differences over time in the values of all DTI parameters measured in this study within the AF and UF.

In this study, the patient's stroke occurred in the left hemisphere, which may have had a greater impact on the UF in the left temporal lobe as compared to the right side [24]. Indeed, we found a decrease in the number of fibers and the volume of UF in within the area affected by the stroke, as compared to the UF in the opposite hemisphere. Perhaps the differences reflect the damage caused by a stroke. However, it is impossible to unequivocally confirm the above thesis because we do not have adequate data from before the onset of a stroke episode. Notably, we observed an increase in the number of fibers and tract volume in both the AF and UF in the left hemisphere, after the application of tDCS and conventional rehabilitation. These parameters were reassessed after three months.

There are a number of changes in the cytoarchitectonics of nervous tissue following ischemic stroke. These neural changes can lead to the loss of axon integrity, which can indirectly result in FA changes. The available data regarding changes in FA in the acute infarction foci are contradictory. Indeed, some studies show reduced FA and others report increased FA [25–27]. One theory for these discrepancies was developed by Ozsunar et al. The authors demonstrated that the FA parameter is inversely correlated with signal intensity in the T2-dependent sequence [27]. Therefore, changes in the value of FA in the early stage of the stroke are secondary to oedema, membrane damage, and cell lysis, and may be an indicative measure of the severity of damage. Post-stroke FA in the early stages may therefore be a potential prognostic indicator of infarct recovery [28].

Several studies have used tractography to visualize damage to the corticospinal tract in patients with motor disorders who experience chronic strokes. These studies demonstrate a correlation between the obtained tractography results and the patients' clinical functioning [29]. Therefore, tractography measures may be a useful prognostic indicator for the return of motor functions following rehabilitation procedures. Indeed, increased FA has been reported following rehabilitation, which may be due to remodeling of white matter motor pathways [30,31]. Tractography can also be used to assess non-motor routes [12,32,33]. Damage to the AF is associated with the occurrence of conductive aphasia, which is characterized by a strongly limited or inability to repeat words heard and a lack of control over active speech [34]. In addition, a study by Breier et al. [35] found that lesions within the AF can cause difficulties not only with repeating heard words, but also with understanding them. These findings point to the relationship between AF damage and changes within posterior superior, middle temporal, and supramarginal gyri that may mediate deficits in speech understanding [35]. A study by Kim and Jang indicates the usefulness of tractography for visualizing the left AF in the early stages of stroke, which suggests that the present approach may be useful for predicting outcomes of aphasia among

stroke patients [36]. DTI may also be a valuable diagnostic tool to assess the presence and severity of AF lesions, track the prognosis of aphasia, and identify mechanisms of aphasia regeneration among stroke patients. Together, these applications may aid in the development of a personalized neurologopedic rehabilitation schedule [36,37].

One of the weaknesses of our study is that we didn't attempt to determine psychological assessment of our patient in terms of empathy and emotional disorders. It was mainly related to the patient's aphasia. Oishi et al. in their study showed a relationship between reduced volume in the uncinate fasciculus and errors on empathy tasks [38]. Previous studies have also proved a relationship between reduced volume of UF and errors on empathy tasks in some neurological disorder. Results confirm that acute damage to the right UF can disrupt performance on a task of emotional empathy [38,39]. This is the reason that the psychological assessment of stroke patients is so important in future studies, taking into account the aspects of emotions and empathy with correlation with the anatomy of UF. The key goal of clinical management among patients with ischemic stroke is to diagnose stroke as early as possible, preferably during the hyperacute phase, in which reperfusion treatment is the most effective. Identification of patients in the hyperacute phase requires an imaging technique that allows for optimal imaging of the infarct focus [40]. These findings also support further investigation into the use of tDCS as a promising method for promoting speech rehabilitation among ischemic stroke patients. Prior studies by Nitche, Paulus, and Jude suggest that tDCS might prime the brain as an adjuvant to behavioral aphasia and motor-limb therapies, and thus optimize recovery. In particular, a low-intensity current (e.g., 1–2 mA) can be useful for modulating neuronal activity during stroke rehabilitation, which may encourage brain plasticity [41,42].

Thus far, the available literature data indicate a low or moderate quality of evidence regarding the use of tDCS in the treatment of aphasia [13]. Nevertheless, numerous reports suggest that the use of tDCS in the rehabilitation of post-stroke aphasia patients may enhance the process of speech recovery [43,44]. At the same time, despite promising reports in the field of neurorehabilitation using tDCS stimulation, this method still has the experimental status. The tDCS method can be used, among others as non-pharmacological support in the treatment of strokes. There is a need for further research, thus constituting a promising additional tool in recovery [44]. Hesse et al. were the first to pay attention to the changes in neurological status after using of tDCS in patients after stroke. The researchers wanted to check 10 patients with paresis in terms of tolerance of transcranial electrostimulation. They joined 30 movement training sessions 7-min 1.5 mA a-tDCS, aimed at the motor cortex hemisphere (anode above C3 / C4 acc. To 10/20 electroencephalographic system). The analysis of the results showed that in 4 out of 5 patients with right-sided paresis accompanied by aphasia, language disorders unexpectedly decreased, assessed using the aphasia test (Aachener Aphasia Test) [45].

In an early phase of ischemic stroke, the phenomenon of spontaneous improvement of the neurological state is observed, including remission in terms of aphasia, especially in groups of young patients, which is directly related to brain neuroplasticity [46,47]. To activate the neuroplasticity process, it is important to implement various forms of neurorehabilitation, including tDCS. In the study, Pelegrino et al. proved that neural plasticity is induced by electrical stimulation of tDCS in sensorimotor areas. In this study, tDCS was compared to sham tDCS. The presented analysis shows that bilateral tDCS stimulation increases the number of gamma waves in the brain, which may be related to the neuroplasticity [48–50].

In the case of ischemic stroke diagnosis, rapid therapeutic interventions are required due to the short therapeutic window. Successful treatment does not end with reperfusion therapy. The next stage of therapy involves the development of a personalized rehabilitation plan, which aims to reduce neurological deficits as quickly and effectively as possible. The present study demonstrates that tractography may be useful in the diagnosis and monitoring of patients with acute ischemic stroke. Of course, the description of one case is a limitation. Therefore, further studies that include a large group of patients and aim to

examine effectiveness are needed. Tractography is a promising new tool for the evaluation of patients following ischemic stroke [51,52].

## 5. Conclusions

This case report demonstrated DTI with tractography as an MRI technique used to detect the microstructural changes and difference in the anatomy and morphology of fiber tracts in patients after ischemic stroke which corresponded with improvement in the patient's clinical functioning. In the described case, the correlation between the patient's clinical improvement and neurorehabilitation enhanced by tDCS cannot be clearly defined. Based on the description of one case, no objective conclusions can be drawn regarding the use of post-stroke tractography and tDCS. The description of this case prompts research on a larger group of patients after ischemic stroke.

**Author Contributions:** Conceptualization, S.K., M.Ś., and P.S.; Data curation, S.K., P.S., and M.Ś.; Formal analysis, S.K., M.Ś., and M.P.; Investigation, S.K., P.S., M.Ś., G.M., and M.P.; Methodology, S.K., P.S., M.Ś., and G.M.; Project administration, S.K., M.Ś., and P.S.; Resources, S.K., P.S., and M.Ś.; Software, S.K., M.Ś., and G.M.; Supervision, S.K. and P.S.; Validation, S.K., P.S., M.Ś., and G.M.; Visualization, S.K., M.Ś., and M.P.; Writing—Original draft, S.K., M.Ś., and P.S.; Writing—Review and editing, S.K. and P.S. All authors have read and agreed to the published version of the manuscript.

**Funding:** This research received no external funding.

**Institutional Review Board Statement:** The study was conducted according to the guidelines of the Declaration of Helsinki, and approved by the Local Ethics Committee in Bydgoszcz N<sup>o</sup> KB 628/2018.

**Informed Consent Statement:** The subject provided written informed consent before enrolling for the treatment in accordance with the Declaration of Helsinki.

**Data Availability Statement:** The datasets generated during and/or analysed during the current study are available from the corresponding author on reasonable request.

**Conflicts of Interest:** The authors declare no conflict of interest.

## References

1. Katan, M.; Luft, A. Global Burden of Stroke. *Semin. Neurol.* **2018**, *38*, 208–211. [[CrossRef](#)] [[PubMed](#)]
2. Bolognini, N.; Russo, C.; Edwards, D.J. The sensory side of post-stroke motor rehabilitation. *Restor. Neurol. Neurosci.* **2016**, *34*, 571–586. [[CrossRef](#)] [[PubMed](#)]
3. Berthier, M.L. Poststroke aphasia: Epidemiology, pathophysiology and treatment. *Drugs Aging* **2005**, *22*, 163–182. [[CrossRef](#)] [[PubMed](#)]
4. Ali, M.; Lyden, P.; Brady, M. Aphasia and dysarthria in acute stroke: Recovery and functional outcome. *Int. J. Stroke* **2015**, *10*, 400–406. [[CrossRef](#)]
5. Donkor, E.S. Stroke in the 21st Century: A Snapshot of the Burden, Epidemiology, and Quality of Life. *Stroke Res. Treat.* **2018**, *2018*. [[CrossRef](#)]
6. Menon, B.K. Neuroimaging in Acute Stroke. *Contin. (Minneapolis, Minn.)* **2020**, *26*, 287–309. [[CrossRef](#)]
7. Taea, W.-S.; Hama, B.-J.; Pyuna, S.-B.; Kang, S.H.; Kim, B.J. Current clinical applications of diffusion-tensor imaging in neurological disorders. *J. Clin. Neurol.* **2008**, *14*, 129–140. [[CrossRef](#)]
8. Denier, C.; Chassin, O.; Vandendries, C.; Bayon De La Tour, L.; Cauquil, C.; Sarov, M.; Adams, D.; Flamand-Roze, C. Thrombolysis in stroke patients with isolated aphasia. *Cerebrovasc. Dis.* **2016**, *41*, 163–169. [[CrossRef](#)]
9. Moura, L.M.; Luccas, R.; De Paiva, J.P.Q.; Amaro, E.; Leemans, A.; Leite, C.D.C.; Otaduy, M.C.G.; Conforto, A.B. Diffusion tensor imaging biomarkers to predict motor outcomes in stroke: A narrative review. *Front. Neurol.* **2019**, *10*, 445. [[CrossRef](#)]
10. Puig, J.; Blasco, G.; Daunis-I-Estadella, J.; Thomalla, G.; Castellanos, M.; Figueras, J.; Remollo, S.; Van Eendenburg, C.; Sánchez-González, J.; Serena, J.; et al. Decreased corticospinal tract fractional anisotropy predicts long-term motor outcome after stroke. *Stroke* **2013**, *44*, 2016–2018. [[CrossRef](#)]
11. Maeshima, S.; Osawa, A.; Nishio, D.; Hirano, Y.; Kigawa, H.; Takeda, H. Diffusion tensor MR imaging of the pyramidal tract can predict the need for orthosis in hemiplegic patients with hemorrhagic stroke. *Neurol. Sci.* **2013**, *34*, 1765–1770. [[CrossRef](#)] [[PubMed](#)]
12. Kieronska, S.; Słoniewski, P. The usefulness and limitations of diffusion tensor imaging—A review study. *Eur. J. Transl. Clin. Med.* **2020**, *2*, 43–51. [[CrossRef](#)]
13. Elsner, B.; Kugler, J.; Pohl, M.; Mehrholz, J. Transcranial direct current stimulation (tDCS) for improving aphasia in adults with aphasia after stroke. *Cochrane Database Syst. Rev.* **2019**. [[CrossRef](#)] [[PubMed](#)]

14. Polanowska, K.; Seniów, J. Influence of transcranial direct current stimulation on cognitive functioning of patients with brain injury. *Neurol. I Neurochir. Pol.* **2010**, *44*, 580–590. [[CrossRef](#)]
15. Fridriksson, J.; Rorden, C.; Elm, J.; Sen, S.; George, M.S.; Bonilha, L. transcranial direct current stimulation vs sham stimulation to treat aphasia after stroke: A randomized clinical trial. *JAMA Neurol.* **2018**, *75*, 1470–1476. [[CrossRef](#)]
16. Monti, A.; Ferrucci, R.; Fumagalli, M.; Mameli, F.; Cogiamanian, F.; Ardolino, G.; Priori, A. Transcranial direct current stimulation (tDCS) and language. *J. Neurol. Neurosurg. Psychiatry* **2013**, *84*, 832–842. [[CrossRef](#)]
17. Enderby, P.M.; Wood, V.A.; Wade, D.T.; Hewer, R.L. The frenchay aphasia screening test: A short, simple test for aphasia appropriate for non-specialists. *Disabil. Rehabil.* **1986**, *8*, 166–170. [[CrossRef](#)]
18. del Toro, C.M.; Bislick, L.P.; Comer, M.; Velozo, C.; Romero, S.; Rothi, L.J.G.; Kendall, D.L. Development of a short form of the boston naming test for individuals with aphasia. *J. SpeechLang. Hear. Res.* **2011**, *54*, 1089–1100. [[CrossRef](#)]
19. Vollmar, C.; Muirheartaigh, J.O.; Barker, G.J.; Symms, M.R.; Thompson, P.; Kumari, V.; Duncan, J.S.; Richardson, M.P.; Koeppe, M.J. NeuroImage identical, but not the same: Intra-site and inter-site reproducibility of fractional anisotropy measures on two 3.0 T scanners. *NeuroImage* **2010**, *51*, 1384–1394. [[CrossRef](#)]
20. Andica, C.; Kamagata, K.; Hayashi, T.; Hagiwara, A.; Uchida, W.; Saito, Y. Scan—rescan and inter-vendor reproducibility of neurite orientation dispersion and density imaging metrics. *Neuroradiology* **2019**, *62*, 483–494. [[CrossRef](#)]
21. Sebastian, R.; Tsapkini, K.; Tippett, D.C. Transcranial direct current stimulation in post stroke aphasia and primary progressive Aphasia: Current knowledge and future clinical applications. *NeuroRehabilitation* **2017**, *39*, 141–152. [[CrossRef](#)]
22. Seghier, M.L.; Lazeyras, F.; Zimine, S.; Saudan-Frei, S.; Safran, A.B.; Hüppi, P.S. Visual recovery after perinatal stroke evidenced by functional and diffusion MRI: Case report. *BMC Neurol.* **2005**, *5*, 17. [[CrossRef](#)] [[PubMed](#)]
23. Furlanis, G.; Ridolfi, M.; Polverino, P.; Menichelli, A.; Caruso, P.; Naccarato, M.; Sartori, A.; Torelli, L.; Pesavento, V.; Manganotti, P. Early recovery of aphasia through thrombolysis: The significance of spontaneous speech. *J. Stroke Cerebrovasc. Dis.* **2018**, *27*, 1937–1948. [[CrossRef](#)]
24. Kierońska, S.; Sokal, P.; Dura, M.; Jabłońska, M.; Rudaś, M.; Jabłońska, R. Tractography-based analysis of morphological and anatomical characteristics of the uncinate fasciculus in human brains. *Brain Sci.* **2020**, *10*, 709. [[CrossRef](#)] [[PubMed](#)]
25. Armitage, P.A.; Bastin, M.E.; Marshal, I.; Wardlaw, J.M.; Cannon, J. Diffusion anisotropy measurements in ischaemic stroke of the human brain. *Magn. Reson. Mater. Phys. Biol. Med.* **1998**, *6*, 28–36. [[CrossRef](#)]
26. Maniega, S.M.; Bastin, M.E.; Armitage, P.A.; Farrall, A.J.; Carpenter, T.K.; Hand, P.J.; Cvorov, V.; Rivers, C.S.; Wardlaw, J.M. Temporal evolution of water diffusion parameters is different in grey and white matter in human ischaemic stroke. *J. Neurol. Neurosurg. Psychiatry* **2004**, *75*, 1714–1718. [[CrossRef](#)] [[PubMed](#)]
27. Ozsunar, Y.; Grant, P.E.; Huisman, T.A.G.M.; Schaefer, P.W.; Wu, O.; Sorensen, A.G.; Koroshetz, W.J.; Gonzalez, R.G. Evolution of water diffusion and anisotropy in hyperacute stroke: Significant correlation between fractional anisotropy and T2. *Am. J. Neuroradiol.* **2004**, *25*, 699–705.
28. García, A.O.; Brambati, S.M.; Brisebois, A.; Désilets-Barnabé, M.; Houzé, B.; Bedetti, C.; Rochon, E.; Leonard, C.; Desautels, A.; Marcotte, K. predicting early post-stroke aphasia outcome from initial aphasia severity. *Front. Neurol.* **2020**, *11*, 120. [[CrossRef](#)] [[PubMed](#)]
29. Provenzale, J.M.; Mukundan, S.; Barboriak, D.P. Diffusion-weighted and perfusion mr imaging for brain tumor characterization and assessment of treatment response. *Radiology* **2006**, *239*, 632–649. [[CrossRef](#)]
30. Puig, J.; Blasco, G.; Schlaug, G.; Stinear, C.M.; Daunis-i-Estadella, P.; Biarnes, C.; Figueras, J.; Serena, J.; Hernández-Pérez, M.; Alberich-Bayarri, A.; et al. Diffusion tensor imaging as a prognostic biomarker for motor recovery and rehabilitation after stroke. *Neuroradiology* **2017**, *59*, 343–351. [[CrossRef](#)]
31. Gonzalez-Aquines, A.; Moreno-Andrade, T.; Gongora-Rivera, F.; Cordero-Perez, A.C.; Ortiz-Jiménez, X.; Cavazos-Luna, O.; Garza-Villareal, E.; Campos-Coy, M.; Elizondo-Riojas, G. The role of tractography in ischemic stroke: A review of the literature. *Med. Univ.* **2019**, *20*, 161–165. [[CrossRef](#)]
32. Szmuda, T.; Kierońska, S.; Ali, S.; Słoniewski, P.; Pacholski, M.; Dzierżanowski, J.; Sabisz, A.; Szurowska, E. Tractography-guided surgery of brain tumors: What is the best method to outline the corticospinal tract? *Folia Morphol.* **2020**. [[CrossRef](#)] [[PubMed](#)]
33. Szmuda, T.; Rogowska, M.; Słoniewski, P.; Abuhaimeed, A.; Szmuda, M.; Springer, J. Frontal aslant tract projections to the inferior frontal gyrus. *Folia Morphol.* **2017**, *76*, 574–581. [[CrossRef](#)] [[PubMed](#)]
34. Catani, M. The arcuate fasciculus and the disconnection theme in language and aphasia: History and current state. *Cortex* **2008**, *44*, 997–1003. [[CrossRef](#)] [[PubMed](#)]
35. Breier, J.I.; Hasan, K.M.; Zhang, W.; Men, D.; Papanicolaou, A.C. Language dysfunction after stroke and damage to white matter tracts evaluated using diffusion tensor imaging. *Am. J. Neuroradiol.* **2008**, *29*, 483–487. [[CrossRef](#)]
36. Kim, S.H.; Jang, S.H. Prediction of aphasia outcome using diffusion tensor tractography for arcuate fasciculus in stroke. *Am. J. Neuroradiol.* **2013**, *34*, 785–790. [[CrossRef](#)]
37. Kim, S.H.; Lee, D.G.; You, H.; Son, S.M.; Cho, Y.W.; Chang, M.C.; Lee, J.; Jang, S.H. The clinical application of the arcuate fasciculus for stroke patients with aphasia: A diffusion tensor tractography study. *NeuroRehabilitation* **2011**, *29*, 305–310. [[CrossRef](#)]
38. Oishi, K.; Faria, A.; Hsu, J.; Tippett, D. The critical role of the right uncinate fasciculus in emotional empathy. *Ann. Neurol.* **2015**, *77*, 68–74. [[CrossRef](#)]
39. Matsuo, K.; Mizuno, T.; Yamada, K. Cerebral white matter damage in frontotemporal dementia assessed by diffusion tensor tractography. *Neuroradiology* **2008**. [[CrossRef](#)]

40. Heiss, W.D.; Kidwell, C.S. Imaging for prediction of functional outcome and assessment of recovery in ischemic stroke. *Stroke* **2014**, *45*, 1195–1201. [[CrossRef](#)]
41. Nitsche, M.A.; Paulus, W. Sustained excitability elevations induced by transcranial DC motor cortex stimulation in humans. *Neurology* **2001**, *57*, 1899–1901. [[CrossRef](#)]
42. Ogretmen, B. tDCS in post-stroke aphasia recovery. *Physiol. Behav.* **2019**, *176*, 139–148. [[CrossRef](#)]
43. Shah-Basak, P.P.; Norise, C.; Garcia, G.; Torres, J.; Faseyitan, O.; Hamilton, R.H. Individualized treatment with transcranial direct current stimulation in patients with chronic non-fluent aphasia due to stroke. *Front. Hum. Neurosci.* **2015**, *9*, 201. [[CrossRef](#)] [[PubMed](#)]
44. You, D.S.; Kim, D.Y.; Chun, M.H.; Jung, S.E.; Park, S.J. Cathodal transcranial direct current stimulation of the right Wernicke's area improves comprehension in subacute stroke patients. *Brain Lang.* **2011**, *119*, 1–5. [[CrossRef](#)] [[PubMed](#)]
45. Alber, R.; Moser, H.; Gall, C.; Sabel, B.A. Combined transcranial direct current stimulation and vision restoration training in subacute stroke rehabilitation: A pilot study. *PM&R* **2017**, *9*, 787–794. [[CrossRef](#)]
46. Fridriksson, J.; Guo, D.; Fillmore, P.; Holland, A.; Rorden, C. Damage to the anterior arcuate fasciculus predicts non-fluent speech production in aphasia. *Brain* **2013**, *136*, 3451–3460. [[CrossRef](#)] [[PubMed](#)]
47. Krajewska, M. Plastyczność ośrodkowego układu nerwowego a modele i mechanizmy poprawy sprawności językowych po udarze niedokrwiennym mózgu. *Logop. Lodz.* **2018**, *2*, 77–92. [[CrossRef](#)]
48. Keci, A.; Tani, K.; Xhema, J. Role of rehabilitation in neural plasticity. *Open Access Maced. J. Med. Sci.* **2019**, *7*, 1540–1547. [[CrossRef](#)]
49. Pellegrino, G.; Arcara, G.; Di, G.; Cristina, P.; Maran, M.; Weis, L.; Piccione, F.; Roman, H. Transcranial direct current stimulation over the sensory-motor regions inhibits gamma synchrony. *Hum. Brain Mapp.* **2019**, *40*, 2736–2746. [[CrossRef](#)]
50. Turolla, A.; Venneri, A.; Farina, D.; Cagnin, A.; Cheung, V.C.K. Rehabilitation induced neural plasticity after acquired brain injury. *Hindawi Neural Plast.* **2018**, *2018*. [[CrossRef](#)]
51. Mukherjee, P. Diffusion tensor imaging and fiber tractography in acute stroke. *Neuroimaging Clin. North Am.* **2005**, *15*, 655–665. [[CrossRef](#)] [[PubMed](#)]
52. Wilson, S.M.; Eriksson, D.K.; Brandt, T.H.; Schneck, S.M.; Lucanie, J.M.; Burchfield, A.S.; Charney, S.; Quillen, I.A.; de Riesthal, M.; Kirshner, H.S.; et al. Patterns of recovery from aphasia in the first 2 weeks after stroke. *J. SpeechLang. Hear. Res.* **2019**, *62*, 723–732. [[CrossRef](#)] [[PubMed](#)]



## 5.5 Omówienie pracy „Tractography-guided surgery of brain tumours: what is the best method to outline the corticospinal tract?”

Tematykę związaną z wyznaczaniem istotnych dróg istoty białej podjęto również w artykule „Tractography-guided surgery of brain tumours: what is the best method to outline the corticospinal tract?” opublikowanym w Folia Morphologica. W pracy wyznaczano drogę korowo-rdzeniową (CST) w oparciu o różne punkty zainteresowania (ROI) celem zoptymalizowania sposobu wyznaczania CST.








Materiał w publikacji stanowiło 32 pacjentów ze zdiagnozowanym guzem mózgu. Dla wykreślenia CST obrano dwa punkty ROI: ROI 1- konar mózgu (CP), ROI 2- odnoga tylna torebki wewnętrznej (PLIC). Jako punkty końcowe wybrano: płat czołowy (FL), pole ruchowe dodatkowe (SMA), zakręt przedśrodkowy, zakręt zaśrodkowy.

Z połączenia punktów ROI i punktów końcowych wytyczono CST na 10 różnych sposobów.

Znaczące różnice w liczbie włókien i ich objętości zaobserwowano, gdy PLIC lub CP stanowiły pojedynczy ROI w porównaniu z metodą dwóch punktów (wszystkie  $p < 0,05$ ). Średnia objętość CST wynosiła 40054U ( $SD \pm 12874$ ) a liczba włókien wynosiła 259,3 ( $SD \pm 87,3$ ), gdy PLIC był pojedynczym obszarem ROI. Nie było różnic między różnymi CST pod względem anizotropii frakcyjnej, średniej dyfuzyjności, pozornego współczynnika dyfuzji, ( $p > 0,05$ ). Droga korowo-rdzeniowa była naciekana przez guz u 17 z 32 pacjentów.

Nie opracowano uniwersalnej metody DTI CST. Z analizy wywnioskowano iż CP lub PLIC jako regiony zainteresowania powinny być w pierwszej kolejności uwzględniane do wyznaczania CST [18,19].

# Tractography-guided surgery of brain tumours: what is the best method to outline the corticospinal tract?

T. Szmuda<sup>1</sup>, S. Kierońska<sup>2</sup>, S. Ali<sup>3</sup>, P. Słoniewski<sup>1</sup>, M. Pacholski<sup>3</sup>, J. Dzierżanowski<sup>1</sup>,  
 A. Sabisz<sup>4</sup>, E. Szurowska<sup>4</sup>

<sup>1</sup>Neurosurgery Department, Medical University of Gdansk, Poland

<sup>2</sup>Neurology and Neurosurgery Department, University Hospital Collegium Medicum Nicolaus Copernicus University, Bydgoszcz, Poland

<sup>3</sup>Student's Scientific Circle, Neurosurgery Department, Medical University of Gdansk, Poland

<sup>4</sup>Radiology Department, Medical University of Gdansk, Poland

[Received: 7 January 2020; Accepted: 27 January 2020]

**Background:** Diffusion tensor imaging (DTI) is the imaging technique used in vivo to visualise white matter pathways. The cortico-spinal tract (CST) belongs to one of the most often delineated tracts preoperatively, although the optimal DTI method has not been established yet. Considering that various regions of interests (ROIs) could be selected, the reproducibility of CST tracking among different centres is low. We aimed to select the most reliable tractography method for outlining the CST for neurosurgeons.

**Materials and methods:** Our prospective study consisted of 32 patients (11 males, 21 females) with a brain tumour of various locations. DTI and T1-weighted image series were acquired prior to the surgery. To draw the CST, the posterior limb of the internal capsule (PLIC) and the cerebral peduncle (CP) were defined as two main ROIs. Together with these main ROIs, another four cortical endpoints were selected: the frontal lobe (FL), the supplementary motor area (SMA), the precentral gyrus (PCG) and the postcentral gyrus (POCG). Based on these ROIs, we composed ten virtual CSTs in DSI Studio. The fractional anisotropy, the mean diffusivity, the tracts' volume, the length and the number were compared between all the CSTs. The degree of the CST infiltration, tumour size, the patients' sex and age were examined.

**Results:** Significant differences in the number of tracts and their volume were observed when the PLIC or the CP stood as a single ROI comparing with the two-ROI method (all  $p < 0.05$ ). The mean CST volume was 40054U ( $SD \pm 12874$ ) and the number of fibres was 259.3 ( $SD \pm 87.3$ ) when the PLIC was a single ROI. When the CP was a single ROI, almost a half of fibres (147.6;  $SD \pm 64.0$ ) and half of the CST volume (26664U;  $SD \pm 10059U$ ) was obtained (all  $p < 0.05$ ). There were no differences between the various CSTs in terms of fractional anisotropy, mean diffusivity, the apparent diffusion coefficient, radial diffusivity and the tract length ( $p > 0.05$ ). The CST was infiltrated by a growing tumour or oedema in 17 of 32 patients; in these cases, the mean and apparent diffusion of the infiltrated CST was significantly higher than in uncompromised CSTs ( $p = 0.04$ ). CST infiltration did not alter the other analysed parameters (all  $p > 0.05$ ).

*Conclusions: A universal method of DTI of the CST was not developed. However, we found that the CP or the PLIC (with or without FL as the second ROI) should be used to outline the CST. (Folia Morphol 2021; 80, 1: 40–46)*

**Key words: diffusion tensor imaging, diffusion tensor tractography, tractography, corticospinal tract, pyramidal tract, glioma surgery, neurosurgery**

## INTRODUCTION

A neurosurgeon's objective is to achieve maximal tumour resection without producing new neurological defects [24, 29]; this includes preserving the cortico-spinal tract (CST). The CST is a white matter bundle that together with corticobulbar tract composes the pyramidal tract and if damaged it may lead to post-operative paresis [6]. Proper preoperative visualisation of the CST and its integration via an intraoperative neuronavigation system could potentially preserve neurological function and simultaneously increase the resection rate [4, 24]. However, several technical obstacles underlie correct delineation of the CST, including: knowledge of an individual's topographical anatomy, a physician's experience and the degree of destruction of the neuronal pathway through the tumour [14, 21].

Magnetic resonance imaging (MRI) scans are routinely acquired when planning brain tumour surgery. Yet, they provide only general information about the brain's pathology and the surrounding structures. Diffusion tensor imaging (DTI) — which provides a quick and non-invasive method for visualising structural changes of the white matter — can be used for visualisation of the CST [10, 12]. This technique not only plays an important role in neurosurgical planning but may predict the extent of safe resection [1, 22, 27]. However, physicians currently select various regions of interest (ROI) to draw the CST as the optimal DTI-derived method to estimate the course of the CST has not yet been established [11]. Due to this lack of standardisation the reliability of tracking the CST in different centres remains low [21].

Our aim was to determine the optimal DTI-derived method to reconstruct the CST as well as to verify if a single ubiquitous method exists. To accomplish this, we compared CST tracking as determined by various ROIs.

## MATERIALS AND METHODS

### Patients

Thirty-two patients with a brain tumour invading the CST were prospectively collected (11 males,

21 females; age 27–81 years, mean  $\pm$  standard deviation (SD) and median age:  $53.4 \pm 17.1/53.5$ ). These patients were treated at the Neurosurgery Department in Gdańsk, Poland, from 2016 to 2019. The protocol of the study was approved by the local bioethical committee, permission number: NKBBN/65/2019.

### Image acquisition

All patients had a preoperative MRI with a DTI sequence performed on a 1.5T Siemens Magnetom Aera scanner (Erlangen, Siemens Medical Solutions, Erlangen, Germany) which was equipped with a 20-channel head coil. The standard imaging protocol for brain tumours covered T1, T2-weighted sequences and T1-weighted post-gadolinium which served as a neuronavigational sequence. Diffusion-weighted imaging (DWI) was obtained using: three repetitions of 20 directions, a b-factor of  $1000 \text{ s/m}^2$ , a slice thickness of 5.0 mm, a  $128 \times 128$  matrix, a  $240 \times 240$  mm field-of-view, a repetition time of 3500 ms, and an echo time of 83.0 ms. A multivariate linear fitting was used to calculate the orientation for a single voxel. The largest eigenvalue denoted the ultimate fibre direction. A total of 60 diffusion sampling directions were acquired. The in-plane resolution was 1.95313 mm. The slice thickness was 2 mm. The diffusion tensor was calculated and a deterministic fibre tracking algorithm was used [28]. The angular threshold was 90 degrees. The step size was 0.977 mm. Diffusion images were processed and all the analyses were conducted using DSI Studio ([dsi-studio.labsolver.org](http://dsi-studio.labsolver.org)). We calculated the fractional anisotropy (FA), the mean diffusivity (MD) and the apparent diffusion coefficient (ADC). The anisotropy threshold was determined automatically by the software. The fibre trajectories were smoothed by averaging the propagation direction with 30% of the previous direction. Tracks with a length less than 30 mm were discarded. A total of 15000 tracts were calculated. When reconstructing the CST, we obtained tract statistics, including: the number of tracks, the mean length, the volume of the CST, the FA, the AD, and the MD values. The ROI

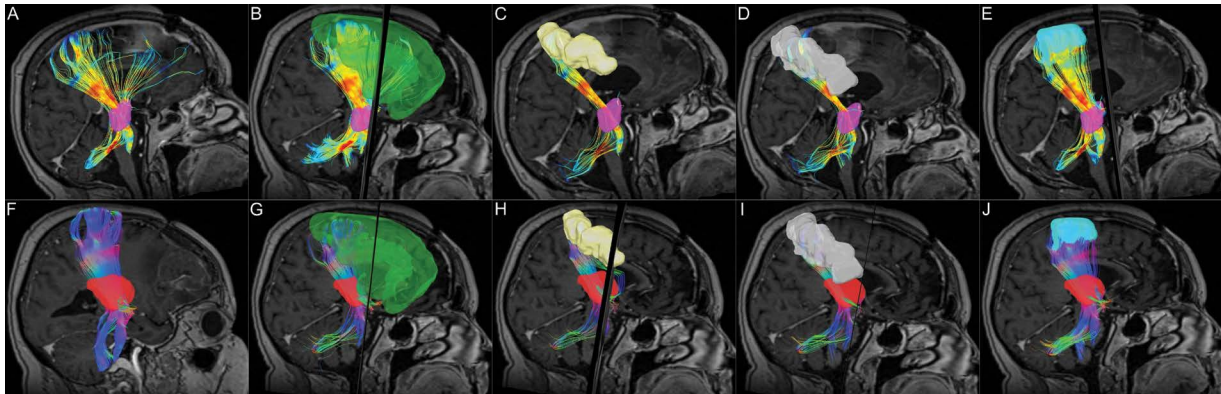


**Figure 1.** A graphic representation of different ways of drawing the cortico-spinal tract, where its course is determined by various regions of interest; **A–E.** Cerebral peduncle (CP, violet); **F–J.** Posterior limb of internal capsule (PLIC, red). **A.** Only CP; **B.** CP and frontal lobe (green); **C.** CP and precentral gyrus (yellow); **D.** CP and postcentral gyrus (white); **E.** CP and supplementary motor area (blue). **F.** Only PLIC; **G.** PLIC and frontal lobe (green); **H.** PLIC and precentral gyrus (yellow); **I.** PLIC and postcentral gyrus (white); **J.** PLIC and supplementary motor area (blue).

**Table 1.** A summary of the average values of the number of tracks of ten corticospinal tracts obtained by a combination of various region-of-interests

ROI	Number of tracts					
	Number	Mean	Median	Minimum	Maximum	SD
CP	32	147.5625	144.5000	22.0000	309.0000	64.01257
CP_preCG	31	31.3548	24.0000	0.0000	211.0000	40.43888
CP_postCG	32	15.1250	12.0000	0.0000	63.0000	15.14819
CP_SMA	32	12.7500	10.0000	0.0000	46.0000	13.77000
CP_FL	32	71.1563	71.0000	3.0000	161.0000	41.26321
PLIC	32	259.2500	248.5000	126.0000	487.0000	87.34581
PLIC_preCG	32	42.3438	39.0000	1.0000	110.0000	27.32199
PLIC_postCG	32	24.0938	22.0000	2.0000	88.0000	20.76654
PLIC_SMA	32	22.4062	18.5000	0.0000	89.0000	21.31614
PLIC_FL	32	115.5938	111.0000	0.0000	287.0000	65.03640

ROI — region of interest, CP — cerebral peduncle, preCG — precentral gyrus, postCG — postcentral gyrus, SMA — supplementary motor area, FL — frontal lobe, PLIC — posterior limb of internal capsule; SD — standard deviation

was selected according to brain landmarks that the CST passed through and the anatomical automatic atlas provided by DSI-Studio. Hence, we verified again all patients and tested methods which were used for drawing CST by other researchers.

After reviewing recent methods of DTI of the CST, we utilised two basic types of ROIs to outline the CST [4, 11, 13, 14, 19, 21, 29]. Two main ROIs were designated as “start points”: the cerebral peduncle (CP) and the posterior limb of internal capsule (PLIC). The following were established as “end points”: the precentral gyrus (PCG), the postcentral gyrus (POCG), the supplementary motor area (SMA) and the frontal lobe (FL). By mixing and matching various combinations of the start point and the end point we obtained ten

different CSTs for analysis. An example is illustrated on Figure 1.

## RESULTS

The CST was reconstructed by 10 different algorithms for each of the 32 patients in the study, resulting in a total of 320 outlines of the CST. The fibres were visualized with DSI-studio to show the anatomical validity of the reconstruction results and we overlay the CST fibres bundles with the FA image. Although the CST was outlined in every patient, a few selected variables could not be calculated due to unknown internal software error(s). The average number of tracts that were obtained with the ten algorithms are summarised in Table 1.

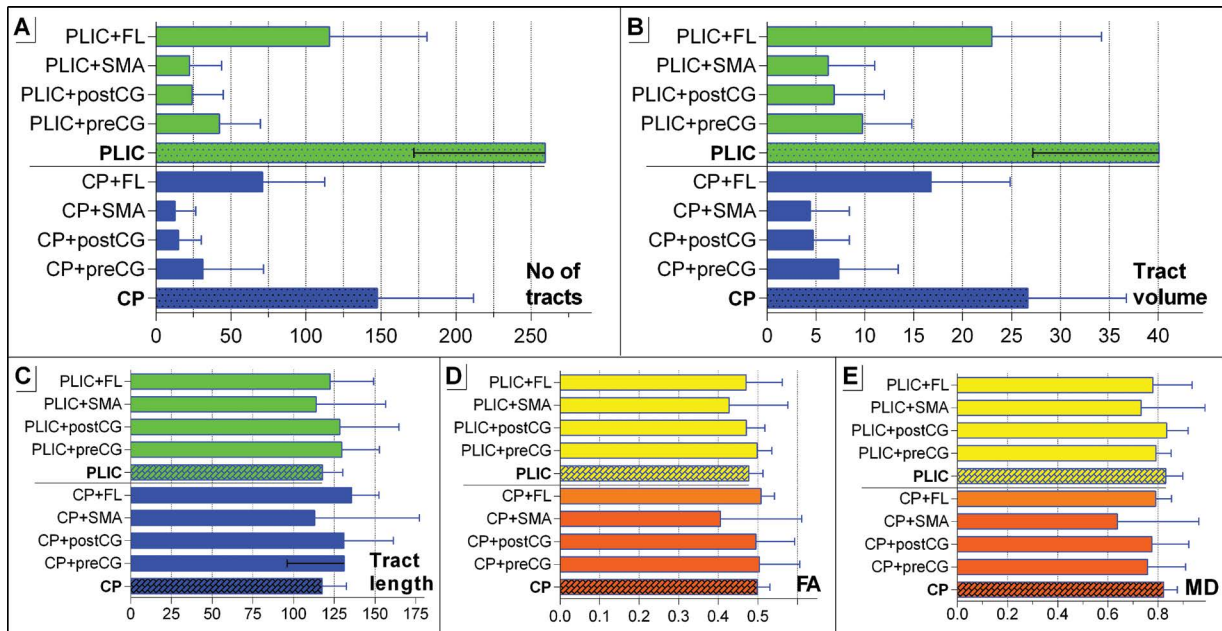


**Figure 2.** The illustration summarises the findings when using 10 different methods of outlining the corticospinal tract, including the mean; **A.** Number of tracts; **B.** Tract volume; **C.** Tract length; **D.** Fractional anisotropy (FA); **E.** The mean diffusivity (MD); PLIC — posterior limb of internal capsule, CP — cerebral peduncle, preCG — precentral gyrus, postCG — postcentral gyrus, SMA — supplementary motor area, FL — frontal lobe.

A significantly higher volume (40054U; SD  $\pm$  12874U) and number of CST tracts (259.3; SD  $\pm$  87.3) were obtained when a single ROI was set at the PLIC comparing to all other ROIs (all  $p < 0.05$ ). In contrast, almost 50% less fibres (147.6; SD  $\pm$  64.0) and volume (26664U; SD  $\pm$  10059U) was achieved when the CP was set as the ROI (both  $p < 0.05$ ) rather than the PLIC. Altogether, the PLIC and CP as starting points comprised a 6.1-fold and 4.7-fold greater number of fibres, respectively than the most common anatomical course of the CST (first ROI set at CP or PLIC, and the cortical ROI set at the precentral gyrus [preCG];  $p < 0.01$ ).

Setting the FL as the endpoint ROI yielded the highest number of tracts (PLIC and FL: 115.6; SD  $\pm$  65.0) and the highest tract volume (CP and FL: 71.1; SD  $\pm$  41.3).

There were no significant differences between the various CSTs in terms of the mean diffusion parameters (FA, MD, apparent diffusion and radial diffusivity) and mean tract length. However, all these values were insignificant when the SMA was set as a ROI (Fig. 2).

Seventeen of the 32 patients (53.1%) with preoperative hemiparesis had a brain tumour or oedema which infiltrated the CST. Even though the degree of infiltration on the CST was not evaluated, the FA, the number of tracts and the tract volumes did not differ between the CSTs drawn in ten configurations

of the ROIs (all  $p > 0.05$ ). However, in patients with CST infiltration through the CP, the MD and the apparent diffusion (AD) was significantly higher than in patients without tract infiltration ( $p = 0.04$ ). This may result from the tumour infiltrating not only the CST but other fibres which are drawn only when the CP is selected as a single ROI. The higher AD was also observed when the postcentral gyrus was added as an additional ROI to the PLIC ( $p = 0.03$ ). This patient group was mostly diagnosed high grade glioblastoma or oligodendroglioma located by the left fronto-parietal lobe, which may explain the finding.

As seen on part D and E on Figure 2, we compared the FA and MD values of the CST between the two brain hemispheres and the patient's sex, yet neither hemisphere yielded significantly different values (all  $p > 0.05$ ). However, patients older than 55 years had a significantly higher MD when the CST was traced from a start point ROI ( $p = 0.031$ ), an endpoint ROI 2 (0.036) and a start point ROI with an end point in the FL ( $p = 0.013$ ). All the statistics comparing the 10 methods of tracking the CST are presented on **Supplementary Table 1** (see journal website) (Fig. 3).

## DISCUSSION

We found that while there is no universal way of determining the CST, the CP or the PLIC should be

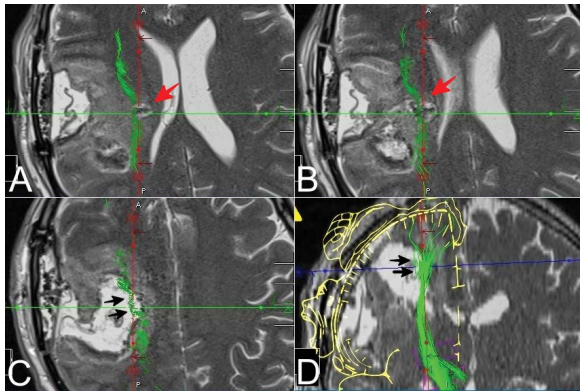


**Figure 3.** A clinical case presentation where an early postoperative magnetic resonance image was fused with a preoperative diffusion tensor imaging (DTI) of the cortico-spinal tract (CST). The subtotal resection of the secondary glioblastoma of the left fronto-parietal region was considered with the preservation of the fibres of the corticospinal tract to preserve foot function. Therefore, only the posterior limb of the internal capsule was selected as a single region of interest to increase DTI sensitivity, regardless of the decreased parallel specificity as many of fibres did not belong to the CST; **A–C.** Axial planes; **D.** Coronal plane, motor homunculus as the injected picture. The red arrows indicate the tumour remnant left deliberately in the CST. The black arrows show the compromised CST fibres responsible for hand movement.

exclusively used as the starting point ROI — regardless of whether the FL is used as the second ROI. This information is invaluable to neurosurgeons as it empowers them to obtain the most optimal view of the CST using DTI. Allowing a surgeon to better understand the spatial orientation between the tumour and the CST fibres may help preserve the CST and therefore minimize the risk of postoperative paresis; since the CST directs the movement of the limbs and the trunk [17]. To the best of our knowledge our findings are novel as our study is the first to compare the various DTI techniques regarding the CST.

It is an established issue that a long fibre bundle may not be recognised as a real fibre. Chenot proved that by using standard ROIs (i.e. PLIC and CP) we obtain a CST far beyond the primary motor cortex [6]. They showed that the CST streamlines from the premotor and parietal cortex. This finding is in contradiction with the well-known course of the pyramidal tract as described by Dejerine in 1901 [7]. To date, the exact origin of CST and the function of its non-primary motor cortex originating fibres remain unclear and unproven [2].

For neurosurgeons, the fibres originating at the precentral gyrus are the most crucial while planning any surgical access near the pyramidal tracts [10, 12, 23, 25]. A study suggests that the remainder of the

CST fibres come from the FL, mainly from the superior frontal gyrus [6]. Our results confirm this since we added the entire frontal lobe as a second ROI to the PLIC or the CP and reduced the number of fibres and the tract volume approximately 2-fold. This suggests that choosing the CP or PLIC as a single ROI does seem to be the most optimal solution when conservative access to the brain pathology is planned to minimise damage to the CST. However, limiting the extent of the ROI-based DTI to the “most anatomical” course of the CST (primary motor cortex as a second ROI to PLIC/CP), decreases the number of potentially valid fibres 6-fold as there is high variability of the CST volume among the population [6, 14]. Thus, there is no universal tractographic approach to delineate the CST due to interference of other crossing fibre tracts (although it may be overcome when the CP or the PLIC stand as a single ROI) [19]. Some authors proposed using the CP and the PLIC as two ROI where all the fibres would run through [13, 29]. At our institution we abandoned this technique and now use a custom DTI technique for all our patients because we believe that estimating the CST around the tumours at the eloquent cortex should utilise a variety of ROIs rather than a standardised set due to several of the reasons indicated before. Of note, DTI operators almost always refer to the CP as a reference for tracking the CST; however, this term is slightly ambiguous. The cerebral crus is a more accurate term anatomically as it refers solely to the anterior part of the CP (which is the correct location for CST tracking).

Setting the ROI at the PLIC was suggested as the approach most resembling the anatomical course of the CST [5]. In our study, the largest volume of the CST was achieved when a single ROI was selected, without indicating any termination points in the brain cortex. In our analysis the ROI point is relatively easy to use and is supported by most DTI data analysis software. The correct ROI may be determined on structural T1-weighted images due to their precisely defined anatomical structures. However, diffusion images that are directionally orientated (DEC sequence) are also useful to define the ROIs especially when white matter structures are being investigated. Thus, special care must be taken when choosing the appropriate ROI [26]. Seeding the termination ROI in a functionally active cortex may be regarded as the most precise method, although, this presurgical task-based functional MRI cannot provide reliable information about the CST in tumours located in the eloquent cortex [15].

In tumours located in or infiltrating the motor cortex the volume of interest (volumetric ROI) may not stand as a single cortical ROI for tracking the CST due to low accuracy [15].

Today, computer software offers automatic (anatomical) atlases to a given brain. This atlas-based method or its combination with DTI has proven to be a similar predictor of clinical outcome when compared with traditional DTI of the CST [21]. Moreover, automatic CST recognition may grant an advantage when planning brain tumour surgery. Recently, O'Donnell et al. [16] proposed the automatic patient-specific method for identifying the CST and the arcuate fasciculus and the DTI predictions corresponded with functional MRIs in 94% of patients. Additionally, the author indicated that the true anatomical termination of the main human tracts remains under debate. Thus, the combination of various techniques, including functional MRI, DTI and computational techniques, could bring scientists closer to discovering the correct CST delineation. On the contrary, the supporters of awake craniotomy for low grade gliomas urge that neuromonitoring and intraoperative stimulation maximize the tumour resection rate while still preserving motor function [8]. Yet, several patients may not be qualified for an awake procedure due to other medical and psychological reasons. We stress that in the absence of functional MRIs, an intraoperative neuromonitoring or motor mapping pathways should be considered to support DTI.

In patients with a high grade glioblastoma, where total resection remains critical, a minor neurological deficit is considered acceptable [24]. In these patients, the CP, the PLIC and the FL were deliberately selected as ROIs as they were the most important CST motor fibres that should be preserved during surgery. With this example, we assert that estimating the CST should be patient-specific as these changes in performing DTI are advantageous. Additionally, literature suggests that the CST's trajectory can change in certain brain pathologies such as a stroke, a brain tumour or a subarachnoid haemorrhage [18]. This may lead to significant alteration in the CST's original route where intraoperative direct stimulation cannot be substituted by other imaging techniques. Bello et al. reported that various types of brain tumours cause modification of white matter fibre trajectory. Based on the DTI analysis, a half of high grade gliomas caused dislocation and some tumours infiltrated or interrupted the course of tracts [3]. On the contrary, low grade gliomas only infiltrated or interrupted

tracts since only a quarter of patients had dislocated fibres. When DTI was compared with intraoperative subcortical mapping, the results illustrated that the CST's course was determined on the basis of DTI depended tumour location and volume [3].

The appropriate choice between these two ROIs lies upon the discretion of the DTI operator. Based on our analysis, seeding the CST from the PLIC results in a significantly greater number of tracks and a larger volume of the CST than seeding from the CP. We postulate that since the CP is smaller than the PLIC, it is less packed in white matter and therefore yields different results [20]. The path of the white matter fibres depends on the degree of precision of the determined ROIs. While plotting points may be determined manually or automatically, in our paper, the CST was determined with an automatic anatomical atlas using two- and three-dimensional planes.

Analysing the CST poses several challenges such as the disturbed anisotropy of water molecules and the reorganisation of nerve fibres. Moreover, tissue swelling around the tumour may disturb the proportions of perpendicular and parallel diffusion, which decreases the FA; this is due to the inversely proportional ratio of average diffusivity and cellularity of the pathology [21]. In addition, the measurement of anisotropy may become a factor differentiating tumours of high and low level of malignancy [21].

In future studies, different tractography methods can be connected with DTI multi-tensor acquisition. Identification of the CST should be carried out based on blood-oxygen-level-dependent and diffusion functional MRIs [9]. These methods may help a physician achieve a better regional and spatial understanding of an area.

## CONCLUSIONS

Our study identified the CST based on various anatomical approaches. We found that while there is no universal method of determining the CST, the CP or the PLIC should be used as the starting point ROIs.

## REFERENCES

1. Anthofer JM, Steib K, Fellner C, et al. DTI-based deterministic fibre tracking of the medial forebrain bundle. *Acta Neurochir (Wien)*. 2015; 157(3): 469–477, doi: [10.1007/s00701-014-2335-y](https://doi.org/10.1007/s00701-014-2335-y), indexed in Pubmed: [25585836](https://pubmed.ncbi.nlm.nih.gov/25585836/).
2. Archer DB, Vaillancourt DE, Coombes SA. A template and probabilistic atlas of the human sensorimotor tracts using diffusion MRI. *Cereb Cortex*. 2018; 28(5): 1685–1699, doi: [10.1093/cercor/bhx066](https://doi.org/10.1093/cercor/bhx066), indexed in Pubmed: [28334314](https://pubmed.ncbi.nlm.nih.gov/28334314/).
3. Bello L, Gambini A, Castellano A, et al. Motor and language DTI fiber tracking combined with intraoperative

- subcortical mapping for surgical removal of gliomas. *Neuroimage*. 2008; 39(1): 369–382, doi: [10.1016/j.neuroimage.2007.08.031](https://doi.org/10.1016/j.neuroimage.2007.08.031), indexed in Pubmed: [17911032](https://pubmed.ncbi.nlm.nih.gov/17911032/).
4. Bonney PA, Conner AK, Boettcher LB, et al. A simplified method of accurate postprocessing of diffusion tensor imaging for use in brain tumor resection. *Oper Neurosurg (Hagerstown)*. 2017; 13(1): 47–59, doi: [10.1227/NEU.0000000000001181](https://doi.org/10.1227/NEU.0000000000001181), indexed in Pubmed: [28931252](https://pubmed.ncbi.nlm.nih.gov/28931252/).
  5. Bürgel U, Amunts K, Hoemke L, et al. White matter fiber tracts of the human brain: three-dimensional mapping at microscopic resolution, topography and intersubject variability. *Neuroimage*. 2006; 29(4): 1092–1105, doi: [10.1016/j.neuroimage.2005.08.040](https://doi.org/10.1016/j.neuroimage.2005.08.040), indexed in Pubmed: [16236527](https://pubmed.ncbi.nlm.nih.gov/16236527/).
  6. Chenot Q, Tzourio-Mazoyer N, Rheault F, et al. A population-based atlas of the human pyramidal tract in 410 healthy participants. *Brain Struct Funct*. 2019; 224(2): 599–612, doi: [10.1007/s00429-018-1798-7](https://doi.org/10.1007/s00429-018-1798-7), indexed in Pubmed: [30460551](https://pubmed.ncbi.nlm.nih.gov/30460551/).
  7. Dejerine J, Dejerine-Klumpke A. *Anatomie des centres nerveux*. Tome 2. Rueff et Cie, Paris 1901.
  8. Duffau H, Taillandier L. New concepts in the management of diffuse low-grade glioma: Proposal of a multistage and individualized therapeutic approach. *Neuro Oncol*. 2015; 17(3): 332–342, doi: [10.1093/neuonc/nou153](https://doi.org/10.1093/neuonc/nou153), indexed in Pubmed: [25087230](https://pubmed.ncbi.nlm.nih.gov/25087230/).
  9. Holodny AI, Ollenschleger MD, Liu WC, et al. Identification of the corticospinal tracts achieved using blood-oxygen-level-dependent and diffusion functional MR imaging in patients with brain tumors. *Am J Neuroradiol*. 2001; 22(1): 83–88, indexed in Pubmed: [11158892](https://pubmed.ncbi.nlm.nih.gov/11158892/).
  10. Kieronska S, Słoniewski P. The usefulness and limitations of diffusion tensor imaging – a review study. *Eur J Transl Clin Med*. 2020; 2(2): 43–51, doi: [10.31373/ejtc/112437](https://doi.org/10.31373/ejtc/112437).
  11. Kim B, Fisher BE, Schweighofer N, et al. A comparison of seven different DTI-derived estimates of corticospinal tract structural characteristics in chronic stroke survivors. *J Neurosci Methods*. 2018; 304: 66–75, doi: [10.1016/j.jneumeth.2018.04.010](https://doi.org/10.1016/j.jneumeth.2018.04.010), indexed in Pubmed: [29684462](https://pubmed.ncbi.nlm.nih.gov/29684462/).
  12. Krakowiak M, Słoniewski P, Dzierżanowski J, et al. Future of the nerve fibres imaging: tractography application and development directions. *Folia Morphol*. 2015; 74(3): 290–294, doi: [10.5603/FM.2015.0044](https://doi.org/10.5603/FM.2015.0044), indexed in Pubmed: [26339808](https://pubmed.ncbi.nlm.nih.gov/26339808/).
  13. Kuczynski AM, Dukelow SP, Hodge JA, et al. Corticospinal tract diffusion properties and robotic visually guided reaching in children with hemiparetic cerebral palsy. *Hum Brain Mapp*. 2018; 39(3): 1130–1144, doi: [10.1002/hbm.23904](https://doi.org/10.1002/hbm.23904), indexed in Pubmed: [29193460](https://pubmed.ncbi.nlm.nih.gov/29193460/).
  14. Leote J, Nunes RG, Cerqueira L, et al. Reconstruction of white matter fibre tracts using diffusion kurtosis tensor imaging at 1.5T: Pre-surgical planning in patients with gliomas. *Eur J Radiol Open*. 2018; 5: 20–23, doi: [10.1016/j.ejro.2018.01.002](https://doi.org/10.1016/j.ejro.2018.01.002), indexed in Pubmed: [29719853](https://pubmed.ncbi.nlm.nih.gov/29719853/).
  15. Niu C, Liu X, Yang Y, et al. Assessing region of interest schemes for the corticospinal tract in patients with brain tumors. *Medicine (Baltimore)*. 2016; 95(12): e3189, doi: [10.1097/MD.00000000000003189](https://doi.org/10.1097/MD.00000000000003189), indexed in Pubmed: [27015212](https://pubmed.ncbi.nlm.nih.gov/27015212/).
  16. O'Donnell LJ, Suter Y, Rigolo L, et al. Automated white matter fiber tract identification in patients with brain tumors. *Neuroimage Clin*. 2017; 13: 138–153, doi: [10.1016/j.nicl.2016.11.023](https://doi.org/10.1016/j.nicl.2016.11.023), indexed in Pubmed: [27981029](https://pubmed.ncbi.nlm.nih.gov/27981029/).
  17. Ottenhausen M, Krieg SM, Meyer B, et al. Functional preoperative and intraoperative mapping and monitoring: increasing safety and efficacy in glioma surgery. *Neurosurg Focus*. 2015; 38(1): E3, doi: [10.3171/2014.10.FOCUS14611](https://doi.org/10.3171/2014.10.FOCUS14611), indexed in Pubmed: [25552283](https://pubmed.ncbi.nlm.nih.gov/25552283/).
  18. Park CH, Kou N, Boudrias MH, et al. Assessing a standardised approach to measuring corticospinal integrity after stroke with DTI. *Neuroimage Clin*. 2013; 2: 521–533, doi: [10.1016/j.nicl.2013.04.002](https://doi.org/10.1016/j.nicl.2013.04.002), indexed in Pubmed: [24179804](https://pubmed.ncbi.nlm.nih.gov/24179804/).
  19. Pujol S, Wells W, Pierpaoli C, et al. The DTI challenge: toward standardized evaluation of diffusion tensor imaging tractography for neurosurgery. *J Neuroimaging*. 2015; 25(6): 875–882, doi: [10.1111/jon.12283](https://doi.org/10.1111/jon.12283), indexed in Pubmed: [26259925](https://pubmed.ncbi.nlm.nih.gov/26259925/).
  20. Radmanesh A, Zamani AA, Whalen S, et al. Comparison of seeding methods for visualization of the corticospinal tracts using single tensor tractography. *Clin Neuro Neurosurg*. 2015; 129: 44–49, doi: [10.1016/j.clineuro.2014.11.021](https://doi.org/10.1016/j.clineuro.2014.11.021), indexed in Pubmed: [25532134](https://pubmed.ncbi.nlm.nih.gov/25532134/).
  21. Ressel V, van Hedel HJA, Scheer I, et al. Comparison of DTI analysis methods for clinical research: influence of pre-processing and tract selection methods. *Eur Radiol Exp*. 2018; 2(1): 33, doi: [10.1186/s41747-018-0066-1](https://doi.org/10.1186/s41747-018-0066-1), indexed in Pubmed: [30426317](https://pubmed.ncbi.nlm.nih.gov/30426317/).
  22. Soni N, Mehrotra A, Behari S, et al. Diffusion-tensor imaging and tractography application in pre-operative planning of intra-axial brain lesions. *Cureus*. 2017; 9(10): e1739, doi: [10.7759/cureus.1739](https://doi.org/10.7759/cureus.1739), indexed in Pubmed: [29209586](https://pubmed.ncbi.nlm.nih.gov/29209586/).
  23. Szmuda T, Ali S. Commentary on: The usefulness and limitations of diffusion tensor imaging – a review study. *Eur J Transl Clin Med*. 2020; 2(2): 85–86, doi: [10.31373/ejtc/114000](https://doi.org/10.31373/ejtc/114000).
  24. Szmuda T, Słoniewski P, Olijewski W, et al. Colour contrasting between tissues predicts the resection in 5-aminolevulinic acid-guided surgery of malignant gliomas. *J Neurooncol*. 2015; 122(3): 575–584, doi: [10.1007/s11060-015-1750-0](https://doi.org/10.1007/s11060-015-1750-0), indexed in Pubmed: [25702194](https://pubmed.ncbi.nlm.nih.gov/25702194/).
  25. Szmuda T, Słoniewski P, Szmuda M, et al. Quantification of white matter fibre pathways disruption in frontal transcortical approach to the lateral ventricle or the interventricular foramen in diffusion tensor tractography. *Folia Morphol*. 2014; 73(2): 129–138, doi: [10.5603/FM.2013.0063](https://doi.org/10.5603/FM.2013.0063), indexed in Pubmed: [24902089](https://pubmed.ncbi.nlm.nih.gov/24902089/).
  26. Van Hecke W, Emsell L, Sunaert S. *Diffusion Tensor Imaging: A Practical Handbook*. Diffus Tensor Imaging A Pract Handb. 2016: 1–440, doi: [10.1007/978-1-4939-3118-7](https://doi.org/10.1007/978-1-4939-3118-7).
  27. Witwer BP, Moftakhar R, Hasan KM, et al. Diffusion-tensor imaging of white matter tracts in patients with cerebral neoplasm. *J Neurosurg*. 2002; 97(3): 568–575, doi: [10.3171/jns.2002.97.3.0568](https://doi.org/10.3171/jns.2002.97.3.0568), indexed in Pubmed: [12296640](https://pubmed.ncbi.nlm.nih.gov/12296640/).
  28. Yeh FC, Wedeen VJ, Tseng WYI. Generalized q-sampling imaging. *IEEE Trans Med Imaging*. 2010; 29(9): 1626–1635, doi: [10.1109/TMI.2010.2045126](https://doi.org/10.1109/TMI.2010.2045126), indexed in Pubmed: [20304721](https://pubmed.ncbi.nlm.nih.gov/20304721/).
  29. Yu Qi, Lin K, Liu Y, et al. Clinical uses of diffusion tensor imaging fiber tracking merged neuronavigation with lesions adjacent to corticospinal tract : a retrospective cohort study. *J Korean Neurosurg Soc*. 2020; 63(2): 248–260, doi: [10.3340/jkns.2019.0046](https://doi.org/10.3340/jkns.2019.0046), indexed in Pubmed: [31295976](https://pubmed.ncbi.nlm.nih.gov/31295976/).



## **5.7. Omówienie pracy „Reliability of diffusion tensor tractography of facial nerve in cerebello-pontine angle tumours”**

Praca zatytułowana „Reliability of diffusion tensor tractography of facial nerve in cerebello-pontine angle tumours” opublikowana w Polish Journal of Neurology and Neurosurgery opisuje metodę wizualizacji przebiegu nerwu twarzowego (FN-facial nerve) u pacjentów z rozpoznaniem guza kąta mostowo-mózdkowego.

Materiał stanowiło 38 pacjentów z rozpoznaniem guza kąta mostowo-mózdkowego (32 nerwiaki osłonkowe nerwu VIII, 5 oponiaki, 1 torbiel naskórkowa). Nerw twarzowy w każdym przypadku został wykreślony na podstawie badania MR głowy z wykorzystaniem programu StealthViz Medtronic wykorzystując protokół deterministyczny. Wizualizacja nerwu VII przedoperacyjnie została porównana z przebiegiem nerwu w warunkach śródoperacyjnych.

U 31 pacjentów wykazano zgodność przebiegu nerwu VII śródoperacyjnie z wytyczonym przebiegiem na podstawie traktografii. Dokładność DTI-FN wyniosła 81,6%, czułość 88,57%. Wiarygodność wizualizacji zintegrowanej z neuronawigacją nie wykazywała korelacji z wielkością guza. Po zabiegu resekcji guzów 86,5% pacjentów prezentowała przydatną funkcję w zakresie nerwu twarzowego (I-III w skali House Brackman).

W artykule przedstawiono również trudności i ograniczenia związane z wykreślaniem przebiegu nerwu twarzowego związane ze stopniem rozproszenia włókien w obrębie kąta mostowo-mózdkowego oraz ograniczeń z nakreśleniem typowego ROI. Wysoki stopień zgodności przebiegu nerwu VII w traktografii z obrazem śródoperacyjnym sugeruje, iż jest to właściwa i skuteczna metoda wizualizacji i planowania zabiegu operacyjnego.



# Reliability of diffusion tensor tractography of facial nerve in cerebello-pontine angle tumours

Tomasz Szmuda<sup>1</sup>, Paweł Słoniewski<sup>1</sup>, Shan Ali<sup>2</sup>, Pedro M. Gonçalves Pereira<sup>3</sup>, Mateusz Pacholski<sup>2</sup>,  
Fanar Timemy<sup>2</sup>, Agnieszka Sabisz<sup>4</sup>, Edyta Szurowska<sup>4</sup>, Sara Kierońska<sup>1</sup>

<sup>1</sup>Neurosurgery Department, Medical University of Gdansk, Poland

<sup>2</sup>Students' Scientific Circle of Neurology and Neurosurgery, Medical University of Gdansk, Poland

<sup>3</sup>Algarve Biomedical Centre, University of Algarve, Faro, Portugal

<sup>4</sup>Radiology Department, Medical University of Gdansk, Poland

## ABSTRACT

**Aim of the study.** This study aimed to verify the accuracy of preoperative visualisation of the facial nerve (FN) by magnetic resonance-based (MR) diffusion tensor imaging-fibre tracking (DTI-FT) with neuronavigation system integration in patients with cerebello-pontine angle (CPA) tumours.

**Clinical rationale for the study.** Complete excision with preservation of the FN remains the critical goal of today's vestibular schwannoma (VS) surgery. DTI-FT of the FN with neuronavigation is yet to be fully evaluated, and could make surgery safer.

**Materials and methods.** This was a prospective cohort study in which 38 consecutive patients with a CPA tumour (32 VSs, five meningiomas and one epidermoid cyst) were operated on via the retrosigmoid route from 2013 to 2019. The course of the FN was simulated before surgery using StealthViz and the images were transferred to the Medtronic S7 neuronavigation system. The FN location reconstructed by DTI-FT was verified during the surgery.

**Results.** MR acquisition was inappropriate in three patients (7.9%). DTI-FT correctly predicted the course of the FN in 31 of the 38 patients; the discordance rate was 18.4%. The accuracy of DTI-FT was 81.6% (95% CI: 65.67–92.26), sensitivity 88.57% (95% CI: 73.26–96.80) and positive predictive value was 91.18% (95% CI: 90.17–92.09). The reliability of the neuronavigation-integrated visualisation of the FN did not depend on the tumour size ( $p = 0.85$ ), but the method was more accurate when the nerve was compact in shape ( $p = 0.03$ , area under curve (AUC) 0.87, 95% CI: 0.60–1.00) and in females ( $p = 0.04$ , AUC 0.78, 95% CI: 0.56–1.00). Following surgery, 86.5% of the patients presented with useful facial function (House-Brackmann grades I–III). Correct simulation of the FN did not prevent postoperative facial palsy ( $p = 0.35$ ).

**Conclusions.** The accuracy of DTI-FT of the FN integrated with neuronavigation remains unsatisfactory. This method does not provide any clinical benefit over non-integrated DTI-FT in terms of nerve function preservation.

**Clinical implications.** Due to the low reliability of the predictions, further technical advances in predicting the course of the FN are awaited by clinicians. However, DTI-FT images in the operating theatre would make tumour excision more comfortable for the surgeon.

**Key words:** cerebello-pontine angle, facial nerve, magnetic resonance imaging, diffusion tensor imaging, vestibular schwannoma  
(*Neurol Neurochir Pol* 2020; 54 (1): 73–82)

**Address for correspondence:** Tomasz Szmuda, Neurosurgery Department, Medical University of Gdansk, Dębinki 7 Str., 80-952 Gdansk, Poland,  
e-mail: tszmuda@gumed.edu.pl

## Introduction

Vestibular schwannomas (VSs), meningiomas and epidermoid cysts account for 80% of the tumours found within the cerebello-pontine angle (CPA) of the posterior fossa [1]. Beyond the excision of these tumours, facial nerve (FN) preservation is of vital importance, especially with VSs [2–6]. Intraoperative nerve injury not only affects a patient's quality of life, but is also a major cause of morbidity following the excision of a VS [3, 5]. To date, the FN's course remains unpredictable [6]. In addition, nerve flattening or compression by a growing tumour limits the reliable visual identification of the FN during the surgery [3]. Due to these variables, safe surgery of VSs remains a challenge. Direct intraoperative electrophysiological monitoring has been used for early FN identification, but this technique remains inadequate [3, 7, 8]. For this reason, imaging techniques—based on conventional magnetic resonance (MR) cisternography [9]—have been developed that preoperatively simulate the position of the FN around the CPA tumour.

One recent example is diffusion tensor imaging-fibre tracking (DTI-FT) which is a non-invasive MR-based imaging modality. Since Taoka et al. first applied this technique to patients with VS, DTI-FT has emerged as a powerful technique in reconstructing the FN [3, 4, 9–11].

Despite the variable acquisition techniques, software and tracking methods, the predictive reliability of the FN's position in VS patients has reached 90.6%. Unfortunately, this is still not complete enough for neurological surgery [4]. Furthermore, the authors of a systematic review on DTI-FT of FN concluded that the integration of preoperative planning with neuronavigation is still to be evaluated [4]. To date, only one 18-patient study has assessed the effect of DTI-FT-integrated neuronavigation [6]. In our study, we evaluated the clinical benefit of preserving the FN offered by this technique.

## Materials and methods

### Study population

Patients with a primary CPA tumour were prospectively enrolled into this study from April 2013 to August 2019 at the Neurosurgery Department of the Medical University of Gdańsk in Poland. The routine local protocol for patients with a suspected VS, meningioma or epidermoid cyst, covered the acquisition of the CPA tumours-adjusted MR protocol prior to surgery. Meningiomas objectively not affecting the course of the FN were excluded from analysis.

The cohort consisted of 38 patients, comprising 19 males and 19 females; the mean and median ages were 54.4 and 57.5 years, respectively. The most common histopathology was VS ( $n = 32$ , 84.2%), followed by meningioma ( $n = 5$ , 13.2%). There was one epidermoid cyst (2.6%) in our series. The mean tumour diameter was 29.6 mm ( $SD \pm 12.7$ , min-max 9–70), and 28.8 mm specifically for VS ( $SD \pm 10.9$ ; min-max 9–48).

Of the VSs, three (9.4%) were graded Koos I, 12 (37.5%) Koos II, 12 (37.5%) Koos III, and five (15.6%) Koos IV [12]. All 32 patients with a VS presented with sensorineural hearing loss, but only one had facial palsy at admission.

All the tumours were approached via retrosigmoid craniectomy; other approaches such as a presigmoid approach were not considered. In order to avoid air embolisms, the patient was positioned prone and the extent of the osteotomy was tailored to the particular tumour size. Following a C-shaped dural incision, the cisterns were opened. The manner of the tumour excision depended on the histopathology. In meningiomas, the tumour was first detached from the dura by an electric cautery and then removed in pieces. In VSs, the internal acoustic meatus was opened by a high-speed coarse and diamond drills following initial debulking. Afterwards, the intracanalicular portion of the tumour was gently removed. The FN was identified with direct mono- or bipolar stimulation by applying pulsed constant-current stimulation (ISIS IOM, Inomed, Emmendingen, Germany; NeuroExplorer software v. 5.1). The nerve, cerebellum and pons were dissected, and then the tumour was excised. An ultrasonic aspiration knife facilitated the excision of most tumours. Facial nerve function was evaluated approximately two weeks after the surgery according to the House-Brackmann (HB) classification [13]. Facial palsy was recognised if the HB grade was II to VI.

Informed consent was obtained from all patients and the protocol of this study was approved by the local Ethics Committee. We adhered to the STROBE Statement, a checklist of items for observational studies [14].

### Imaging acquisition

MR scans were acquired on a 1.5 tesla Siemens Magnetom Aera 1.5T (Erlangen, Germany) with a 20-channel head coil. The imaging protocol for CPA tumour included: T1, T2-weighted, constructive interference in steady state (CISS) and post-gadolinium T1-weighted (the last sequence served as a reference for neuronavigation). Diffusion-weighted imaging (DWI) was obtained by readout segmentation of long variable echo-trains high-definition protocol (predefined by the manufacturer, *syngo* RESOLVE™). The number of diffusion-encoding gradient directions was 20, the b-factor was 0, 1,000 s/mm<sup>2</sup> (see Table 2 for MR acquisition details). Except for bone masking, we did not perform any additional digital transformations such as motion or edgy corrections. The diffusion tensor of a single voxel was calculated using multivariate linear fitting. In that way, each voxel owned three eigenvectors, and the voxel associated with the largest eigenvalue denoted the ultimate fibre direction.

### Data processing

The entire MR exam was imported to StealthViz software with a StealthDTI™ module (Medtronic Inc., Minneapolis, MN, USA), and later fused and manually verified. Based on the DWI sequence, the particular DTI derivate images were

**Table 1.** Patient characteristics, outcomes and facial nerve fibre tracking

No.	Year of surgery	Age	Sex	Side	Pathology	Koos grade	Tumour diameter (mm)	Facial nerve position (DTI-FT)	Facial nerve position (intraoperative)	Facial nerve (flat/compact)	Agreement (DTI— intraoperative)	Facial nerve function (House-Brackmann grade)	Complete excision
1	2013	38	F	R	VS	1	9	anterior	anterior	C	1	1	1
2	2013	30	M	R	VS	2	21	antero-superior	antero-inferior	Flat	0	2	1
3	2013	57	M	R	VS	2	25	antero-superior	antero-superior	Flat	1	3	1
4	2013	58	M	R	Epidermoid cyst	NA	70	anterior	anterior	C	1	1	0
5	2014	69	F	L	VS	3	22	antero-superior	antero-superior	C	1	4	1
6	2014	51	F	R	VS	2	27	anterior	anterior	C	1	1	1
7	2014	65	M	R	MG	NA	19	wrong MR acquisition	antero-medial	C	0	1	1
8	2014	43	M	L	VS	4	45	penetrating	penetrating	Flat	1	1	0
9	2014	70	M	L	VS	4	45	superior	superior	Flat	1	1	0
10	2014	62	M	R	VS	3	38	superior	antero-superior	UNK	0	death	0
11	2014	37	M	R	VS	1	19	superior	superior	Flat	1	2	1
12	2014	60	F	L	VS	1	10	antero-superior	antero-superior	C	1	1	1
13	2015	61	M	L	VS	3	39	posterior	anterior	Flat	0	6	1
14	2015	35	F	R	VS	4	48	inferior	inferior	UNK	1	6	1
15	2015	71	M	L	VS	3	32	antero-inferior	antero-inferior	C	1	1	0
16	2015	81	M	L	VS	3	23	UNK	antero-superior	Flat	0	1	1
17	2015	71	F	R	VS	4	38	postero-superior	postero-superior	Flat	1	3	0
18	2016	54	F	L	VS	3	27	antero-inferior	antero-inferior	C	1	1	1
19	2016	57	M	R	VS	2	10	antero-superior	antero-superior	C	1	1	1
20	2016	25	M	R	VS	2	36	antero-superior	antero-superior	C	1	1	0
21	2017	49	M	R	VS	2	29	wrong MR acquisition	antero-superior	C	0	2	1
22	2017	56	F	R	MG	NA	43	anterior	anterior	C	1	1	1
23	2017	50	F	L	VS	4	43	postero-inferior	postero-inferior	Flat	1	1	0
24	2017	43	F	L	VS	2	16	wrong MR acquisition	anterior	C	0	1	1
25	2017	35	F	L	VS	3	35	antero-superior	antero-superior	C	1	4	1
26	2017	32	F	R	VS	3	41	antero-superior	antero-superior	Flat	1	5	1
27	2018	63	F	L	VS	2	37	antero-superior	antero-superior	C	1	2	1
28	2018	48	M	R	VS	2	33	superior	superior	C	1	1	1
29	2018	72	F	L	VS	2	17	antero-superior	antero-superior	C	1	1	1
30	2018	50	F	L	VS	3	30	antero-superior	antero-superior	C	1	1	0
31	2018	58	F	L	VS	2	31	antero-superior	antero-superior	C	1	1	1
32	2018	59	M	R	VS	3	19	superior	superior	C	1	1	1
33	2018	62	M	L	VS	3	36	antero-superior	antero-superior	Flat	1	2	0
34	2018	44	F	R	MG	NA	12	anterior	anterior	C	1	1	1
35	2019	62	F	R	VS	3	22	antero-superior	antero-superior	C	1	3	1
36	2019	67	M	L	MG	NA	23	anterior	anterior	C	1	1	1
37	2019	61	M	R	VS	2	18	antero-superior	antero-superior	C	1	2	1
38	2019	60	F	L	MG	NA	35	anterior	anterior	C	1	1	1

C — compact; DTI-FT — diffusion tensor imaging-fibre tracking; F — female; M — male; NA — not applicable; VS — vestibular schwannoma; MG — meningioma; L — left; R — right

**Table 2.** Main parameters of magnetic resonance sequences

Sequence type	Plane	Name of specific technique	Field-of-view [mm x mm]	Voxel size [mm x mm x mm]	Gap [%]	Number of slices	Repetition Time [ms]	Echo Time [ms]	Time of Inversion [ms]	Signal Averaging
T2-weighted	sagittal	blade	250 x 250	0.7 x 0.7 x 4.0	20	30	4,430	146	-	1
T2-weighted	coronal	TSE	250 x 250	0.5 x 0.5 x 4.0	20	28	5,180	109	-	2
T2-weighted FLAIR	transverse	TIR	260 x 187	0.4 x 0.4 x 4.0	20	30	9,000	106	2,500	1
T2-weighted	transverse	CISS	220 x 165	0.4 x 0.4 x 0.7	20	88	5.66	2.83	-	1
DTI	transverse	RESOLVE	230 x 230	1.5 x 1.5 x 1.5	0	30	4,870	74 and 111	-	2
T2-weighted	transverse	TSE	250 x 187	0.6 x 0.6 x 2.0	0	80	15,960	89	-	1
T1-weighted	transverse	MPRAGE	260 x 260	1.0 x 1.0 x 1.0	50	176	1,730	3.27	800	1

mm — millimetres; TSE — turbo spin echo; TIR — triple inversion recovery; CISS — constructive interference in steady state; DTI — diffusion tensor imaging

automatically calculated, including directionally encoded colours, apparent diffusion coefficient, fractional anisotropy (FA) and mean diffusivity. In order to track the nerve, a single region-of-interest was set in the entire internal acoustic meatus. The FA start value was 0.2 and the angle threshold was  $> 60^\circ$ , although these values were balanced individually during post-processing. The thicker bundle starting from the meatus and rounding the tumour was visualised and recorded as a predicted location of the FN. To define the course of the FN, the angle of view was adjusted to the perspective proposed by Sampath et al. [15].

Accordingly, the FN location in relation to the tumour was categorised as: anterior, antero-superior, superior, posterior or inferior. Multiplanar reconstructions as well as three-dimensional modelling enabled assessment of the structures in various planes as well as with the retrosigmoid approach. Both the tumour volume and the predicted course of the FN were segmented, and exported, together with the reference exam (contrast-enhanced T1-weighted sequence) to the neuronavigation system (StealthStation S7, Medtronic Inc., Minneapolis, MN, USA). The surgical microscope (Pentero 800, Carl Zeiss AG, Oberkochen, Germany) was fully integrated with the navigation system, with a display that was updated in real time with the microscope's movement. Both the surgeries and the neuronavigation display were recorded simultaneously; these videos were used for post-hoc analysis between the predicted course of the FN and the actual course found during the surgery. Unlike other studies [7, 16], the surgeon was not blinded to the results of preoperative DTI-FT. The segmented tumour and the FN (prepared by the first author) were seen by the surgeon (the senior author) in the navigation display and/or in the injected picture in the surgical microscope. **See the supplementary video** showing how the FN was tracked.

### Outcome measures

The single outcome measure was the prediction accuracy of the FN's path made with DTI-FT integrated with

a neuronavigation system. Intraoperative monitoring and/or visual recognition of the FN confirmed the actual course of the FN. The sensitivity and specificity of DTI-FT was calculated. We also aimed to associate the clinical and radiological factors with agreement between the predicted and the actual position of the nerve.

### Statistical methods

Continuous variables were described by the mean, standard deviation and range, and were compared using the Mann-Whitney U test. Chi-square and two-tailed Fisher's exact test was used for the analysis of categorical data.

We used software for particular statistical analyses: Statistica v. 13.1 (StatSoft Co, Tulsa, OK, USA) and Prism v. 6.07 (GraphPad Software, La Jolla, CA, USA). A p value below 0.05 was deemed significant. Receiver operating characteristic curves for significant variables were created and the

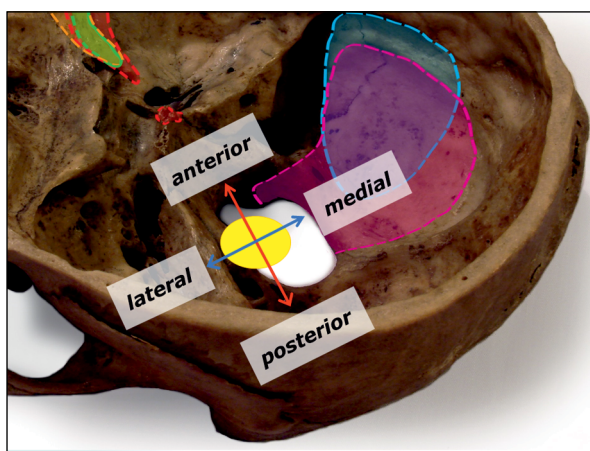


**Figure 1.** This illustration of the left-sided vestibular schwannoma demonstrates the possible positions of the facial nerve according to the Sampath classification [15]. Typical retrosigmoid craniectomy is marked in blue, and the extended craniectomy to the foramen magnum that was used for large tumours is marked in violet.

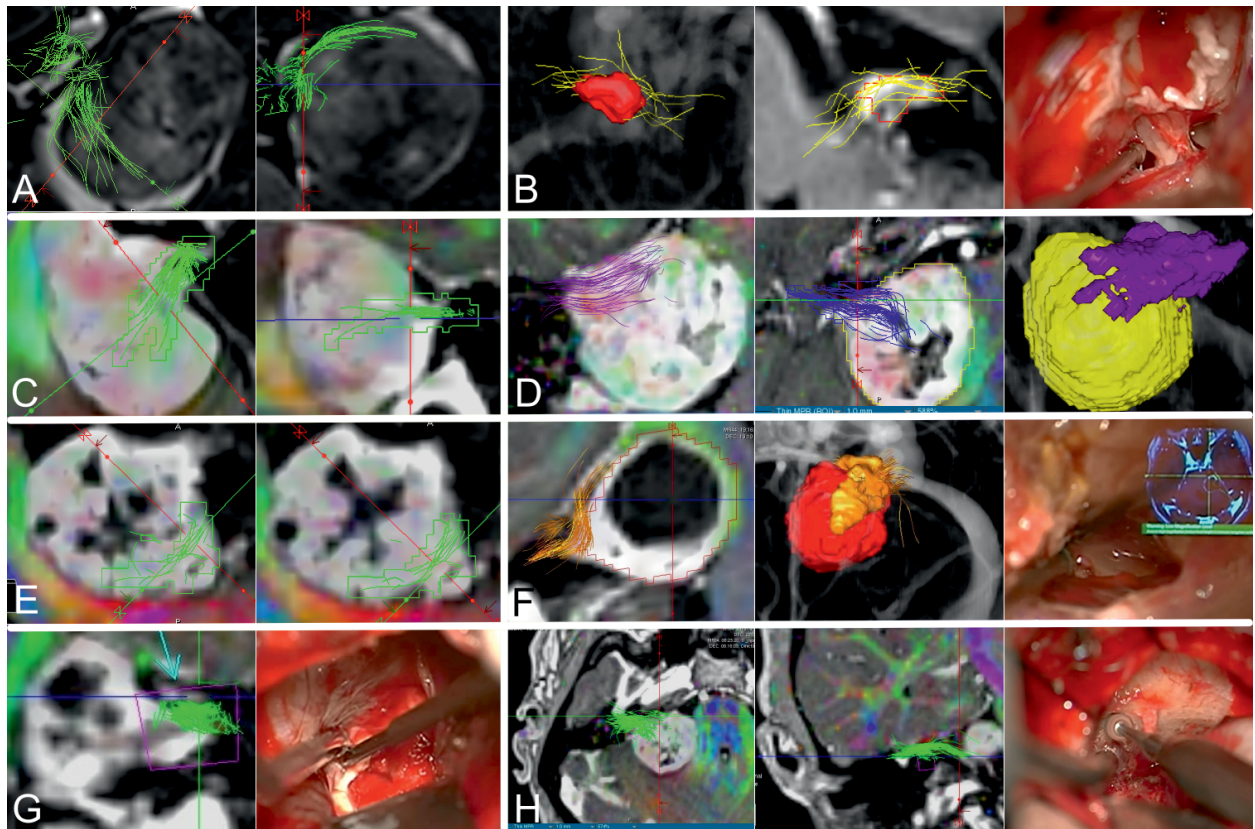


**Figure 2.** Illustration of facial nerve (FN) courses (colour bundles) tracked by diffusion tensor imaging. All presented cases are vestibular schwannomas.

A. Case 17: Postero-superior, axial view, coronal view.

B. Case 12: Antero-superior, three-dimensional model, axial view and intraoperative snapshot.

C. Case 32: Superior, axial views.

D. Case 9: Superior, axial views and three-dimensional model.

E. Case 33: Antero-superior, axial views.

F. Case 3: Antero-superior, axial view, three-dimensional model and intraoperative snapshot with injected quarter-screen picture of real-time neuronavigation.

G. Case 5: Antero-superior, sagittal view and intraoperative snapshot.

H. Case 6: Anterior, axial, coronal view and intraoperative snapshot.

area under the curves (AUC) were compared in MedCalc v. 11.4 (MedCalc Software; Mariakerke, Belgium).

## Results

### Surgical outcome

The postoperative course, as well as the final clinical outcome, were uneventful in all patients, except for one mortality due to an idiopathic vast pontine oedema. Surgery-related facial palsy (HB grade II-VI) was recognised in 14 patients (14/37; 36.8%). No or minor facial palsy (known as 'useful facial function'; HB grades I-III) was present in 32 patients (32/37; 86.5%). Since all surgeries were done in the prone position, we did not encounter any air embolism. There was no sinus or vertebral artery injury during the craniotomy. Other intraoperative complications included a local haematoma requiring surgical revision in one patient. Postoperative cerebrospinal

fluid leakage was encountered in 4/37 patients (10.8%) and was treated successfully by external lumbar drainage, although the hospital stay was prolonged in these patients.

### Facial nerve prediction

In the 35 patients where DTI was comprehensive, the correct course of the FN was seen in 24 cases (24/35; 68.6%). In 10 cases (10/35; 28.6%) the nerve's path was highly predictive as the main fibre bundle determined the FN's position. The FN was not visualised in one individual (1/35; 2.9%) with a cystic VS (23 mm in diameter).

In our study, DTI-FT correctly predicted the course of the FN in 31 out of 38 patients (81.6%). However, the prediction accuracy jumped to 31 out of 35 patients (88.6%) when we only included patients in whom DTI-FT was performed properly. Regarding the subset of VSs, DTI-FT was correct in simulating the FN's position in 26 out of 30 patients (86.7%).

Among VSs, the antero-superior (17/38, 44.7%) and anterior (9/38, 23.7%) were the most common positions of the FN around the tumour according to the Sampath classification [15]. DTI-FT was more accurate when the nerve was not flat ( $p = 0.03$ ) and in females ( $p = 0.04$ ). The identification rate did not differ significantly ( $p = 0.43$ ) in regard to the FN's position. The reliability of DTI-FT for the FN did not depend on other analysed factors such as tumour size ( $p = 0.85$ ). Receiver operating characteristic curves for the FN shape and sex were subsequently compared; AUC was 0.87 (95% CI: 0.60-1.00) and 0.78 (95% CI: 0.56-1.00), respectively. We found that the shape of the FN was the dominant component influencing the accuracy of DTI-FT, as there was a larger AUC for a compactly shaped FN. However, the comparison of AUCs was not significant ( $p = 0.63$ ).

The accuracy of the preoperative visualisation of the FN did not prevent facial palsy ( $p = 0.35$ ); the AUC for the House-Brackmann grade was 0.69 (95% CI: 0.34-1.00).

The calculated accuracy DTI-FT was 81.58% (95% CI: 65.67 to 92.26). The comprehensive predictive capability of DTI-FT was additionally evaluated by tools for a diagnostic test evaluation. These values were respectively: sensitivity 88.57% (95% CI: 73.26 to 96.80), specificity 0% (95% CI: 0 to 70.76) and positive predictive value of 91.18% (95% CI: 90.17 to 92.09).

## Discussion

We found that the FN's path can be predicted correctly with preoperative DTI-FT visualisations in four-fifths of patients (81.6%) with a CPA tumour; but this is far from the long-desired goal in neurosurgery. Moreover, the integration of surgical planning with the neuronavigation system did not increase the prediction rate when compared to previous studies solely relying on non-integrated preoperative DTI-FT simulations [3, 4]. Today, there is growing interest in the reliable identification of the FN in CPA angle tumours, so further advances are necessary [3, 4]. Our findings are novel because the integration of preoperative planning with neuronavigation is only just beginning to be explored in neurological surgery.

Since DTI-FT of cranial nerves first came to the attention of the neurosurgical community, fewer than 30 research groups have investigated its benefits in the surgery of CPA [11]. Yet during these 13 years, the concordance between the radiological reconstruction of the FN and intraoperative findings has substantially improved. Taoka et al. was the first to report the use of DTI-FT in VSs, but attained a low agreement that barely exceeded 60% [9]. Our initial results were also not promising [17]. However, three later studies overcame some technical constraints and demonstrated significant correlations between preoperative imaging and the FN's actual position [18–20]. Notably, these initial reports included only a small number of patients. Larger studies revealed that DTI-FT-based nerve predictions were not always correct [6, 21, 22]. In larger

series, the DTI-FT-based reconstruction of the FN yielded 91% reliable predictions [23]. Researchers have tried DTI-FT augmented with high-definition ultrasonography, although their initially promising results have not been followed up by other physicians [8]. We feel that these varying results are due to the highly variable methodology, MR field strengths, number of diffusion directions, software and tracking techniques used in each study.

Four systematic reviews have summarised the findings of DTI-FT in VSs [3, 4, 11, 24]. Two of these reviews pooled all the published cases into one artificial single subset by using the individual patient data PRISMA methodology (or equivalent) [3,4]. In that way, Baro et al. attempted to conclude from a highly unselected cohort of 223 individuals [3]. The overall incongruence between DTI-FT reconstruction and intraoperative nerve position was 13.3% (95% CI: 5.7-27.8), and the overall accuracy was 85.5% [3]. We did not surpass that figure, given that only 81.6% of our predictions were true. Baro et al. listed the main factors responsible for the incongruence: structural alterations of the FN, cystic VSs, technical problems related to the acquisition, post-processing, and anatomical alterations in large VSs [3]. The second systematic review, by Savardekar et al., pooled 234 original VSs and obtained a high, 90.6%, accuracy of DTI-FT of the FN [4]. Although they did not analyse the factors related to discordance, integration of the neuronavigation system with the prepared DTI-FT images needs verification in terms of decreasing the neurological complication rate [4].

Therefore, our study met the demand for preoperative visualisation of the FN by DTI-FT and a tumour that is integrated with the neuronavigation system [4]. Li et al. first integrated neuronavigation with the preoperative DTI-FT images with correct predictions in 17 out of 18 patients [6]. The authors suggested that integration with neuronavigation offered a wide range of applications, such as removing unnecessary worry when debulking in the region where the FN is not indicated by the navigation [6]. We feel that stereotactic localisation of the FN could be clinically useful to the neurosurgeon, but only with complete or nearly complete reliability. Failing that, a surgeon could mistakenly injure a nerve, or look for a nerve where it is not present. Our study proved that this imaging technique currently requires more development.

All DTI-FT software settings, including the thresholds of various values, region-of-interests and cropping fibres, are highly operator-dependent. This creates a situation where two DTI-FT operators can produce two different tracing results [6]. Therefore, the value of literature reviews mentioned earlier is debatable because studies differ substantially in their imaging methodology. In our study, we modified the FA thresholds and other parameters to obtain a more reliable FN visualisation based on previous research [25]. However, we deliberately set only one region-of-interest in the entire internal auditory canal since we found that setting an additional region-of-interest at the pons was ineffective. Peculiar diffusion around the CPA

**Table 3.** Factors associated with accuracy of diffusion tensor tractography-fibre tracking of facial nerve

Factor	Correct prediction		Incorrect prediction
<b>Age</b> (mean $\pm$ SD)	54.0 $\pm$ 12.7		58.5 $\pm$ 21.1
		<i>p</i> = 0.47	
<b>Sex</b> (n, % of females)	18/31, 58.1%		0/4, 0%
		<i>p</i> = 0.04	
<b>Side</b> (n, % of left)	15/17, 88.2%		2/17, 11.8%
		<i>p</i> = 1.00	
<b>Years from study initiation</b> (mean $\pm$ SD)	3.3 $\pm$ 2.0		1.3 $\pm$ 1.0
		<i>p</i> = 0.09	
<b>Tumour and facial nerve</b>			
Pathology			
Vestibular schwannoma (n, %)	26/30, 86.7%		4/30, 100%
Meningioma (n, %)	4/4, 100%		0/4, 0%
		<i>p</i> = 0.69	
Intracanalicular growth (n, %)	23/27, 85.2%		4/27, 14.8%
		<i>p</i> = 0.55	
Diameter (mean $\pm$ SD)	30.3 $\pm$ 13.4		30.2 $\pm$ 9.6
		<i>p</i> = 0.86	
Koos grade (mean $\pm$ SD)	2.6 $\pm$ 0.9		2.8 $\pm$ 0.5
		<i>p</i> = 0.78	
Koos grade $\geq$ 3 (n, %)	14/17, 82.4%		3/17, 17.6%
		<i>p</i> = 0.61	
Tumour diameter (mean $\pm$ SD)	30.3 $\pm$ 13.4		30.3 $\pm$ 9.6
		<i>p</i> = 0.86	
Tumour diameter $\geq$ 3cm (n, %)	17/19, 89.5%		2/19, 10.5%
		<i>p</i> = 1.00	
Compact shape of facial nerve (n, %)	8/11, 72.7%		3/11, 27.3%
		<i>p</i> = 0.03	
Facial nerve position (Sampath [15], n, %)			
Antero-superior	14/16, 87.5%		2/14, 12.5%
		<i>p</i> = 1.00	
Anterior	7/8, 87.5%		1/8, 12.5%
		<i>p</i> = 1.00	
Superior	4/4, 100%		0/4, 0%
		<i>p</i> = 1.00	
Other	6/7, 85.7%		1/7, 14.3%
		<i>p</i> = 1.00	
<b>Outcome</b>			
HB grade $\geq$ 2 (n, %)	11/13, 84.6%		2/13, 15.4%
		<i>p</i> = 0.57	
HB grade (mean $\pm$ SD)	1.8 $\pm$ 1.4		3.0 $\pm$ 2.6
		<i>p</i> = 0.35	
Complete excision (n, %)	18/21, 85.7%		3/21, 14.3%
		<i>p</i> = 1.00	

HB — House-Brackmann grade of facial palsy; SD — standard deviation



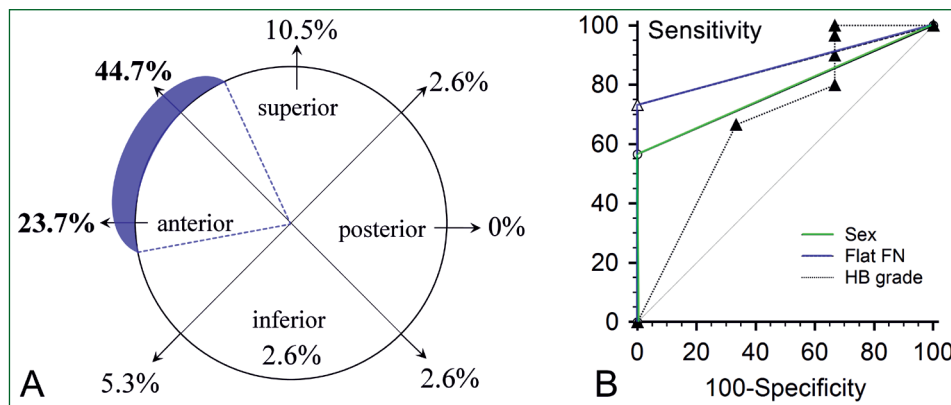


**Figure 3.** A. Illustration showing frequency of locations of facial nerve (according to classification proposed by Sampath et al. [15]). B. Receiver operating characteristic curves of factors influencing prediction rate for diffusion tensor imaging-fibre tracking (DTI-FT) of facial nerve (FN). House-Brackmann grading used to demonstrate that DTI-FT of FN had positive influence on neurological outcome, although not significant FN – facial nerve, HB grade – House-Brackmann grade of facial palsy

**Table 4.** Prediction of facial nerve location in relation to intraoperative findings

DTI-FT visualised position of FN	FN position confirmed during surgery	
	-	+
-	FN was <b>NOT</b> visualised by DTI-FT, and for some reason it was <b>NOT</b> exposed during surgery <b>n = 0</b>	FN was <b>NOT</b> visualised by DTI-FT, but its position was identified during surgery <b>n = 4</b> (case nos. 7, 16, 21, 24)
+	FN was visualised by DTI-FT, but its actual position was different to that predicted <b>n = 3</b> (case nos. 2, 10, 13)	FN was visualised by DTI-FT, and its correct position was confirmed during surgery <b>n = 31</b> (all other cases)

DTI-FT — diffusion tensor imaging-fibre tracking; FN — facial nerve

precludes drawing long fibres, hence we selected the main DTI bundle around the tumour which was passing through the internal auditory canal.

Even so, the low accuracy of our method may indicate that we performed DTI-FT ineffectively. FN reconstructions using probabilistic tractography were considered to solve the problem of many fibres which are densely packed around the VS. Unfortunately, the obtained accuracy was not satisfactory and reached only 81% [26]. A fully reliable method visualising the FN is still needed. Recalculation of a few co-registered MR sequences could be the solution. Initially, this did not increase the reliability of FN prediction, although DTI together with CISS sequence could somewhat differentiate the FN from the cochlear nerve [23, 27]. Recently, Pereira et al. developed a promising concept involving fusing sequences: CISS, T1 and contrast-enhanced T1. This method takes advantage of the non-contrasting regularity of the FN as compared to the tumour [28]. In this preliminary report on five cases, the agreement between the fused CISS/T1 and intraoperative findings was always correct.

Therefore, we feel that determining the right course of the FN in CPA tumours is not just a matter of improving a single DTI sequence, but also of combining semi-automated and

acquired sequences. Skilful fusion techniques have not reached the limits of their capabilities, and are promising in terms of forthcoming FN identification [28]. Perhaps in the future neural networks could help streamline imaging of the cranial nerves and overcome human limitations. Unless augmented by other technical advances, we assert that the development of an isolated DTI technique for FN tracking will not attain optimal accuracy.

We compared our complication rates with a recent study on 502 VSs [29]. In this study, approximately 25% had facial palsy (HB grades II-VI), whereas 36.8% of our patients had it. In terms of preserved useful facial functions (HB grades I-III), we encountered the same percentage: 86%. 10% of our patients encountered cerebrospinal fluid leakage, which was similar to other series [29]. Complications, both neurological and general surgical, are the major concern in the modern approach to a VS. Over the last decade, we have witnessed the treatment paradigm of large VSs favouring subtotal resection, and subsequent stereotactic radiosurgery; this approach offers excellent functional outcomes while achieving a tumour control rate comparable to that after total resection [2].

Even with 38 patients in our study, we could have encountered some degree of a type II error. However, we emphasise

that even if the study period was prolonged (and so the number of patients was increased) the FN prediction rate would not be affected significantly. We feel that the limitations of DTI-FT are in part associated with the practical application of the imaging technique. For example, it is not unusual to encounter a brain shift related to head misalignment, hardware micro-movements and cerebrospinal fluid release following partial tumour debulking. All these factors increase the inaccuracy of DTI-FT of the FN. Fortunately, future technical advances may address some of these variables e.g. making machinery more stable. An anatomical limitation also exists; the FN is usually tracked together with the vestibulo-cochlear nerve, and it is not always possible to distinguish them by DTI-FT.

## Conclusions

The reliability of DTI-FT when predicting the FN's course remains unsatisfactory. Our study shows no benefit with DTI-FT neuronavigation integration over only preoperative DTI-FT visualisation. However, introducing surgical planning to the operating theatre can make excising the CPA tumour more comfortable for the surgeon. Combining more imaging modalities would increase the ability to predict the course of the FN, and reduce surgery-related complications.

## Abbreviations:

AUC — area under the curve  
 CISS — constructive interference in steady state  
 CPA — cerebello-pontine angle  
 DTI — diffusion tensor imaging  
 DTI-FT — diffusion tensor imaging-fibre tracking  
 FA — fractional anisotropy  
 FN — facial nerve  
 HB — House-Brackmann  
 MRI — magnetic resonance imaging  
 VS — vestibular schwannoma

**Funding:** *No funding was received for this research.*

**Conflict of Interest:** *All authors certify that they have no affiliation with or involvement in any organisation or entity with any financial interest (such as honoraria, educational grants, participation in speakers' bureaux, membership, employment, consultancies, stock ownership, or other equity interest, and expert testimony or patent-licensing arrangements), or non-financial interest (such as personal or professional relationships, affiliations, knowledge or beliefs) in the subject matter or materials discussed in this manuscript.*

**Ethical permission:** *For preparation of this article, ethical approval was obtained from the institution (IRB Committee number: NKEBN/98/2012, NKEBN/65/2019).*

**Informed consent:** *Informed consent for treatment and data processing was obtained from all individual participants included in this study.*

## References

1. Rinaldi V, Casale M, Bressi F, et al. Facial nerve outcome after vestibular schwannoma surgery: our experience. *J Neurol Surg B Skull Base.* 2012; 73(1): 21–27, doi: [10.1055/s-0032-1304559](https://doi.org/10.1055/s-0032-1304559), indexed in Pubmed: [23372991](https://pubmed.ncbi.nlm.nih.gov/23372991/).
2. Staronni D, Daniel RT, Tuleasca C, et al. Systematic review and meta-analysis of the technique of subtotal resection and stereotactic radiosurgery for large vestibular schwannomas: a “nerve-centered” approach. *Neurosurg Focus.* 2018; 44(3): E4, doi: [10.3171/2017.12.FOCUS17669](https://doi.org/10.3171/2017.12.FOCUS17669), indexed in Pubmed: [29490553](https://pubmed.ncbi.nlm.nih.gov/29490553/).
3. Baro V, Landi A, Brigadoi S, et al. Preoperative Prediction of Facial Nerve in Patients with Vestibular Schwannomas: The Role of Diffusion Tensor Imaging-A Systematic Review. *World Neurosurg.* 2019; 125: 24–31, doi: [10.1016/j.wneu.2019.01.099](https://doi.org/10.1016/j.wneu.2019.01.099), indexed in Pubmed: [30708084](https://pubmed.ncbi.nlm.nih.gov/30708084/).
4. Savardekar AR, Patra DP, Thakur JD, et al. Preoperative diffusion tensor imaging-fiber tracking for facial nerve identification in vestibular schwannoma: a systematic review on its evolution and current status with a pooled data analysis of surgical concordance rates. *Neurosurg Focus.* 2018; 44(3): E5, doi: [10.3171/2017.12.FOCUS17672](https://doi.org/10.3171/2017.12.FOCUS17672), indexed in Pubmed: [29490547](https://pubmed.ncbi.nlm.nih.gov/29490547/).
5. Samala R, Borkar SA, Sharma R, et al. Effectiveness of preoperative facial nerve diffusion tensor imaging tractography for preservation of facial nerve function in surgery for large vestibular schwannomas: Results of a prospective randomized study. *Neurol India.* 2019; 67(1): 149–154, doi: [10.4103/0028-3886.253631](https://doi.org/10.4103/0028-3886.253631), indexed in Pubmed: [30860114](https://pubmed.ncbi.nlm.nih.gov/30860114/).
6. Li H, Wang L, Hao S, et al. Identification of the Facial Nerve in Relation to Vestibular Schwannoma Using Preoperative Diffusion Tensor Tractography and Intraoperative Tractography-Integrated Neuronavigation System. *World Neurosurg.* 2017; 107: 669–677, doi: [10.1016/j.wneu.2017.08.048](https://doi.org/10.1016/j.wneu.2017.08.048), indexed in Pubmed: [28826862](https://pubmed.ncbi.nlm.nih.gov/28826862/).
7. Borkar SA, Garg A, Mankotia DS, et al. Prediction of facial nerve position in large vestibular schwannomas using diffusion tensor imaging tractography and its intraoperative correlation. *Neurol India.* 2016; 64(5): 965–970, doi: [10.4103/0028-3886.190270](https://doi.org/10.4103/0028-3886.190270), indexed in Pubmed: [27625239](https://pubmed.ncbi.nlm.nih.gov/27625239/).
8. Simon NG, Cage T, Narvid J, et al. High-resolution ultrasonography and diffusion tensor tractography map normal nerve fascicles in relation to schwannoma tissue prior to resection. *J Neurosurg.* 2014; 120(5): 1113–1117, doi: [10.3171/2014.2.JNS131975](https://doi.org/10.3171/2014.2.JNS131975), indexed in Pubmed: [24628610](https://pubmed.ncbi.nlm.nih.gov/24628610/).
9. Taoka T, Hirabayashi H, Nakagawa H, et al. Displacement of the facial nerve course by vestibular schwannoma: preoperative visualization using diffusion tensor tractography. *J Magn Reson Imaging.* 2006; 24(5): 1005–1010, doi: [10.1002/jmri.20725](https://doi.org/10.1002/jmri.20725), indexed in Pubmed: [17031835](https://pubmed.ncbi.nlm.nih.gov/17031835/).
10. Jacquesson T, Frindel C, Kocevar G, et al. Overcoming Challenges of Cranial Nerve Tractography: A Targeted Review. *Neurosurgery.* 2019; 84(2): 313–325, doi: [10.1093/neuros/nyy229](https://doi.org/10.1093/neuros/nyy229), indexed in Pubmed: [30010992](https://pubmed.ncbi.nlm.nih.gov/30010992/).
11. Shapey J, Vos SB, Vercauteren T, et al. Clinical Applications for Diffusion MRI and Tractography of Cranial Nerves Within the Posterior Fossa: A Systematic Review. *Front Neurosci.* 2019; 13: 23, doi: [10.3389/fnins.2019.00023](https://doi.org/10.3389/fnins.2019.00023), indexed in Pubmed: [30809109](https://pubmed.ncbi.nlm.nih.gov/30809109/).
12. Koos WT, Day JD, Matula C, et al. Neurotopographic considerations in the microsurgical treatment of small acoustic neurinomas. *J Neurosurg.* 1998; 88(3): 506–512, doi: [10.3171/jns.1998.88.3.0506](https://doi.org/10.3171/jns.1998.88.3.0506), indexed in Pubmed: [9488305](https://pubmed.ncbi.nlm.nih.gov/9488305/).

13. Sun MZ, Oh MC, Safaee M, et al. Neuroanatomical correlation of the House-Brackmann grading system in the microsurgical treatment of vestibular schwannoma. *Neurosurg Focus*. 2012; 33(3): E7, doi: [10.3171/2012.6.FOCUS12198](https://doi.org/10.3171/2012.6.FOCUS12198), indexed in Pubmed: 22937858.
14. Elm Ev, Altman D, Egger M, et al. The Strengthening the Reporting of Observational Studies in Epidemiology (STROBE) statement: guidelines for reporting observational studies. *Journal of Clinical Epidemiology*. 2008; 61(4): 344–349, doi: [10.1016/j.jclinepi.2007.11.008](https://doi.org/10.1016/j.jclinepi.2007.11.008).
15. Sampath P, Rini D, Long DM. Microanatomical variations in the cerebellopontine angle associated with vestibular schwannomas (acoustic neuromas): a retrospective study of 1006 consecutive cases. *J Neurosurg*. 2000; 92(1): 70–78, doi: [10.3171/jns.2000.92.1.0070](https://doi.org/10.3171/jns.2000.92.1.0070), indexed in Pubmed: 10616085.
16. Churi ON, Gupta S, Misra BK. Correlation of Preoperative Cranial Nerve Diffusion Tensor Tractography with Intraoperative Findings in Surgery of Cerebellopontine Angle Tumors. *World Neurosurg*. 2019; 127: e509–e516, doi: [10.1016/j.wneu.2019.03.190](https://doi.org/10.1016/j.wneu.2019.03.190), indexed in Pubmed: 30928584.
17. Szmuda T, Słoniewski P, Sabisz A, et al. Traktografia nerwu twarowego w guzach kąta mostowo-mózdkowego. *Otorynolaryngologia*. 2015; 13: 42–50.
18. Roundy N, Delashaw JB, Cetas JS. Preoperative identification of the facial nerve in patients with large cerebellopontine angle tumors using high-density diffusion tensor imaging. *J Neurosurg*. 2012; 116(4): 697–702, doi: [10.3171/2011.12.JNS111404](https://doi.org/10.3171/2011.12.JNS111404), indexed in Pubmed: 22283188.
19. Choi KS, Kim MS, Kwon HG, et al. Preoperative identification of facial nerve in vestibular schwannomas surgery using diffusion tensor tractography. *J Korean Neurosurg Soc*. 2014; 56(1): 11–15, doi: [10.3340/jkns.2014.56.1.11](https://doi.org/10.3340/jkns.2014.56.1.11), indexed in Pubmed: 25289119.
20. Zhang Y, Chen Y, Zou Y, et al. Facial nerve preservation with preoperative identification and intraoperative monitoring in large vestibular schwannoma surgery. *Acta Neurochir (Wien)*. 2013; 155(10): 1857–1862, doi: [10.1007/s00701-013-1815-9](https://doi.org/10.1007/s00701-013-1815-9), indexed in Pubmed: 23877233.
21. Yoshino M, Kin T, Ito A, et al. Feasibility of diffusion tensor tractography for preoperative prediction of the location of the facial and vestibulocochlear nerves in relation to vestibular schwannoma. *Acta Neurochir (Wien)*. 2015; 157(6): 939–46; discussion 946, doi: [10.1007/s00701-015-2411-y](https://doi.org/10.1007/s00701-015-2411-y), indexed in Pubmed: 25862170.
22. Wei PH, Qi ZG, Chen Ge, et al. Identification of cranial nerves near large vestibular schwannomas using superselective diffusion tensor tractography: experience with 23 cases. *Acta Neurochir (Wien)*. 2015; 157(7): 1239–1249, doi: [10.1007/s00701-015-2431-7](https://doi.org/10.1007/s00701-015-2431-7), indexed in Pubmed: 25948078.
23. Gerganov VM, Giordano M, Samii M, et al. Diffusion tensor imaging-based fiber tracking for prediction of the position of the facial nerve in relation to large vestibular schwannomas. *J Neurosurg*. 2011; 115(6): 1087–1093, doi: [10.3171/2011.7.JNS11495](https://doi.org/10.3171/2011.7.JNS11495), indexed in Pubmed: 21962081.
24. Jacquesson T, Cotton F, Frindel C. MRI Tractography Detecting Cranial Nerve Displacement in a Cystic Skull Base Tumor. *World Neurosurg*. 2018; 117: 363–365, doi: [10.1016/j.wneu.2018.06.182](https://doi.org/10.1016/j.wneu.2018.06.182), indexed in Pubmed: 29966790.
25. Yoshino M, Kin T, Ito A, et al. Diffusion tensor tractography of normal facial and vestibulocochlear nerves. *Int J Comput Assist Radiol Surg*. 2015; 10(4): 383–392, doi: [10.1007/s11548-014-1129-2](https://doi.org/10.1007/s11548-014-1129-2), indexed in Pubmed: 25408307.
26. Zolal A, Juratli TA, Podlesek D, et al. Probabilistic Tractography of the Cranial Nerves in Vestibular Schwannoma. *World Neurosurg*. 2017; 107: 47–53, doi: [10.1016/j.wneu.2017.07.102](https://doi.org/10.1016/j.wneu.2017.07.102), indexed in Pubmed: 28754643.
27. Yoshino M, Kin T, Ito A, et al. Combined use of diffusion tensor tractography and multifused contrast-enhanced FIESTA for predicting facial and cochlear nerve positions in relation to vestibular schwannoma. *J Neurosurg*. 2015; 123(6): 1480–1488, doi: [10.3171/2014.11.JNS14988](https://doi.org/10.3171/2014.11.JNS14988), indexed in Pubmed: 26053235.
28. Pereira P, Manacas R. Magnetic Resonance Imaging Fusion of Cranial Nerves Impaired by Skull Base Tumors: A Technical Development. *Journal of Nuclear Medicine & Radiation Therapy*. 2019; 10(1), doi: [10.4172/2155-9619.1000396](https://doi.org/10.4172/2155-9619.1000396).
29. Breun M, Nickl R, Perez J, et al. Vestibular Schwannoma Resection in a Consecutive Series of 502 Cases via the Retrosigmoid Approach: Technical Aspects, Complications, and Functional Outcome. *World Neurosurg*. 2019; 129: e114–e127, doi: [10.1016/j.wneu.2019.05.056](https://doi.org/10.1016/j.wneu.2019.05.056), indexed in Pubmed: 31100515.

## 6. Podsumowanie

W neurochirurgii tematyka poszukiwania nowych metod obrazowania i diagnostyki, które ułatwiłyby codzienną pracę oraz zwiększyłyby bezpieczeństwo zabiegów operacyjnych należy do częstych obszarów badań. W przedłożonej pracy doktorskiej podsumowano i przedstawiono możliwości jakie wynikają z wykorzystania traktografii zarówno w zakresie anatomii dróg nerwowych w populacji zdrowej oraz zaprezentowano zmiany w zakresie pęczków nerwowych u chorych nowotworowych lub po udarze niedokrwiennym mózgu [7-10].

Prezentowane wyniki wiążą wykorzystanie traktografii jako metodę diagnostyczną w neurochirurgii, neurologii oraz anatomii [16].

W większości zaprezentowanych artykułów wykorzystywano deterministyczny algorytm traktograficzny. W przyszłości kierunki dalszych analiz mogą skupiać się na porównaniu algorytmu deterministycznego i probabilistycznego co może skutkować większą precyzją otrzymywanych danych oraz zmniejszyć ograniczenia wynikającej m.in. ze stopniem rozproszenia włókien nerwowych.

Uzyskane wyniki w zaprezentowanych publikacjach pokazują złożoność roli traktografii. Przeprowadzona analiza użyteczności i wykorzystania traktografii w oparciu o tensor dyfuzji potwierdziła potencjał metody w wyznaczaniu pęczków nerwowych oraz wizualizacji nerwów czaszkowych [11-13].

Skojarzenie jej z innymi technikami z zakresu neuroobrazowania czy elektrofizjologii znajduje coraz szersze zastosowanie w diagnostyce, monitorowaniu oraz terapii patologii układu nerwowego [22,23]. W bieżącym przeglądzie pokazaliśmy przykłady, w których traktografia jest cennym dodatkiem do codziennego obrazowania [19,24]. Ze względu na coraz częściej stosowane połączenia traktografii z monitorowaniem śródoperacyjnym możliwe jest dokładniejsze planowanie przedoperacyjne oraz zwiększenie bezpieczeństwa operacji [14,15].

## **7.Wnioski**

1.Zaprezentowany cykl publikacji wykazał iż wykorzystanie traktografii oraz poszukiwanie nowych metod wyznaczania istotnych dróg nerwowych w oparciu o zróżnicowane ROI jest użyteczną i nieinwazyjną metodą, która może być wykorzystana w neurochirurgii i neurologii.

2.Zastosowane algorytmy deterministyczne mogą zostać wykorzystane w codziennej pracy m.in. podczas resekcji guzów mózgu zwiększając bezpieczeństwo operacji i zmniejszając ryzyko wystąpienia deficytów neurologicznych.

3. Traktografia może być wykorzystana w diagnostyce i monitorowaniu zmian w anatomii i przebiegu dróg nerwowych i nerwu twarzowego u chorych z naciekiem nowotworowym i niedokrwieniem mózgu.

## 8. Piśmiennictwo

1. Abdullah K.G., Lubelski D., Nucifora P.G.P., Brem S., 2013. Use of diffusion tensor imaging in glioma resection. *Neurosurgical Focus* 34, E1. <https://doi.org/10.3171/2013.1.focus12412>
2. Al-Okaili R.N., Krejza J., Wang S., Woo J.H., Melhem E.R. 2006. Advanced MR Imaging Techniques in the Diagnosis of Intraaxial Brain Tumors in Adults. *RadioGraphics* 26, S173–S189. <https://doi.org/10.1148/rg.26si065513>
3. Bette S., Huber T., Wiestler B., Boeckh-Behrens T., Gempt J., Ringel F., et al. 2016. Analysis of fractional anisotropy facilitates differentiation of glioblastoma and brain metastases in a clinical setting. *European Journal of Radiology* 85(12), 2182–2187. doi:10.1016/j.ejrad.2016.10.002
4. Costabile J. D., Alaswad E., D'Souza S., Thompson J. A., Ormond D. R. 2019. Current applications of diffusion tensor imaging and tractography in intracranial tumor resection. *Frontiers in oncology* 9, 426. <https://doi.org/10.3389/fonc.2019.00426>
5. Czarnecka A., Zimny A., Szewczyk P. 2010. Zaawansowane techniki rezonansu magnetycznego w diagnostyce guzów wewnątrzczaszkowych. *Polski Przegląd Neurologiczny* 6(1), 2010, 27-37.
6. Demir A., Ries M., Moonen C.T.W., Vital J.M., Dehais J., Arne P., Caillé J.M., Dousset V. 2003. Diffusion-weighted MR imaging with apparent diffusion coefficient and apparent diffusion tensor maps in cervical spondylotic myelopathy. *Radiology* 229, 37–43. <https://doi.org/10.1148/radiol.2291020658>

7. Eliassen J. C., Boespflug E. L., Lamy M., Allendorfer J., Chu W. J., Szaflarski J. P. 2008. Brain-mapping techniques for evaluating poststroke recovery and rehabilitation: a review. *Topics in stroke rehabilitation* 15(5), 427–450. <https://doi.org/10.1310/tsr1505-427>
8. Essayed W.I., Zhang F., Unadkat P., Cosgrove G.R., Golby A.J., O'Donnell L.J. 2017. White matter tractography for neurosurgical planning: A topography-based review of the current state of the art. *NeuroImage: Clinical* 15, 659–672. <https://doi.org/10.1016/j.nicl.2017.06.011>
9. Facon D., Ozanne A., Fillard P., Tournoux-Facon C., Ducreux D. 2005. MR diffusion tensor imaging and fiber tracking in spinal cord compression. *Am J Neuroradiol* 26(6):1587–94 1587–1594. <https://doi.org/10.1016/j.jns.2013.07.1941>
10. Gierek T., Paluch J., Pencak P., Kaźmierczak B., Klimczak-Gołab L. 2009. Magnetic resonance tractography in neuroradiological diagnostic aspects. *Otolaryngologia polska = The Polish otolaryngology* 63, 403–6. [https://doi.org/10.1016/S0030-6657\(09\)70151-9](https://doi.org/10.1016/S0030-6657(09)70151-9)
11. Jiang R., Du F. Z., He C., Gu M., Ke Z. W., Li J. H. 2014. The value of diffusion tensor imaging in differentiating high-grade gliomas from brain metastases: a systematic review and meta-analysis. *PloS one* 9(11), e112550. <https://doi.org/10.1371/journal.pone.0112550>

12. Kim SH., Jang SH. 2013. Prediction of aphasia outcome using diffusion tensor tractography for arcuate fasciculus in stroke. *AJNR Am J Neuroradiol* 34:785–790.
13. Krakowiak M., Słoniewski P., Dzierżanowski J., Szmuda T. 2015. Future of the nerve fibres imaging : tractography application and development directions. *Folia Morphologica* 74, 290–294. <https://doi.org/10.5603/FM.2015.0044>
14. Marcinkowska A., Sabisz A., Szurowska E. 2017. Nowoczesne techniki rezonansu magnetycznego w obrazowaniu guzów mózgu. *Forum Medycyny Rodzinnej* 11, 216–224.
15. Min Z.G., Niu C., Zhang Q.L., Zhang M., Qian Y.C. 2017. Optimal factors of diffusion tensor imaging predicting corticospinal tract injury in patients with brain tumors. *Korean Journal of Radiology* 18, 844–851. <https://doi.org/10.3348/kjr.2017.18.5.844>
16. O’neill B.E., Hochhalter C.B., Carr C., Strong M.J., Ware M.L. 2018. Advances in neuro-oncology imaging techniques. *Ochsner Journal* 18, 236–241. <https://doi.org/10.31486/toj.17.0062>
17. Potgieser A. R. E., Wagemakers M., van Hulzen A. L. J., de Jong B. M., Hoving E. W., Groen R. J. M. 2014. The role of diffusion tensor imaging in brain tumor surgery: A review of the literature. *Clinical Neurology and Neurosurgery* 124, 51–58. doi:10.1016/j.clineuro.2014.06.009



18. Provenzale J.M., Mukundan S., Barboriak D.P. 2006. Diffusion-weighted and Perfusion MR Imaging for Brain Tumor Characterization and Assessment of Treatment Response. *Radiology* 239, 632–649. <https://doi.org/10.1148/radiol.2393042031>

19. Song F. Hou Y., Sun G., Chen X., Xu B., Huang J.H., Zhang J. 2016. In vivo visualization of the facial nerve in patients with acoustic neuroma using diffusion tensor imaging-based fiber tracking. *J. Neurosurg* 125:787–794.

20. Sotak C. H. 2002. The role of diffusion tensor imaging in the evaluation of ischemic brain injury - a review. *NMR in Biomedicine* 15(7-8), 561–569. [doi:10.1002/nbm.786](https://doi.org/10.1002/nbm.786)

21. Tae W. S., Ham B. J., Pyun S. B., Kang S. H., Kim B. J. 2018. Current Clinical Applications of Diffusion-Tensor Imaging in Neurological Disorders. *Journal of clinical neurology* (Seoul, Korea), 14(2), 129–140. <https://doi.org/10.3988/jcn.2018.14.2.129>

22. Ulmer J.L., Salvan C. V., Mueller W.M., Krouwer H.G., Stroe G.O., Aralasmak A., Prost R.W. 2004. The role of diffusion tensor imaging in establishing the proximity of tumor borders to functional brain systems: Implications for preoperative risk assessments and postoperative outcomes. *Technology in Cancer Research and Treatment* 3, 567–576. <https://doi.org/10.1177/153303460400300606>

23. Wu J.S., Zhou L.F., Tang W.J., Mao Y., Hu J., Song et al. 2007. Clinical evaluation and follow-up outcome of diffusion tensor imaging-based functional

neuronavigation. Neurosurgery 61(5), 935–949.  
doi:10.1227/01.neu.0000303189.80049.ab

24.Zhang Y., Chen Y., Zou Y., Zhang W., Zhang R., Liu X., et al. 2013. Facial nerve preservation with preoperative identification and intraoperative monitoring in large vestibular schwannoma surgery. *Acta Neurochir* 155:1857–1860